ARTICLE

The utilization of post-synthetic modification in covalent organic frameworks

Received 00th January 20xx,
Accepted 00th January 20xx

DOI: 10.1039/x0xx00000x

José L. Segura,*[a] Sergio Royuela [a,b] and María M. Ramos [b]

Covalent organic frameworks (COFs) are organic porous materials with many potential applications, which very often depend on the presence of chemical functionality at the organic building blocks. Functionality that cannot be introduced into COFs directly *via de novo* syntheses can be accessed through post-synthetic modification (PSM) strategies. Current strategies for the post-synthetic modification of COFs involve (i) incorporation of a variety of active metal species by using metal complexation through coordination chemistry, (ii) covalent bond formation between existing pendant groups and incoming constituents and (iii) chemical conversion of linkages. (iv) The post-synthetic modification is sometimes assisted by a monomer truncation strategy for the internal functionalization of COFs. (v) Even more intriguing methods that go beyond PSM are herein termed building block exchange (BBE) which encompasses framework-to-framework transformations taking advantage of the fact that reversible bond formation is a characteristic feature of COFs. This strategy allows the use of protoCOF structures (i.e., the utilization of a parent COF as a template) for the evolution of new COF structures with completely new components.

1. Introduction

In 2005, Yaghi and co-workers reported the first successful examples of covalent organic frameworks (COFs) which demonstrated the utility of dynamic covalent chemistry and the topological design principle in the synthesis of these porous organic frameworks connected *via* covalent bonds.[1] This seminal work paved the way for the development of new families of robust, stable, ordered and highly accessible porous materials with associated functionalities in their framework. These characteristics have allowed research on COFs to address some of the important challenges identified in materials science when searching for advanced solids for separation, catalysis, energy storage, adsorption, sensors, electronic or photoluminescence devices.[2, 3] Thus, as recently reviewed by Lohse and Bein,[4] COFs have already found applications in the storage and separation of gases, in catalysis, in electrochemical energy storage, in electrical devices, in optoelectronics, in sensing or in drug delivery among others. Because of this interest, research related with COFs has experienced an enormous growth in the last few years and the literature of the field has been already reviewed in a number of review articles. Thus, some general review articles,[4-11] reviews centered in the fundamentals,[12] the applications,[13-27] the synthesis,[28] and the design of COFs[29, 30] have been already published. Other reviews have focused in more specific aspects such as the development of COFs as nanolayers or synthesized on surface,[31, 32] on the morphologic control,[33] growth mechanism, scalability and stability[11, 34] of COFs.

The purpose of this review article is not to duplicate those aspects previously reviewed in the different fields summarized above but to focus on the post-polymerization modification of covalent organic frameworks due to the great development of this particular area of research related with the field of COFs in the last four years. As stated by Yaghi and co-workers, the promise of COFs lies in the fact that COFs, though being extended solids, are amenable to the versatile toolbox of molecular synthesis. Thus, by the use of post-synthetic modifications, COFs can be subjected to reactions normally carried out in molecular organic chemistry, leading to completely new COFs without the need of the trial and error and inherent uncertainties of *de novo* synthesis.[35] Therefore, the aim of the article is to review the post-polymerization modification of COFs from a broad point of view considering (i) the incorporation of a variety of active metal species by using metal complexation through coordination chemistry, (ii) the covalent bond formation between existing pendant groups and incoming constituents and (iii) the chemical conversion of linkages. Furthermore, (iv) the post-synthetic modification assisted by a monomer truncation strategy for the functionalization of COFs will be also reviewed. (v) An important development in the field that will be also reviewed involves the strategy known as building block exchange (BBE) which encompasses framework-to-framework transformations taking advantage of the fact that reversible bond formation is a characteristic feature of COFs. Thus, in the review we will briefly mention the basic principles for the synthesis of COFs and then

[a] *Departamento de Química Orgánica, Facultad de Química, Universidad Complutense de Madrid, 28040 Madrid, Spain. E-mail: segura@ucm.es.*
[b] *Departamento de Tecnología Química y Ambiental, Universidad Rey Juan Carlos, 28933 Madrid, Spain.*

concentrate on the post-polymerization modification of this unique family of organic macromolecular materials.

2. Principles for the design and synthesis of covalent organic frameworks

The development of novel precision polymers and macromolecular materials has been possible due to the advances in novel synthetic methods with exceptional stereospecificity, chemoselectivity as well as polymer size, architecture, composition, and uniformity.[36, 37] However, there is still a challenge related with the polymerization of monomers into well-defined two-dimensional (2D) or three-dimensional (3D) structures. In this respect, development of novel 2D and 3D structures has been possible due to complementary contributions from different research areas including coordination chemistry,[38, 39] dynamic bond formation,[40-42] topochemical polymerization,[43] supramolecular assembly,[44, 45] as well as due to advances in the techniques for the characterization of nanostructured materials.[46]

In this context, the development of methods for the preparation of covalent organic frameworks (COFs) represents a unique strategy in order to access 2D and 3D polymer networks. Thus, the directional bonding principles established for supramolecular assemblies[47-49] and coordination polymers[50] are used for the design of COF monomers. However, in contrast with the parent supramolecular and coordination polymers, COFs are linked by covalent bonds that confer superior chemical and thermal stability. In these systems, the shape of the monomers determines the topology and dimensionality of the network (Fig. 1) as well as the size and shape of the pores that are usually retained after solvent removal. In this respect, it is worth pointing out that COFs are designed by using modular design principles related in many ways with the reticular design concepts used for the synthesis of other classes of porous materials including metal–organic frameworks (MOFs).[39] However, in comparison with other porous crystalline materials, COFs offer a singular combination of properties that make them unique materials and that include modularity, crystallinity, porosity, stability and low density.[33]

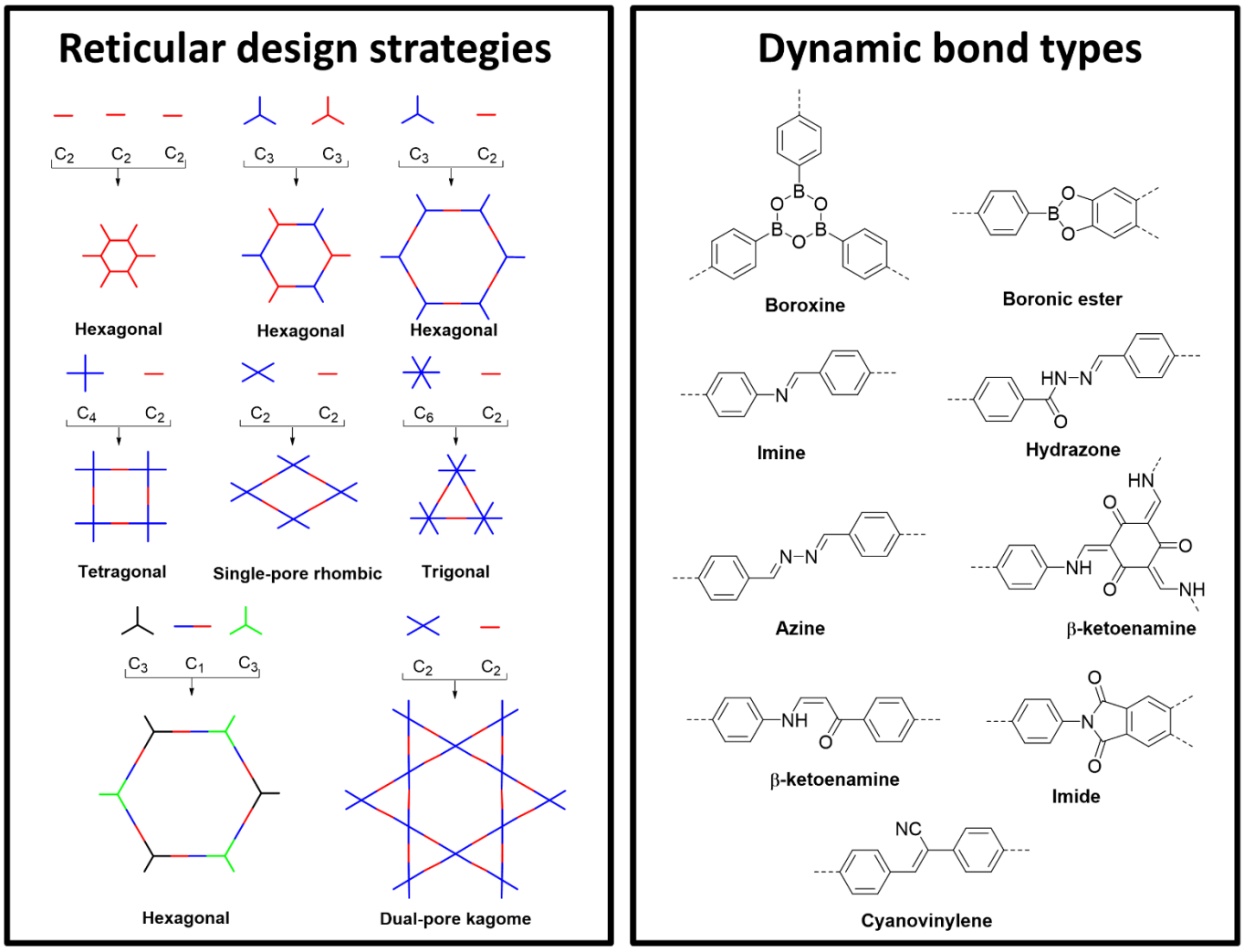

Fig. 1 Left: Reticular design strategies used in the synthesis of COFs. Right: Most common types of dynamic covalent bonds used to make COFs.

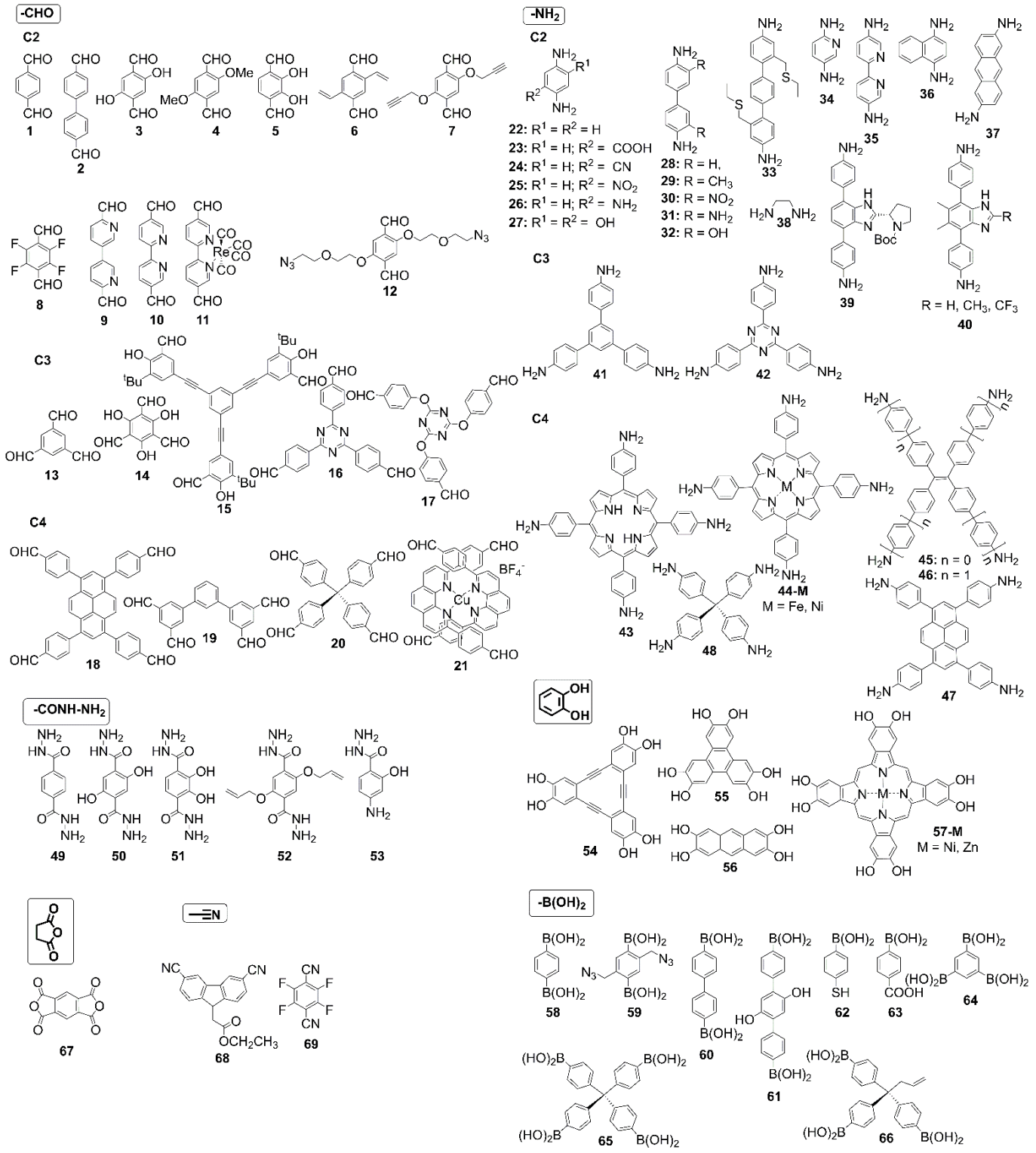

Fig. 2 Constituting building blocks used for the synthesis of the COFs reviewed in this article.

An important point in the production of COFs is related with the selection of suitable reactions for the construction of the crystalline frameworks. COFs can be built by using organic linkers with slightly reversible condensation reactions. The reactions must permit the regulation of the thermodynamic equilibrium during bond formation, thus allowing self-correction and formation of thermodynamically stable crystalline architectures. In Fig. 1 are depicted the most common types of covalent bonds used to make COFs including boroxine,[1] boronic ester,[51] imine,[52] hydrazone,[53] azine,[54] β-

ketoenamine,[55] imide[56] or cyanovinylene[57] linkages. The first pages on the COFs' field were written with the use of boroxine and boronic esters that provided highly crystalline materials. However, they are rather sensitive toward hydrolysis and it was necessary to develop more stable coupling motifs like the C=N linkages present in hydrazones, azines and imines, which exhibit superior resistance to hydrolysis. COFs based on imine linkages[9] have been the most extensively used for post-functionalization modification not only because of their stability but also because they can be formed by the condensation between aldehydes (**1-21**, Fig. 2) and primary amines (**22-48**, Fig. 2) which are readily accessible. COFs based on hydrazine linkages have been also used for post-synthetic modifications. These COFs can be obtained by the reversible condensation of hydrazides (**49-53**, Fig. 2) and aldehydes. There are also some examples of post-functionalization modification of COFs based on boroxines that can be obtained by self-condensation of boronic acids as well as modification of COFs based on boronic esters obtained by condensation of boronic acids (**58-66**, Fig. 2) and catechols (**54-57**, Fig. 2). Less explored is the post-synthetic modification of imide-linked COFs that can be obtained by reaction between primary amines and anhydrides (**67**, Fig. 2) as well as the modification of COFs based on triazines that can be obtained by cyclotrimerization reaction of nitriles (**68, 69**, Fig. 2). An in-depth description of the reactions used for the synthesis of COFs is out of the scope of the present review and the reader is referred to excellent feature articles covering this particular area.[8, 58]

In general, the building blocks for the synthesis of COFs should contain reactive groups that trigger the corresponding dynamic covalent bond formation. In addition, they should be conformationally rigid with the bond formation direction being discrete. In this regard, it is worth pointing out that in Fig. 2 are depicted the constituting building blocks used for the synthesis of COFs that have been used for post-synthetic transformations. This Figure can be used to guide the reader throughout the text in order to avoid duplication of structures in other figures and schemes.

The post-synthetic modification of two-dimensional COFs is the primary focus of this review, although the few examples reported for the post-synthetic modification of three-dimensional COFs will be also highlighted. The difference between these two types of COFs lies mainly in the design of their monomers.[24] Thus, monomers for the synthesis of 3D-COF are designed such that they can be polymerized through the formation of covalent bonds in all directions. On the other hand, the growth of 2D-COFs is controlled by two orthogonal processes: (i) thermodynamically controlled covalent-bond formation in two dimensions by using dynamic covalent polymerization[59] and (ii) crystallization of these layers through supramolecular interactions including dipolar forces or aromatic stacking.

3. Post-synthetic modification of covalent organic frameworks through metalation

The strong coordination between organic ligands and metal ions is a general method to introduce metal active sites in catalysts. The modular nature of COFs provides a unique platform to incorporate various molecular building blocks which can be used as organic ligands uniformly distributed throughout COFs. Furthermore, the interaction of the uniformly distributed organic ligands with metal active sites allows for the effective isolation of the active sites of the catalyst at a molecular level.[60] Thus, several inorganic ions including Ca,[61, 62] Sr,[62] Ti,[63] V,[64, 65] Mn,[62, 66] Fe,[67-70] Co,[66, 69-73] Ni,[66, 69, 74] Cu,[66, 75-78] Zn,[66] Mo,[79] Rh,[80] Pd,[72, 80-85] Re,[86] and Ir[87] have been incorporated in covalent organic frameworks through post-treatment of COFs with salts of suitable inorganic ions taking advantage of metal-ligand interactions. At this point it is worth mentioning that there are metalated COFs in which a metalated ligand is used as a monomer in the polymerization reaction (i.e. monomers based on metalated porphyrins).[88] This kind of systems are not reviewed in this article because there is no post-synthetic modification of the COF, given that the metal is already incorporated in the monomer in a pre-polymerization step. For this kind of COFs, the post-synthetic step would involve the demetalation of the COF. In fact, some nice examples of post-synthetic demetalation of phenanthroline-based COFs have been recently reported and will be discussed below.[76, 89]

In this section of the review we will focus mainly on COFs that incorporate metal species in a post-synthetic step. In this regard, the types of COFs containing ligands that are used for the incorporation of metals can be grouped in the following different types: (i) COFs in which the ligands are the linkers formed in the polymerization reaction, (ii) COFs in which the ligands are constituted by the newly formed linkers and other substituents present in the monomers and (iii) COFs in which the ligands are already part of the structure of the monomers used in the synthesis of COFs. In Fig. 3 are depicted the main types of ligands present in COFs which include tetradentated, tridentated, bidentated and monodentated ligands.

The first type of COFs that incorporate metal species in a post-synthetic step are those in which the ligands are the linkers formed in the polymerization reaction. Linker metalation is an effective approach to create catalytically active centers in crystalline frameworks. The most representative examples correspond to COFs with imine linkages (Fig. 3). Imines are ubiquitous as ligands for transition metals, forming σ dative bonds by donation of the lone pair of the nitrogen atom. In fact, Schiff bases are able to stabilize many different metals in various oxidation states, controlling the performance of metals in a large variety of useful catalytic transformations.[90] Thus, COFs based on imine moieties have efficiently immobilized Pd^{II}, Fe^{II}, Co^{II} and Ni^{II}. Among them, the most investigated derivatives are those with immobilized Pd^{II}, which have been successfully used as catalysts for the Suzuki-Miyaura coupling,[61] for the hydrogenation of nitrobenzene to aniline[83] and for cross

coupling reactions between silanes and aryl halides.[82] It is worth mentioning that the Pd ions are located in between adjacent layers of the COFs and efficiently coordinated with two nitrogen atoms from different layers. This type of coordination is very effective in COFs exhibiting an eclipsed layered-sheet arrangement with interlaminar distances allowing an efficient π-π stacking.

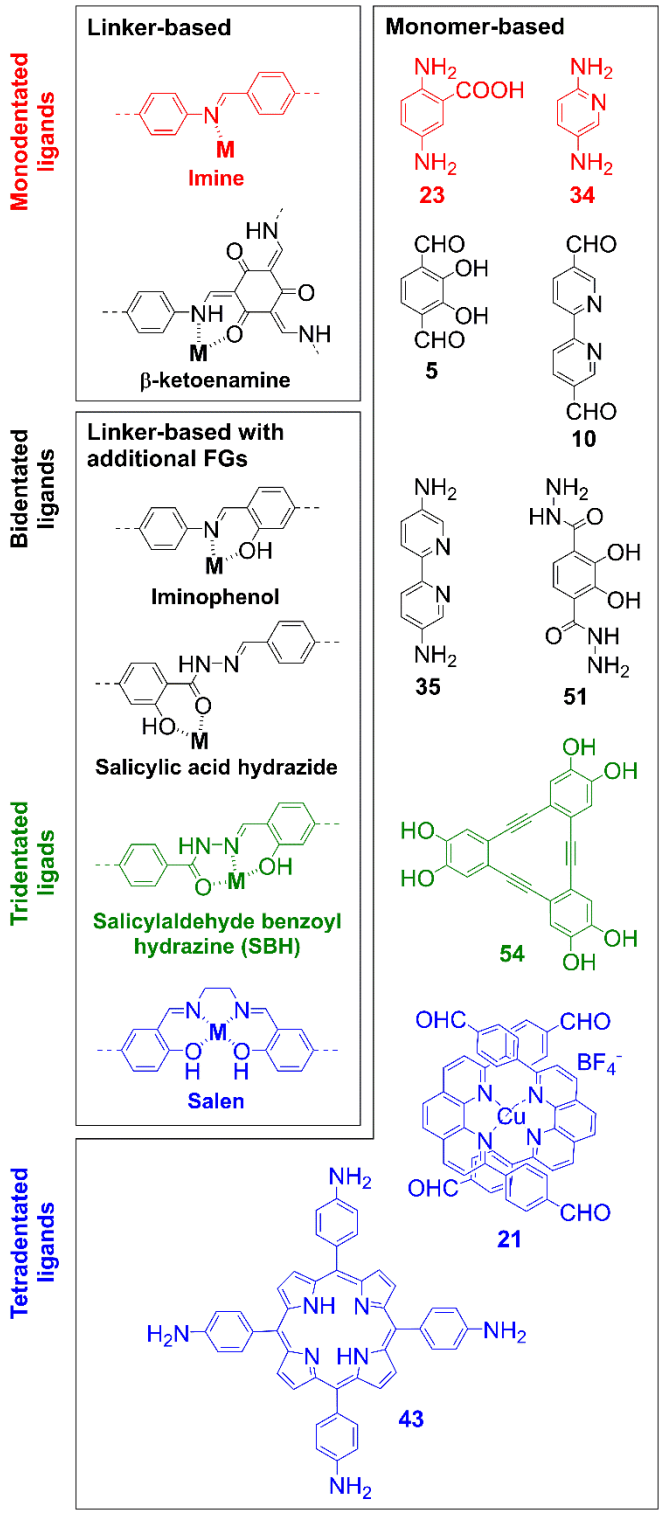

Fig. 3 Ligands used for the post-synthetic metalation of COFs.

The second type of COFs that incorporate metal species in a post-synthetic step are those in which the ligands are constituted by the newly formed linkers and other substituents present in the monomers. Representative examples of this type of COFs are those containing bidentated iminophenol (Fig. 3), β-ketoenamine (Fig. 3) or salicylic acid hydrazide (Fig. 3) units as well as those bearing tetradentated *N*,*N*′-bis(salicylidene)-ethylenediamine (Salen) (Fig. 3), and salicylaldehyde benzoyl hydrazone (SBH) groups (Fig. 3).

Iminophenol ligands can be generated by using suitably functionalized *o*-hydroxybenzaldehyde monomers. Thus, these imine-based COFs with hydroxyl groups allow the incorporation of copper ions into the pores of the eclipsed structure *via* the coordination interaction with hydroxyl groups and imine linkers.[77] In the context of these imine-based COFs with hydroxyl groups, when monomers containing salicylaldehyde moieties are combined with suitable diamines a particular chelating Schiff base is produced. The so-called Salen ligands (Fig. 3), with four coordinating sites and two axial sites open to ancillary ligands, are very much like porphyrins, but more easily prepared.[90]

Similarly to the other imine-based COFs, these COFs based on Salen ligands exhibit excellent thermal stability with no degradation below 350 °C. In addition, the crystalline structure of Salen-COFs is preserved in aqueous solutions at pH = 1-13.[66] For comparison purposes, it is worth pointing out that the above mentioned imine-based COFs used to immobilize Pd^{II} species do not survive in aqueous solutions at pH = 1. These COFs can be efficiently metalated with different metal ions including Co^{II}, Cu^{II}, Ni^{II}, Zn^{II} and Mn^{II}. Those COFs metalated with Co^{II} exhibited activity in the Henry reaction.

Other COFs based on ligands constituted by the newly formed linkers and other substituents present in the monomers are those based on β-ketoenamine (Fig. 3). These COFs can be obtained by reaction between 1,3,5-triformylphloroglucinol (**14**, Fig. 2) and different diamines to yield COFs with β-ketoenamine functionalities. The tautomerism exhibited by these functionalities provides exceptional stability to the networks. Concerning with the metalation, the enaminone group connected by a carbon-carbon double bond and an *N*-substituted amine allows them to act as bidentated ligands for metal ions such as Cu^{II}. By copper complexation with homochiral COFs bearing the β-ketoenamine moiety, it is possible to develop materials which can be used as heterogeneous catalysts for the asymmetric Henry reaction.[78] Ti^{IV} can be also immobilized in COFs bearing β-ketoenamine ligands. In this case, the Ti^{IV} ions are located in between adjacent layers of the COF and efficiently tetracoordinated with two β-ketoenamine groups from different layers.[63]

Reaction between 1,3,5-triformylphloroglucinol (**14**, Fig. 2) and terephthalohydrazide (**51**, Fig. 2) yields the corresponding salicylaldehyde benzoyl hydrazine (SBH) ligand (Fig. 3). These ligands can efficiently order molybdenum sites into the channel

walls of COFs through robust coordination involving the two oxygen atoms and the enamine nitrogen atoms of the SBH ligand. However, the thermal stability of these metalated COFs is slightly lower than those observed for the above mentioned metalated COFs and they start to decompose at around 260 °C. This behavior can be attributed to the destruction of the hydrogen bonding located in the 2D framework.[79]

By using a similar reaction between 1,3,5-triformylphloroglucinol (**14**, Fig. 2) with a terephthalohydrazide bearing hydroxyl functionalities (**50**, **51**, Fig. 2) it is possible to obtain COFs bearing salicylic acid hydrazide ligands (Fig. 3), which can efficiently immobilize Co^{II} ions via coordination with the two oxygen atoms of the salicylic acid hydrazide.[73] This metalated COF exhibits Lewis acid catalytic activity towards the cyanosilylation of aldehydes.

The third type of COFs that incorporate metal species in a post-synthetic step are those that contain ligands which are already part of the structure of the monomers used in the synthesis of the COFs. This type of COFs involves those based on monomers containing tetradentated porphyrin (**43**, Figs. 2, 3),[91] tridentated dehydrobenzoannulene (**54**, Figs. 2, 3),[92] bidentated catechol (**5**, **51**, Figs. 2, 3)[93] and monodentated pyridine (**34**, Figs. 2, 3),[94] as well as other polypyridine systems including the bidentated bipyridine (**10**, **35**, Figs. 2, 3).[95]

Porphyrins are the most widely studied macrocyclic compounds because of their several important roles in nature as well as their special coordinative, spectral and redox features. In fact, the cavity of porphyrins containing four pyrrolic nitrogens is ideally suited for binding the vast majority of metal ions of the periodic table.[96, 97] In spite of it, the amount of metal ions used for the metalation of porphyrin-based COFs is still very limited. Thus, Fe-porphyrin-based COFs exhibit a peroxidase-like activity in the presence of hydrogen peroxide and have been used to catalyze the oxidation of highly ordered pyrolytic graphite (HOPG).[67] Additionally, they also catalyze the oxidation of chromogenic substrates to produce color.[68] On the other hand, COFs composed of rhenium-bipyridine and iron- or cobalt-metalated porphyrins have been used as heterobimetallic frameworks in the electrocatalytic reduction of CO_2.[70] In this last contribution, the synthesis of the complexated COFs by using an already metalated porphyrin as monomer is also attempted. The reaction does not proceed and therefore the post-synthetic metalation was the only feasible alternative to obtain the metalated-porphyrin COF.

Dehydrobenzoannulene derivatives (DBAs) are planar triangular shaped macrocycles capable of forming strong metal complexes with Li,[98] Ca,[99] and low oxidation state transition metals.[100] The planarity and metal binding properties of DBAs are comparable to porphyrin ligands, which typically use hard nitrogen atoms to bind metals. In contrast, DBAs are neutral compounds that contain soft ligands capable of donating 2–4 electrons per alkyne depending on the electronic demands of the metals.[92] Concerning with DBA-based COFs, they have been used to complex Ni(0) and the metalated COF has been successfully used for the uptake of ethane and ethylene gas.

Catechol moieties are interesting functionalities given that Group 5 elements, especially vanadium and other high-valent transition-metal ions such as molybdenum, are well known to form a range of complexes with bidentate O,O-donors.[93] Thus, COFs complexated with vanadium have been used as catalyst for the Prins reaction and sulfide oxidation.

The most versatile COFs in order to be used for metalation reactions have been imine-based COFs containing 2,2'-bipyridine (bpy) moieties. 2,2'-Bipyridine is a neutral, bidentated, chelating heterocyclic ligand which forms charged complexes with metal cations, and this property has been exploited in the design and synthesis of a variety of metal-bipyridine complexes.[101] Thus, 2,2'-bipyridine and its C-substituted derivatives are probably the most commonly used bidentate nitrogen-donor ligands in coordination chemistry because of their ability to form metal complexes with almost all metals in the periodic table including many main-group metal ions, lanthanoid ions, actinoid ions, and transition-metal ions.[95] Concerning with bpy-based COFs, Co^{II} ions have been successfully immobilized into 2,2'-bipyridyl-derived COFs and further used as efficient oxygen evolution reaction (OER) catalysts.[71] On the other hand, a 2,2'-bipyridyl-derived COF has been efficiently used to form the corresponding iridium complex, which can heterogeneously catalyze the C–H borylation of arenes.[87] Furthermore, the strong interaction between Cu species and bipyridine has been also used to prepare copper complexes of 2,2'-bipyridyl-derived COFs, which have been used to catalyze the cycloaddition reaction of CO_2 with epoxides.[75] Specially interesting are those imine-based bpy-COFs used as bimetallic docks with catalytic activity in tandem reactions. Thus, Mn/Pd bimetallic docked 2D COFs can be prepared through a programmed synthetic procedure that involves first selective Mn coordination with the bipyridine ligands, followed by Pd coordination with the imine moieties. This bimetallic docked material can be efficiently used as heterogeneous catalyst in a Heck-epoxidation tandem reaction.[72] By using a similar two-step complexation strategy, a Rh/Pd bimetallic docked 2D COF has been prepared and used as heterogeneous catalyst in one-pot addition-oxidation cascade reactions.[80]

To sum up, the broad potential scope as heterogeneous catalysts of COFs post-synthetically modified through metalation can be realized by taking into account the variety of reactions that have been already catalyzed by this family of COF derivatives and which include (Table 1): (i) cross-coupling reactions such as the Suzuki-Miyaura, Heck or the cross-coupling reaction between silane and aryl aldehydes; (ii) addition reactions such as the cyanosilylation of aldehydes, the addition of phenylboronic acids to aldehydes, the Henry reaction or the epoxidation of alkenes; (iii) reduction reactions including the reduction of CO_2 to CO or the hydrogenation of nitrobenzene to aniline; (iv) oxidation reactions such as the

selective oxidation of alkenes or the oxidation of diphenylmethanol to benzophenone; (v) cyclization reactions like the cycloaddition of epoxides with CO_2 to form cyclic carbonates or the Prins-type cyclization which is used to synthesize nopol, an important bicyclic primary alcohol used in the agrochemical industry to form pesticides, perfumes, detergents, etc.; and (vi) one-pot cascade reactions including addition-oxidation, Heck-epoxidation or oxidation-Knoevenagel.

Table 1 Post-synthetic metalation of COFs and their potential applications.

Metal	COF	Monomers	Application	Ref.
Ca	$[CaOOC]_{17}$-COF	14+22+23	Ammonia uptake	62
Ti	TpPa-2-Ti^{4+}	14+22	Phosphopeptide enrichment	63
V	VO@Py-2,3-DHPh COF	5+47	----------	64
	VO-TAPT-2,3-DHTA-COF	5+42	Catalyst for Prins reaction and sulfide oxidation	65
Mn	Mn/Salen-COF	15+38	----------	66
	Mn@Bpy-COF	10+47	Catalyst in the epoxidation of trans-stilbene	72
	$[MnOOC]_{17}$-COF	14+22+23	Ammonia uptake	62
Fe	Fe-DhaTph-COF	5+43	Catalyst for the synthesis of holey graphene by HOPG oxidation	67
	Fe-COF	1+43	Peroxidase-like activity and colorimetric assay for the detection of glucose	68
	RT-COF-1-Fe	13+41	Electrodes in supercacitors[a]	69
Co	Co-COF-TpBpy	14+35	Electrocatalyst for oxygen evolution reaction	71
	NUS-50-Co	14+50	Catalyst for the cyanosilylation of aldehydes	73
	NUS-51-Co	14+51	Catalyst for the cyanosilylation of aldehydes	73
	RT-COF-1-Co	13+41	Electrodes in supercacitors[a]	69
	Co/Salen-COF	15+38	Catalyst for the Henry reaction	66
Ni	Ni-DBA-3D-COF	54+65	Ethane and ethylene uptake	74
	RT-COF-1-Ni	13+41	Electrodes in supercacitors[a]	69
	Ni/Salen-COF	15+38	----------	66
Cu	Cu-COF	3+42	Catalyst for the selective oxidation of alkenes	77
	PPS@COF-TpBpy-Cu	14+35	Catalyst in the cycloaddition of epoxides with CO_2 to form cyclic carbonates	75
	CCOF-TpTab-Cu	14+41	Catalyst for the asymmetric Henry reaction of nitroalkanes with aldehydes	78
	demetaled COF-505	21+28	Mechanical properties	76
	demetaled COF-500	21+46	Mechanical properties	89
	Cu/Salen-COF	15+38	----------	66
Zn	Zn/Salen-COF	15+38	----------	66
Sr	$[SrOC]_{17}$-COF	14+22+23	Ammonia uptake	62
Mo	Mo-COF	14+49	Catalyst for the epoxidation of cyclohexene	79
Rh	Rh@Bpy-COF	10+47	Catalyst in the addition of phenylboronic acid to benzaldehyde to produce diphenyl-methanol	80
Pd	Pd/COF-LZU-1	13+22	Catalyst for Suzuki-Miyaura coupling	61
	Pd/COF-LZU-1	13+22	Catalyst for the hydrogenation of nitrobenzene to aniline[a]	83
	Pd/MOF@COF	13+22	Photocatalyst for tandem dehydrogenation and hydrogenations reactions	84
	Pd/H_2P-Bph-COF	2+43	Catalyst for Suzuki coupling between bromoarenes and arylboronic acids	81
	Pd/COF-SDU1	17+22	Cross coupling between silanes and aryl halides	82
	$Pd(OAc)_2$-TpPa-H	14+22	Catalyst for Suzuki-Miyaura coupling	173
	Pd/COF-TpPa-Py	14+34	Catalyst in cascade oxidation-Knoevenagel condensation	85
	Pd@Bpy-COF	10+47	Catalyst in the oxidation of diphenylmethanol to benzophenone	80
	Pd@Bpy-COF	10+47	Catalyst in the Heck reaction between iodobenzene and styrene	72
Re	Re-COF	10+42	Photocatalyst to reduce CO_2 to CO	86
Ir	Ir-4-R	10+41	Catalyst in the C-H borylation of arenes	87
Pd and Rh	Rh/Pd@Bpy-COF	10+47	Catalyst in one-pot addition-oxidation cascade reaction	80
Pd and Mn	Mn/Pd@Bpy-COF	10+47	Catalyst in Heck-epoxidation tandem reaction	72
Fe and Co	Fe,Co-COF	14+35	Electrocatalyst for ORR, OER and HER[a]	108
Re and Co	COF-Re_Co	11+43	Catalyst for the reduction of CO_2 to CO	70
Re and Fe	COR-Re_Fe	11+43	Catalyst for the reduction of CO_2 to CO	70

[a]Application described for the calcinated COF.

The precise location of the ligands on porous crystalline COFs allows for high and homogeneous loading of metal ions. Although incorporation of preformed ligands (such as porphyrins) can be used to synthesize COFs which can be further modified through the post-synthetic approach, one limitation of this strategy is the relatively difficult access to this type of monomers. In addition, monomers not only must have suitable receptors but also orthogonal functionalities to those necessary for the COF formation, and the required geometry to synthesize COFs with appropriate topology and pore size. In this respect, the possibility to generate COFs in which the ligands are the linkers formed in the polymerization reaction are much more versatile. This strategy enables the use of a variety of monomers with different size and shape in order to generate COF derivatives endowed with ligands in which the topology of the COF as well as the pore size and shape can be finely tuned.

In the following sections we will classify the different types of COFs post-synthetically modified through metalation based on the variety of ligands used for the complexation. We will comment on the preservation or not of the COFs' crystallinity after the complexation. For comparison purposes, the metal ion content and the stability of the metal-containing COFs will be included when they are specified in the original articles. Furthermore, the applicability of these metalated COFs will be reviewed and the reusability in catalytic applications will be also included.

3.1. COF-Metals based on COFs with imine linkages

Concerning with the different families of covalent organic frameworks it is worth pointing out that the imine-type (Schiff base) ligands are versatile groups for incorporating a variety of active metal species as it has been well demonstrated in coordination chemistry.[10, 102] This initial premise was the incentive to use imine-linked COFs as macromolecular ligands for the incorporation of metal ions.

Thus, in 2011 Wang and co-workers showed that the imine-linked **COF-LZU1** (Scheme 1), that presents a two-dimensional eclipsed layered-sheet structure, was able to incorporate stabilized metal ions.[61] Through a simple post-treatment of **COF-LZU1** by solution-impregnation with palladium acetate, a Pd^{II}-containing **COF-LZU1** material, **Pd/COF-LZU1**, can be prepared. The eclipsed layered-sheet arrangement of **COF-LZU1** offered a robust scaffold for $Pd(OAc)_2$ incorporation and the distance (~3.7 Å) of eclipsed nitrogen atoms in adjacent layers fell into the ideal requirement for strong coordination of $Pd(OAc)_2$. The crystal structure of **COF-LZU1** is well preserved after the treatment with palladium acetate as demonstrated by the comparison of the powder X-ray diffraction (PXRD) patterns of **COF-LZU1** and **Pd/COF-LZU1**. Interestingly, X-ray photoelectron spectroscopy (XPS) measurements were carried out to further investigate the incorporation of palladium within **COF-LZU1**. Thus, it was observed that the Pd^{II} species in **Pd/COF-LZU1** shifted negatively by 0.7 eV in comparison with that of 338.4 eV for free $Pd(OAc)_2$. This negative shift can be rationalized in terms of a strong coordination of $Pd(OAc)_2$ with the imine groups of **COF-LZU1** by which the imine groups further donate electrons to Pd^{II}, making the Pd species less electron-deficient. In addition to the robust incorporation of $Pd(OAc)_2$, **Pd/COF-LZU1** exhibits regular channels with a diameter of ~1.8 nm which provides fast diffusion and efficient easy access to the active sites of even bulky molecules. Because of this, the catalytic activity of **Pd/COF-LZU1** was examined in one of the representative Pd-catalyzed reactions, i.e., the Suzuki-Miyaura coupling reaction, showing excellent catalytic activity (yields of 96–98%), high stability and easy recyclability.

In 2016, Li and co-workers used a similar impregnation method for the post-treatment of **COF-LZU1** with palladium acetate. In this case, the **Pd/COF-LZU1** material was further annealed at 500 °C. During the annealing process under an inert atmosphere, Pd cations are reduced to form Pd nanoparticles which are encapsulated in the shell of the nitrogen doped hollow carbon material. The carbonized products show a similar morphology compared to the precursor. The catalytic efficiencies of the as-synthesized nanohybrid materials were evaluated using the hydrogenation of nitrobenzene to aniline as a model reaction showing unprecedented catalytic performances, in terms of activity and selectivity, which are superior to conventional Pd nanoparticles supported on N doped carbon and commercial carbon materials. The highly dispersed Pd nanoparticles and the uniform distribution of N dopants are responsible for the excellent catalytic properties obtained.[83]

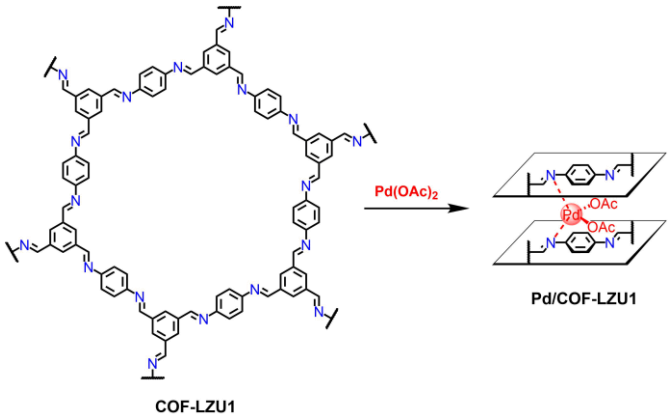

Scheme 1 Schematic representation for the synthesis of **Pd/COF-LZU1** materials.

In 2018 Kim and co-workers have reported the production of metal doped hybrid MOFs@COFs based also on **COF-LZU1** and an $-NH_2$ containing metal organic framework (MOF) (Fig. 4). The $-NH_2$ containing MOF was used for the direct interfacial growing of the COF shell without any extra functionalization step. The subsequent treatment of the **MOF@COF** hybrid with $Pd(OAc)_2$ by using the impregnation method mentioned above allows the incorporation of Pd^{II} into the **MOF@COF** hybrid. The XPS analysis of the spectrum of **Pd^{2+}/MOF@COF** confirms the strong coordination of Pd^{II} with the imine groups of the LZU1 shell,

comparable with that of **Pd^{2+}/COF-LZU1** in the previous report. The **Pd^{2+}/MOF@COF** material shows excellent photocatalytic performance for tandem dehydrogenation and hydrogenation reactions in a continuous-flow microreactor as well as in a batch system. The excellent performance of this system is due to the synergy that exists among the three components with the metal elucidated to be the active center, the MOF core as an electron donor, and the COF shell as a mediator for electron transfer.[84]

Not only **COF-LZU1** has been used for the immobilization of Pd. Following also a post-treatment with palladium acetate, Jiang and co-workers immobilize Pd into porphyrin containing imine-based COFs and used them also as catalysts in Suzuki-coupling reactions.[81] The abundant and periodically distributed N atoms from both the central porphyrin moiety and the C=N bonds in the COF are able to stabilize and uniformly disperse the Pd ions inside the COF structure. XPS analysis confirms the strong coordination of $Pd(OAc)_2$ with the imine groups. The Suzuki-coupling reaction between bromoarenes and arylboronic acids was efficiently catalyzed under mild condition with high yields of 97.1-98.5%.

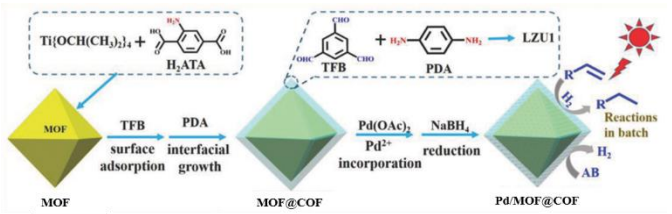

Fig. 4 Schematic scope of the preparation of Pd doped MOF@COF core–shell. Figure extracted from ref. 82. Reproduced with permission from Wiley-VCH.

Also, a triazine containing imine-based COF with two-dimensional eclipsed layer-sheet structure and nitrogen-rich content was used to immobilize $Pd(OAc)_2$ by a similar solution-infiltration method. The catalytic activity of this COF toward one-pot silicon-based cross-coupling reaction of silanes and aryl halides was accessed.[82]

Fe^{III}, Co^{II} and Ni^{II} have been also immobilized in imine-based COFs. A yellow gel of the so-called **RT-COF-1** can be obtained by the direct reaction between a 1:1 molar ratio of 1,3,5-tris(4-aminophenyl)benzene (**41**, Fig. 2) and 1,3,5-benzenetricarbaldehyde (**13**, Fig. 2) in *m*-cresol at room temperature.[103] The subsequent treatment of the material with a methanol solution of $M(acac)_n$ (M = Fe^{III}, Co^{II}, Ni^{II}; acac = acetylacetonate) under vigorous stirring for 24 h at 25 °C produces the incorporation of the metal ions into the **RT-COF-1** structure (Scheme 2). The metal ion content was evaluated by total reflection X-ray fluorescence (TXRF) showing that Fe^{III} is incorporated in a 1 : 280 Fe : N atomic ratio. For Co^{II} the atomic ratio is similar (1 : 190 Co : N), while Ni^{II} is incorporated in a smaller ratio (1 : 760 Ni : N). It is worth mentioning that these values are significantly smaller than that observed in **Pd/COFLZU1** (Scheme 1) in which the Pd content as determined by ICP analysis, corresponds to ~0.5 Pd atom per unit cell.[61] Nevertheless, a dramatic quenching of the characteristic fluorescence of **RT-COF-1** was observed after metal incorporation due to metal-to-ligand charge transfer (MLCT), thus indicating metal ion incorporation into the **RT-COF-1** structure rather than physisorption. Synchrotron radiation grazing incidence X-ray diffraction (GIXRD) data of the iron-containing COF show a general broadening of the peaks indicating a partial amorphization of the initial structure which is associated to a layer-to-layer separation. The incorporation of Co^{II} and Ni^{II} causes an even more pronounced effect with a complete loss of structural order. This behavior contrasts with that observed in **Pd/COF-LZU1** (Scheme 1) for which the crystal structure is well preserved after the treatment with palladium acetate.[61]

Subsequent controlled thermal treatment of the **RT-COF-1-Metal** hybrids carried out in a tubular oven at 900 °C under a nitrogen atmosphere favors corrugated N-doped graphenes formation which can be efficiently used as electrode materials in supercapacitors.[69]

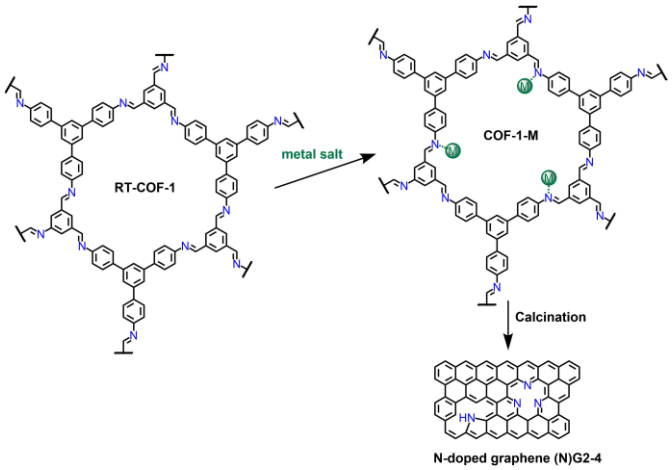

Scheme 2 General scheme of the work showing the **RT-COF-1** and **RT-COF-1-Metal** structures, as well as the calcination process to produce N-doped graphenes.

3.2. COF-Metals based on imine-based COFs with additional functionalities

3.2.1. Hydroxyl groups

Additional functionalities such as hydroxyl groups have been incorporated in imine-based COFs in order to favor the metalation process. Thus, Chen and co-workers immobilize Cu^{II} in an ordered 2D-COF containing imine linkages as well as hydroxyl units.[77] By simple post-treatment of the COF with copper acetate, copper ions are efficiently incorporated into the pores of the COF *via* the coordination interaction with hydroxyl groups and imine linkers. Interestingly, XPS analysis shows that when the synthesis of the COF is carried out in a mixture of *o*-dichlorobenzene, *n*-butanol and acetic acid, the COF obtained coordinates with Cu^{II} ions through the imine linkages and the hydroxyl groups (Scheme 3). On the other hand, the XPS analysis shows also that when the synthesis of the COF is carried out in DMF, Cu^{II} ions only coordinate with oxygen to form metal complexes. The different behavior is due to the fact that the COF obtained in dimethylformamide is more disordered than the analogue obtained in a mixture of *o*-dichlorobenzene,

n-butanol and acetic acid. PXRD analysis for the COFs with immobilized Cu suggested that framework integrity is maintained but the crystallinity of **Cu-COF** is relative lower compared to that of the COFs prior to Cu immobilization. This behavior is similar to that previously observed for the imine-based COFs with immobilized Fe.

These copper-containing COFs were explored as heterogeneous catalyst for the selective oxidation of alkenes showing catalytic performances above 75% conversion for a variety of alkenes. Interestingly, the material can be easily recovered from the reaction mixture by centrifugation and reused three times without significant loss of catalytic activity, which confirms that copper is robustly immobilized onto the COF resulting in a reusability and stability of these copper-containing COFs similar to that previously mentioned for imine-based COFs with immobilized Pd.

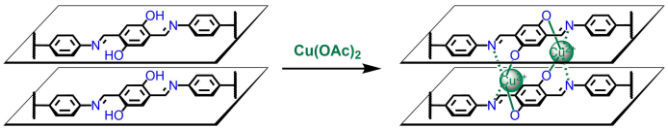

Scheme 3 Schematic representation of the coordination of Cu^{II} with the hydroxyl groups and imine linkages of consecutives sheets of the COF.

One interesting type of hydroxyl groups-containing imine-based COFs are those based on the *N*,*N*′-bis(salicylidene)ethylenediamine (Salen) unit, that represents one of the most important ligands in coordination chemistry.[104] However, one limitation of Salen-based small molecules is their lack of stability under acidic conditions, which prevents their separation by flash chromatography from reaction mixtures when they are used as homogenous catalysts. Accordingly, a great deal of effort has been dedicated to the construction of Salen-based materials *via* immobilization.[105] Thus, in 2017, Ding, Wang and co-workers have reported the one-step construction of a Salen-based porous COF (**Salen-COF**, Scheme 4) through imine-bond formation by direct co-condensation reaction between ethylene diamine (**38**, Fig. 2) and 1,3,5-tris[(5-*tert*-butyl-3-formyl-4-hydroxyphenyl)ethynyl]benzene (**15**, Fig. 2), a salicylaldehyde-based C3-geometric monomer (Scheme 4).[66] The obtained **Salen-COF** material possesses high crystallinity and excellent stability. Thus, the crystalline structure of **Salen-COF** was preserved in aqueous solutions at pH = 1–13 while other imine-based COFs, such as **COF-LZU1** (Scheme 1), could not survive in aqueous solution at pH = 1. A series of metallo-Salen-based COFs were prepared *via* metalation by treatment of a methanolic dispersion of **Salen-COF** with methanol solutions of metal salts including $Co(OAc)_2$, $Cu(OAc)_2$, $Ni(OAc)_2$, $Zn(OAc)_2$ and $Mn(OAc)_2$. ICP analysis on the resulting metallo-Salen-based COFs (denoted as M/Salen-COF) showed that most of the Salen pockets are occupied by the metal ions. This represent a high degree of metalation in comparison with the above mentioned metalation of imine moieties in imine-based COFs, in which the metal content was lower than 0.5 atoms per unit cell. The unchanged PXRD patterns of the metallo-Salen-based COFs verified that the crystalline structure of **Salen-COF** was preserved after metalation. The chemical stability of **Co/Salen-COF** was also tested and its crystalline structure was maintained in aqueous solutions at pH = 2-13.

As a proof of concept, catalytic activity of **Co/Salen-COF** in the Henry reaction was demonstrated. The metallo-Salen-COF can be separated by centrifugation for the recycle use and the catalytic activity and the crystalline structure remained after four recycles.

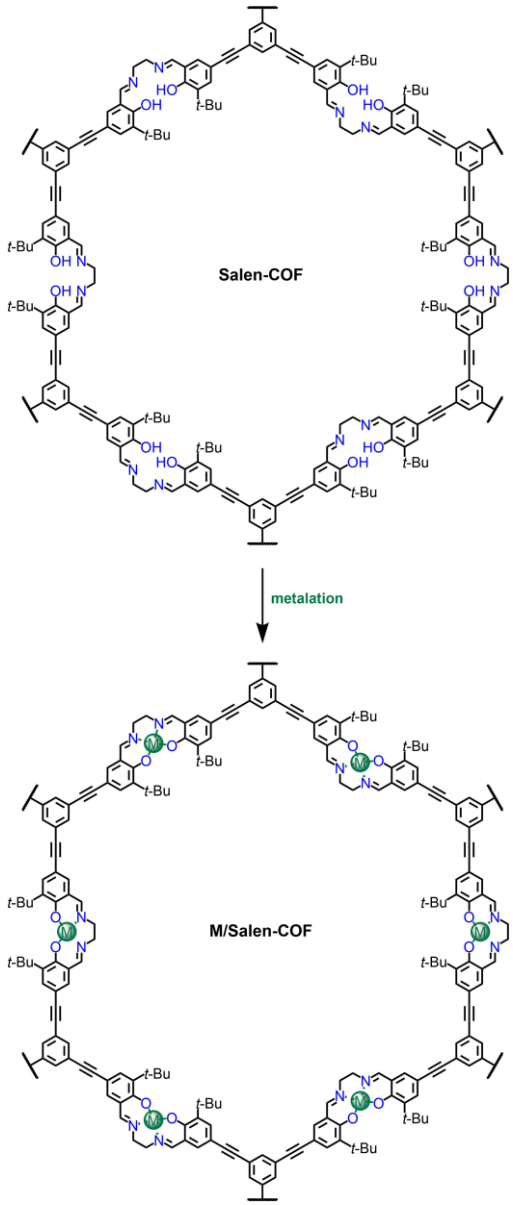

Scheme 4 Metalation of a Sale-based COF to afford a series of metallo-Salen-based COFs (M = Co, Cu, Ni, Zn and Mn).

Other hydroxyl groups-containing imine-based COFs used for post-functionalization are those containing catechol moieties.[64] Catechol moieties are interesting functionalities given that Group 5 elements, especially vanadium and other high-valent transition-metal ions such as molybdenum, are well known to form a range of complexes with bidentated O,O-donors.[93] Thus,

catechol-containing COFs can be efficiently metalated with vanadium(IV)-oxy acetylacetonate [$VO(acac)_2$]. Similarly to the metalation of other hydroxyl groups-containing imine-based COFs the crystallinity is maintained in the metalated COF as demonstrated by the PXRD patterns. In contrast to the above COFs, the level of metalation is not reported in the study. However, energy dispersive X-ray spectroscopy (EDX) *via* SEM showed the presence and even distribution of all the elements (C, N, O, V) in the modified framework, thereby implying a uniform post-synthetic modification. The UV-vis absorption band of the COF was broadened to longer wavelengths after metalation due to the coordination of V=O to the catechol units of the COF. The material is stable in a variety of solvents and thermally stable up to 400 °C. The good catalytic characteristics of the V=O sites[106] together with the thermal and solvent stability of this COF pave the way for its use as heterogeneous catalyst. In fact, in 2019 it has been reported the synthesis of a COF decorated with vanadium as catalyst for Prins reaction and sulfide oxidation.[65]

3.2.2. Bipyridine moieties

Recently, the field of heterogeneous catalysis has turned its attention to the study of bimetallic catalysts because they offer the potential of increased activity and selectivity combined with enhanced stability as compared to their monometallic counterparts. However, it is unlikely that the use of only one type of nitrogen ligand could be satisfactory to allow for differential bimetallic docking.[107] With this aim, in 2016 Gao and co-workers carried out the synthesis of a 2D-COF containing bipyridine groups and imine linkages to allow for controllable bimetallic binding.[72, 80] Reaction between 4,4',4'',4'''-(pyrene-1,3,6,8-tetrayl)tetraaniline (**47**, Fig. 2) and bipyridine 2,2-bipyridyl-5,5-dialdehyde (**10**, Figs. 2, 3) allows for the synthesis of **BPy-COF** containing both imine linkages and bipyridine moieties (Scheme 5).

When monometallic $Pd(OAc)_2$ was first loaded into the **BPy-COF** by using the simple solution-infiltration method mentioned above, the corresponding **Pd^{II}@BPy-COF** can be obtained. XPS analysis shows that the $Pd(OAc)_2$ molecules coordinate to the imine groups that are located between adjacent COF sheets as well as with the bipyridine groups (Scheme 5, Route 1). On the other hand, to realize the bimetallic loading, a programmed synthetic procedure was used (Scheme 5, Route 2). Rh(COD)Cl (7.4x6.6x5.3 Å) is bulky and more rigid than $Pd(OAc)_2$ (10.6x5.0x4.3 Å) but could still be readily immobilized by the bipyridine units. However, in contrast with $Pd(OAc)_2$ molecules, it is difficult for Rh(COD)Cl to enter the space between adjacent COFs sheets. Therefore, when the docking of Rh(COD)Cl was carried out first, the resulting sample named **Rh^{I}@BPy-COF** was obtained in which Rh-loading is produced *via* the coordination with the bipyridine units. After the subsequent loading of $Pd(OAc)_2$, the resulting hybrid named as **Rh^{I}/Pd^{II}@BPy-COF** was obtained with successful bimetallic loading.[80]

The Pd-loading content of the **Rh^{I}/Pd^{II}@BPy-COF** was determined to be close to that of an analogous bipyridine-free COF but much lower than that of the **Pd^{II}@BPy-COF**. These results further indicate that $Pd(OAc)_2$ molecules mainly occupy the imine sites in the space between adjacent COF layers as in the previously reported imine-based COFs with immobilized Pd atoms. Thus, the incorporation of bipyridine moieties in imine-based COFs is an efficient strategy in order to enhance Pd loading.

A similar bimetallic loading can be achieved by docking first with $MnCl_2$ followed by docking with $Pd(OAc)_2$ to yield the analogue **Mn^{II}/Pd^{II}@BPy-COF**.[72] The Pd-loading content of **Mn^{II}/Pd^{II}@BPy-COF** is similar to that observed in **Rh^{I}/Pd^{II}@BPy-COF**. In contrast the Mn content is only 0.8 wt % in **Mn^{II}/Pd^{II}@BPy-COF** while the Rh content in **Rh^{I}/Pd^{II}@BPy-COF** is of 7.9 wt %. It is also worth pointing out that the pre-loaded Mn and Rh are neither lost nor replaced by the subsequently loaded Pd.

The bimetallic **Rh^{I}/Pd^{II}@BPy-COF** and **Mn^{II}/Pd^{II}@BPy-COF** show excellent catalytic activity in tandem reactions. Thus, **Mn^{II}/Pd^{II}@BPy-COF** performs efficiently as catalyst in a Heck-epoxidation tandem reaction while **Rh^{I}/Pd^{II}@BPy-COF** catalyzes a one-pot addition-oxidation cascade reaction between diphenylboronic acid and benzaldehyde to yield first diphenylmethanol and then benzophenone. In order to elucidate the respective functions of Pd^{II} and Rh^{I} in the cascade reaction, COFs only loaded with Pd^{II} or Rh^{I} were investigated. It is observed that the monometallic **Pd^{II}@BPy-COF** does not catalyze the addition of phenylboronic acid to benzaldehyde. On the other hand, this COF exhibits an excellent catalytic activity in the oxidation of diphenylmethanol to benzophenone with a yield of 99%. Likewise, the monometallic **Rh^{II}@BPy-COF** does not catalyze the oxidation of diphenylmethanol to benzophenone, but exhibited a high catalytic activity in the addition of phenylboronic acid to benzaldehyde to produce diphenylmethanol. The results obtained in this study clearly indicate that Rh^{I} catalyzes the addition reaction and Pd^{II} catalyzes the oxidation reaction, as expected. This is a good example of how the incorporation of additional ligands in imine-based COFs acts efficiently in order to obtain bimetallic-docked COFs that catalyze tandem reactions.

Zhang, Huang and co-workers have recently reported an imine-based COF containing bipyridine units that can incorporate a Re moiety by using simple solution-infiltration method upon treatment with $Re(CO)_5Cl$ in toluene.[86] Similarly to Mn^{II} and Rh^{I}, the Re moiety is incorporated in the COF via reaction with the bipyridine ligand. The 2D-COF with incorporated Re complex exhibits intrinsic light absorption and charge separation (CS) properties. In addition, it can be used as heterogenous photocatalyst to efficiently reduce CO_2 to form CO under visible light illumination with high selectivity (98%) and better activity than a homogeneous Re counterpart. On the other hand, metalation of 2D imine-based bipyridine containing COFs with $[Ir(COD)(OMe)]_2$ has been also recently carried out.[87] Interestingly, a series of similar imine-based bipyridine containing 2D COFs with AA, AB, or ABC stacking are metalated

and the metalated COFs were tested as catalysts in the C–H borylation of arenes. In this particular case, the ABC packing in the COF divides the large hexagonal open channels into smaller triangular micropores with more suitable pore widths and therefore the COF with ABC packing exhibits much higher catalytic activity than the parent analogues with AA and AB stackings. This contribution provides a good evidence of how the control of layer stacking can be an efficient strategy in order to provide better accessibility to catalytic centers.

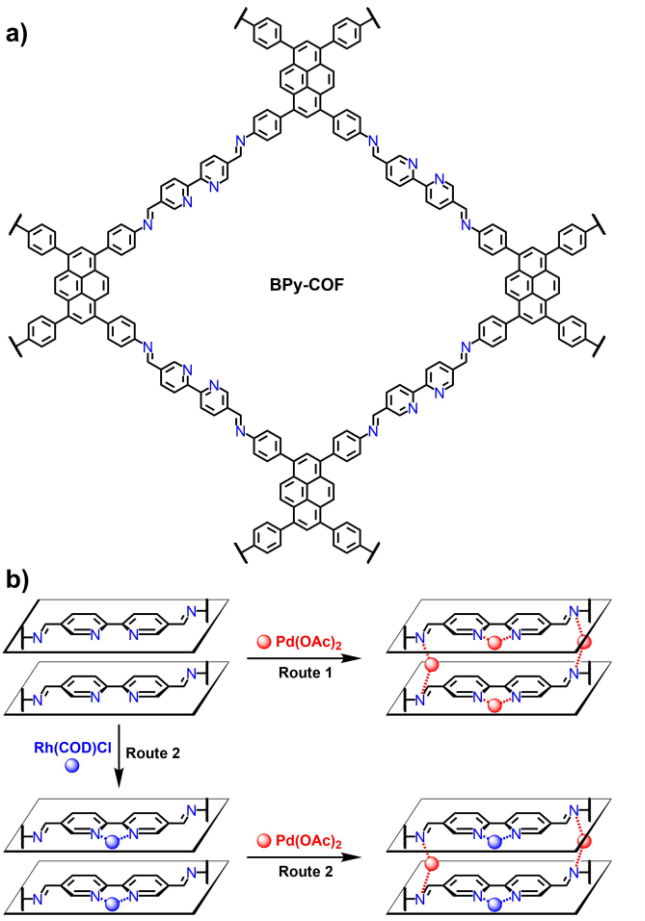

Scheme 5 (a) Schematic representation of **BPy-COF**. (b) Designed strategies for the monometallic (Route 1) and bimetallic docking (Route 2).

A cobalt modified COF containing bipyridine moieties has been prepared by Banerjee, Kurungot and co-workers from a COF (**COF-TpBpy**, Fig. 5) obtained by condensation between 1,3,5-triformylphloroglucinol (**14**, Fig. 2) and 5,5'-diamino-2,2'-bipyridine (**35**, Figs. 2, 3). The cobalt-modified COF (**Co-COF-TpBpy**) was prepared by solution-infiltration method by soaking a known amount of the COF in methanolic cobalt acetate solution. [71] Thermogravimetric analysis (TGA) of **Co-TpBpy** in air revealed ~12% cobalt content in the framework. XPS and local EDX analyses confirm the presence of cobalt. The FTIR spectrum suggests the coordination of Co ions to the bipyridinic N atoms in the COF framework. Nothing is mentioned about the possible coordination of Co with the imine moieties which was observed upon treatment of **RT-COF-1** with $Co(acac)_2$ (Scheme 2).[69] Furthermore, the incorporation of Co^{II} in **RT-COF-1** upon treatment with $Co(acac)_2$ causes a complete loss of structural order while the crystal structure is well preserved after treatment of **COF-TpBpy** with cobalt acetate solution. The behavior observed in the metalation of **COF-TpBpy** is indicative of the coordination of the Co moieties with the bipyridine and not with the imine sites in the space between adjacent COF layers.

On the other hand, the solid-state UV-vis spectra of **Co-COF-TpBpy** shows the characteristic band corresponding to the charge transfer transition, usually observed in Co^{II}-bipyridine complexes.[71] **Co-COF-TpBpy** has been used as electrocatalyst for the efficient oxygen evolution reaction (OER) showing an unusual catalytic stability which arises from the synergetic effect of the inherent porosity and presence of coordinating units in the COF skeleton.

COF-TpBpy (Fig. 5) has been also used to accommodate linear ionic polymers in close proximity to surface Lewis acid active sites based on Cu-bpy complexes in order to combine two reactive centers working in concert on a single material.[75] To accommodate the linear polymers in the COF channels, in situ radical polymerization of ionic monomers (PS, ethyldiphenyl(4-vinylphenyl)phosphonium bromide) in **COF-TpBpy** was performed, affording the product denoted as **PPS⊂COF-TpBpy**. The subsequent treatment of **PPS⊂COF-TpBpy** with $Cu(OAc)_2$ affords **PPS⊂COF-TpBpy-Cu**. XPS analysis confirms that strong interactions exist between the Cu species and the bipyridine moieties in **PPS⊂COF-TpBpy-Cu** (Fig. 5). Thus, bipyridine moieties are good alternatives to hydroxyl groups in COFs in order to form Cu complexes.

The movability of the catalytically active sites on the highly flexible PPS together with the great potential cooperation with the Lewis acid sites (Cu species) anchored on the COF walls make these composite catalysts excellent candidates in the cycloaddition of epoxides with CO_2 to form cyclic carbonates. Thus, the essential catalytic components enriched in the confined space are beneficial to boosting cooperation and promoting catalytic efficiency. In fact, the composite exhibited significantly improved catalytic efficiency compared to the individual catalytic components. Concerning with recyclability, **PPS⊂COF-TpBpy-Cu** can readily be recycled with negligible loss of its catalytic performance for at least ten cycles, thus highlighting its heterogeneous nature.

Very recently, **COF-TpBpy** has been simultaneously metalated with Fe^{II} and Co^{II} by treatment with metal acetate salts.[108] XPS analysis revealed the homogenous complexation of both metals with the bpy units, and the Fe^{II} and Co^{II} contents were calculated to be 1.65% and 1.06% respectively. The bimetallic **Fe,Co-COF** was carbonized at 900 °C under nitrogen affording metal nanoparticles uniformly distributed on the nitrogen doped carbon support. This material presented excellent electrochemical catalytic activity in the oxygen reduction reaction (ORR), oxygen evolution reaction (OER) and hydrogen evolution reaction (HER).

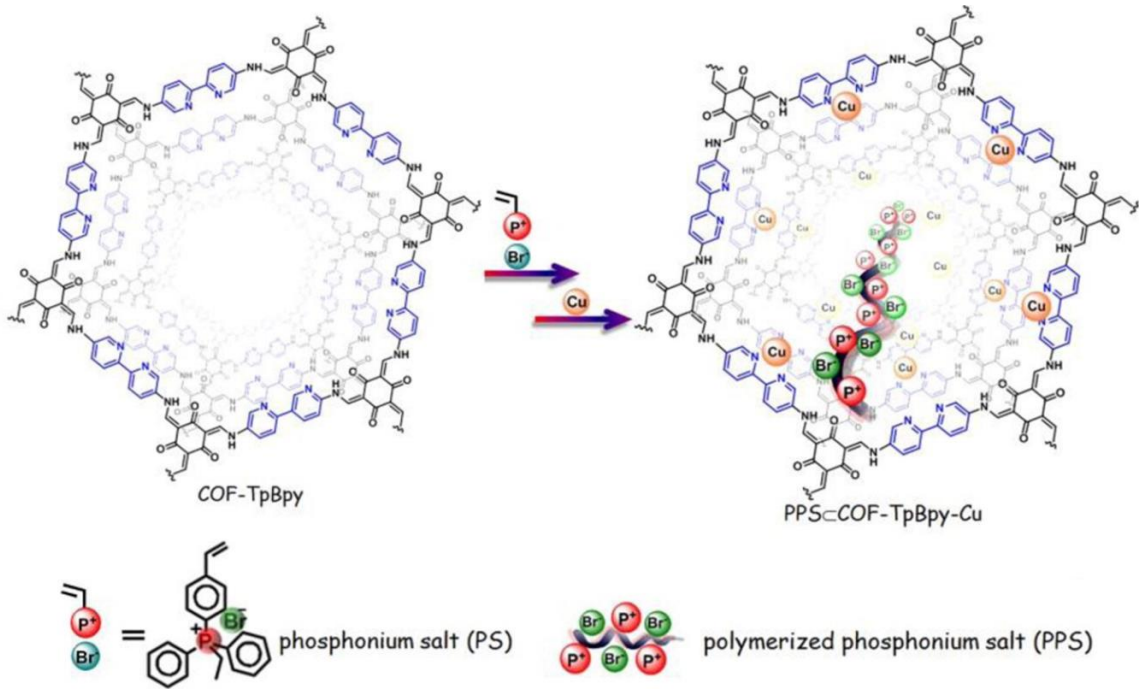

Fig. 5 Schematic representation for the synthesis of **PPS⊂COF-TpBpy-Cu** from **COF-TpBpy**. Adapted with permission from *J. Am. Chem. Soc.*, 2016, **138**, 15790-15796. Copyright 2016 American Chemical Society

3.2.3. Porphyrin moieties

Porphyrin is a component of hemoglobin which consists of abundant functionalized nitrogen groups and which can be metalated *via* pre- and post-metalation methods. Porphyrins are ideal building blocks for the development of functional COFs due to their planar geometry and rigidity coupled with inherent functionalities such as photosensitizing and redox-active properties. Thus, porphyrins-based COFs, which consist of π–π stacking of porphyrin units in adjacent layers, have already enabled the use of porphyrinic COFs in sensing,[109] energy harvesting[110] and storage,[111] photochemical,[112, 113] catalytic[81, 114-116] and electrocatalytic[117] applications. With this background in mind, porphyrin-based COFs have been recently synthesized also by post-synthetic strategies.

In 2017 Star and co-workers reported the synthesis of a bifunctional, metalated porphyrin-based COF (**Fe-DhaTph-COF**, Scheme 6) which serves as a surface catalyst and as master template for creating holes on graphite that can be subsequently exfoliated into multiple patterned graphene sheets.[67] **Fe-DhaTph-COF** can be synthesized by following two different strategies. The first one involves the preparation of iron(III)-tetrakis(4-aminophenyl)porphyrin chloride (**Fe-TAP-Cl**, Scheme 6) by metalation of 5,10,15,20-tetrakis(4-aminophenyl)porphyrin (**43**, Figs. 2, 3) upon treatment with iron(II) chloride tetrahydrate ($FeCl_2{\cdot}4H_2O$). To grow **Fe-DhaTph-COF** directly on graphite, condensation of **Fe-TAP-Cl** and 2,3-dihydroxybenzene-1,4-dicarbaldehyde (**5**, Figs. 2, 3) was performed in a flame-sealed pyrex tube in which several pieces of mechanically cleaved HOPG (0.5x0.5 mm) flakes were immersed in the reaction mixture before the flame seal. Alternatively, **Fe-DhaTph-COF** catalyst could be also prepared by complexation of Fe^{III} with already synthesized **DhaTph-COF** in a separate post-polymerization step. Then, a suspension of **DhaTph-COF** coordinated with Fe^{III} can be deposited on HOPG by either dip-coating or drop-casting. The fabricated few-layer graphene sheets exhibited holey structures after treatment with H_2O_2 or H_2O_2/NaOCl.

Marinescu and co-workers have recently reported the synthesis of a COF with two distinct metal sites (**COF-Re_Co** and **COF-Re_Fe**, Scheme 7) by post-synthetic modification of a COF with integrated rhenium bipyridine moieties and free porphyrin units (**COF-Re**) upon treatment with cobalt and iron chloride salts respectively.[70] PXRD analysis confirms the preservation of the ordered structure following post-metalation. It is worth pointing out that attempts to directly synthesize the metalloporphyrin-based COFs (**COF-Re_Co** and **COF-Re_Fe**) with metalated tetraaminoporphyrin monomers proved unsuccessful and therefore the post-synthetic modification strategy was employed, whereby the free-base porphyrins were successfully post-metalated with either cobalt or iron precursors. XPS spectra of **COF-Re_Co** and **COF-Re_Fe** show retention of the rhenium peaks as well as additional peaks corresponding to cobalt and iron which are consistent with reported Co and Fe porphyrin molecular species, thus indicating successful incorporation of two distinct metal centers in the COF. ICP analyses of the frameworks indicate that cobalt incorporation into **COF-Re_Co** is 53.4%, whereas the iron incorporation into **COF-Re_Fe** is 30.7%. For comparison purposes it is worth pointing that the loading content by post-metalation with $Co(OAc)_2$ of imine-based COFs bearing

bipyridine moieties is *ca.* 60%.[71] However, these loading contents contrast with other reported post-metalations of porphyrin-based frameworks which led to near-unity incorporation of metal ions.[118]

Given that these metal sites are well-known molecular catalysts for the reduction of CO_2 to CO, electrochemical studies were performed to determine the ability of the frameworks to reduce CO_2. It was found that **COF-Re_Co** had the highest activity towards CO_2 reduction, achieving a faradaic efficiency of 18%.

A COF synthesized from tetraaminoporphyrin (**43**, Figs. 2, 3) and terephthalaldehyde (**1**, Fig. 2) has been recently metalated by using an analogue post-synthetic strategy which involves solution-impregnation with $FeSO_4{\cdot}7H_2O$ (instead of $FeCl_2{\cdot}4H_2O$ as in the previous examples).[68] The catalytic application of this COF as enzymatic mimic has been investigated. Thus, in the presence of hydrogen peroxide, the Fe-porphyrin-containing COF can catalyze a chromogenic substrate (3,3',5,5'-tetramethylbenzidine) to produce color, and this just goes to show that it has an inner peroxidase-like activity. In fact, the intrinsic peroxidase-like catalytic activity of this COF is superior to that of horse radish peroxidase (HRP) in terms of stability and catalytic activity. In addition, the peroxidase-like Fe-porphyrin-containing-COF can be used in combination with glucose oxidase to build a one-pot colorimetric assay with a high sensitivity and selectivity for the detection of glucose. This contribution certainly paves the way for the use of COF-based porous composites as enzymatic mimics in bioanalysis and medical diagnostics.

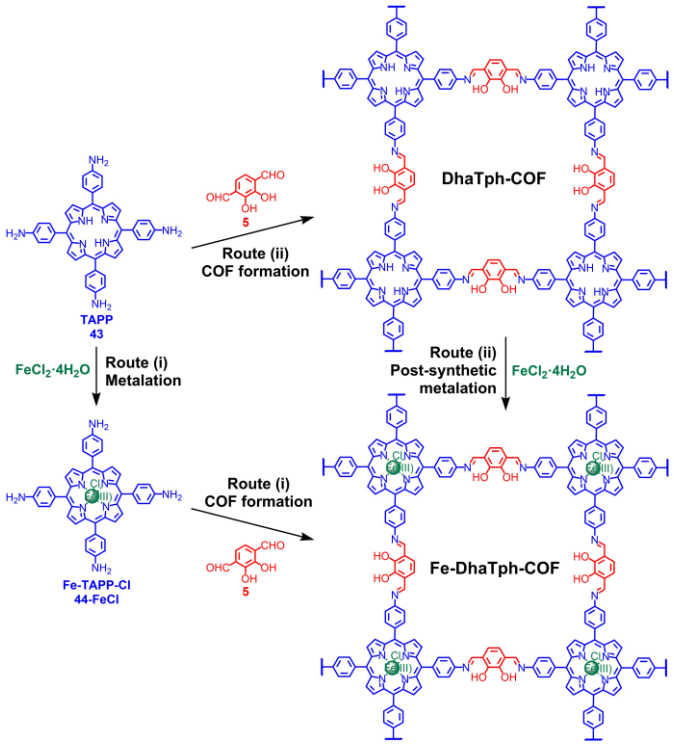

Scheme 6 Schematic representation for the synthesis of **Fe-DhaTph-COF** by either (i) metalation followed by COF formation or (ii) COF formation followed by post-synthetic metalation.

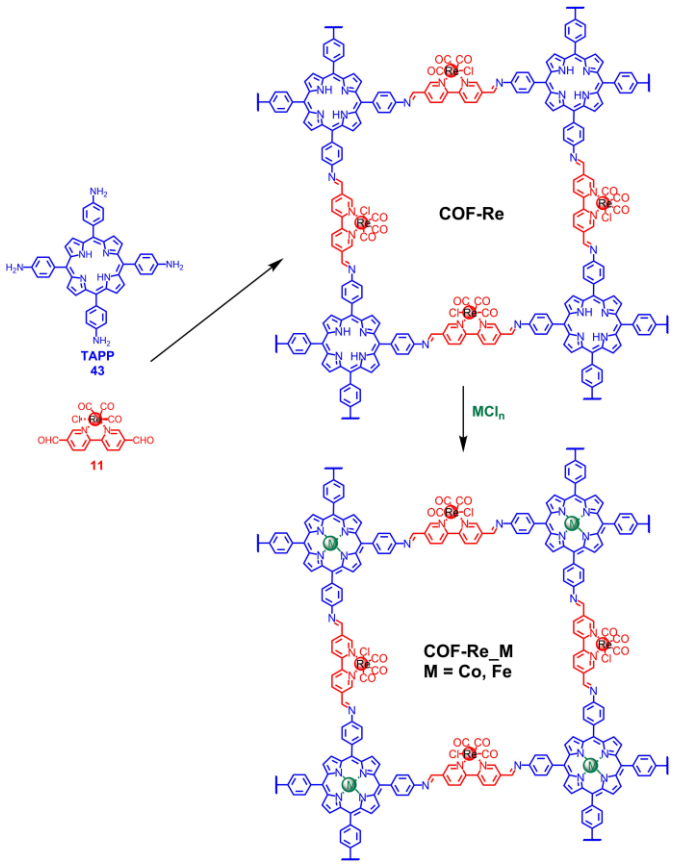

Scheme 7 Schematic representation for the synthesis of **COF-Re_Co** and **COF-Re_Fe** covalent-organic frameworks with both metalloporphyrin and metal bipyridine moieties.

3.2.4. Phenanthroline moieties

Terasaki, Yaghi and co-workers have carried out imine condensation reactions between aldehyde functionalized copper(I)-bisphenanthroline tetrafluoroborate (**$Cu(PDB)_2(BF_4)$**, **21**, Figs. 2, 3) and benzidine (**BZ**, **28**, Fig. 2) to afford a three-dimensional (3D) COF constructed from helical organic threads, designed to be mutually weaving at regular intervals (**COF-505**, Scheme 8).[76] Because the **PDB-BZ** threads are topologically independent of the Cu^I ions, the resulting woven structure can be formally considered a COF. In this case, the post-synthetic strategy involves the removal of Cu^I ions by heating **COF-505** in a KCN methanol-water solution. By using ICP analysis it is found that under these conditions 92-97% of the Cu^I ions are removed. Although the crystallinity of the demetalated material decreased in comparison with **COF-505**, SEM images show similar morphology before and after demetalation. In addition, the material can be remetalated with Cu^I ions by stirring in a $CH_3CN/CHCl_3$ solution of $Cu(CH_3CN)_4(BF_4)$ to give back crystalline **COF-505**. After remetalation, the Cu content was determined to be 82-88% of that in **COF-505** before demetalation. Thus, this type of COFs based on phenanthroline moieties are good alternatives to COFs with bipyridine moieties or hydroxyl groups in order to form Cu complexes. The remetalated **COF-505** has identical crystallinity to the original as-synthesized **COF-505**. Furthermore, the peak representing imine C=N stretch in the FTIR spectrum is retained, which

indicates that the framework is chemically stable and robust under the reaction conditions.

The effective Young's moduli (neglecting the anisotropy of the elasticity) determined for the two **COF-505** materials is ~12.5 and 1.3 GPa for the metalated and demetalated materials, respectively. The loose interaction between the threads upon removal of copper is responsible for the increase of elasticity. Interestingly, the elasticity of the original **COF-505** can be fully recovered after the process of demetalation and remetalation. This is a remarkable example of how the mechanical properties of a COF can be modified through post-synthetic modification.

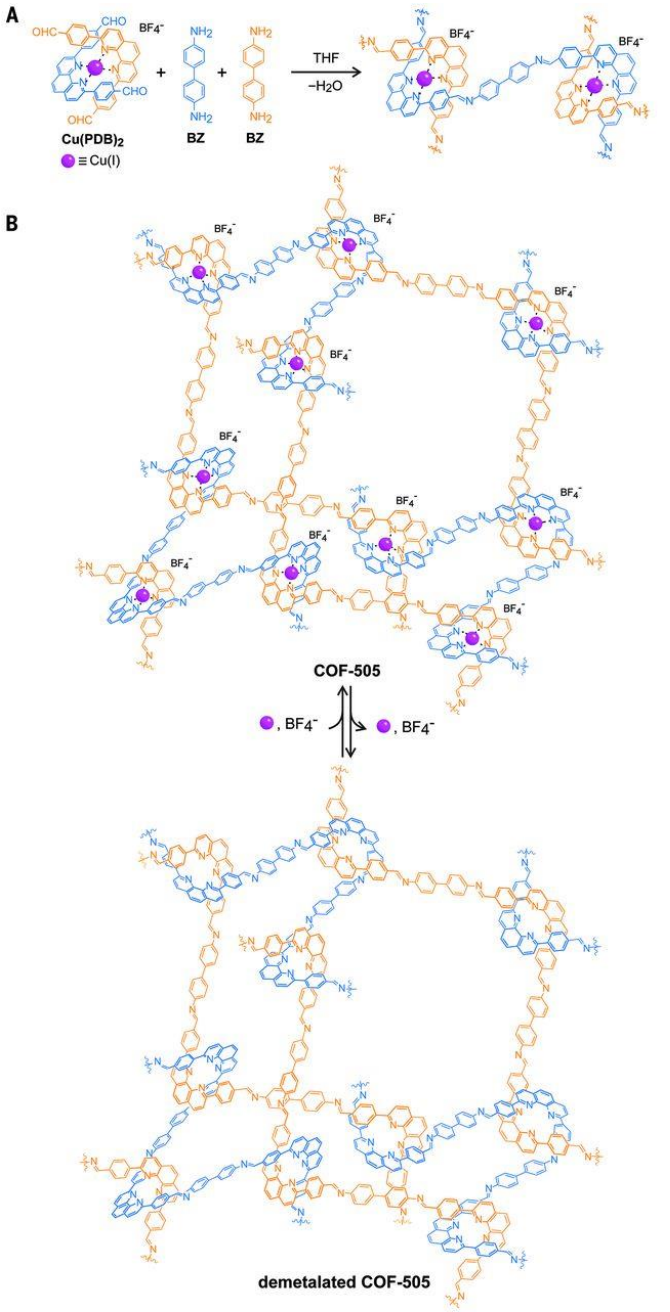

Scheme 8 (A) Synthetic strategy for the synthesis of **COF-505** as a weaving structure and (B) post-synthetic metalation and demetalation of this COF. From *Science*, 2016, **351**, 365-369. Reprinted with permission from AAAS.

In 2019, Yaghi and co-workers have used this post-synthetic strategy that involves the removal of Cu^{I} ions by heating in a KCN methanol solution with another COF constructed from helical organic threads based on copper(I)-bisphenanthroline moieties. By removing the Cu^{I} ions, the individual 1D square ribbons in the demetalated form are held together only by mechanical interlocking of rings. The copper content determined by ICP-AES in the demetalated COF is less than 1% of the original amount. The COF can be remetalated by stirring in a $CH_3CN/CHCl_3$ solution of $Cu(CH_3CN)_4(BF_4)$ and the Cu content in the remetalated COF is 99% that of the COF before demetalation. This fact confirms the excellent ability of this type of phenanthroline-based COFs to coordinate Cu ions.

In the demetalated COF, because of the particular mechanical linkages, the individual 1D square ribbons can move in a collective manner to produce a narrow-pore form. Furthermore, it was observed that these interlocking ribbons can dynamically move away from each other to reopen up the structure when exposed to tetrahydrofuran vapor. Interestingly, the structural integrity of the COF is maintained during this dynamic motion.[89]

3.3. COF-Metals based on COFs with β-ketoenamine linkages

In 2012, Banerjee *et al.* introduced a new protocol for the synthesis of highly acid- and base-stable crystalline covalent organic frameworks by a combination of reversible and irreversible organic reactions.[119] Triformylphloroglucinol (C3, **14**, Fig. 2) together with different diamines (C2) are employed in the design of [C3+C2] COFs. The total reaction can be divided into two steps which include a reversible Schiff base reaction for the formation of a crystalline framework followed by an irreversible enol-to-keto tautomerization, which enhances the chemical stability. Furthermore, the presence of new functional groups in the COFs backbone can be used for the subsequent post-modification of the COFs. Thus, the presence of the carbonyl group connected by a carbon–carbon double bond and an *N*-substituted amine in enaminones allow them to act as bidentated ligands for metal ions.

Thus, Shen, Zhang and co-workers have recently immobilized Ti^{IV} into **TpPa-2** (Scheme 9). Titanium ions were immobilized in the nitrogen-rich frameworks of **TpPa-2** COFs by treatment with a $Ti(SO_4)_2$ solution.[63] After metal-chelating, the XPS spectrum of **TpPa-2-Ti^{4+}** composites demonstrates the successful grafting of titanium ions onto **TpPa-2** COFs by the coordination reaction between Ti^{IV} and the β-ketoenamine groups. PXRD analysis shows that the crystal structure of **TpPa-2** is almost maintained after treatment with $Ti(SO_4)_2$ although the intensity of the PXRD pattern slightly decreases, in agreement with that observed for the metalation of some of the above mentioned imine-based COFs when the imine linkage is involved in the complexation. In order to address the loading ability of this COF for Ti^{IV} ions, the atom and weight percentages of titanium were estimated and found to be 12.61% and 33.49% respectively.

The feasibility of **TpPa-2-Ti^{4+}** for phosphopeptide enrichment was investigated using tryptic digests of standard phosphoprotein β-Casein. The specificity and selectivity of the **TpPa-2-Ti^{4+}** for phosphopeptide enrichment were further evaluated using relatively complex peptide mixtures of tryptic digestion including β-casein and bovine serum albumin (BSA). Even the practicability of **TpPa-2-Ti^{4+}** for low-abundance phosphopeptide enrichment in a real sample, namely non-fat milk, was carried out. The results obtained demonstrate the high selectivity and great capacity for phosphopeptide identification as well as the potential for deep phosphoproteomics research using the novel COF as immobilized metal ion affinity chromatography (IMAC) material.

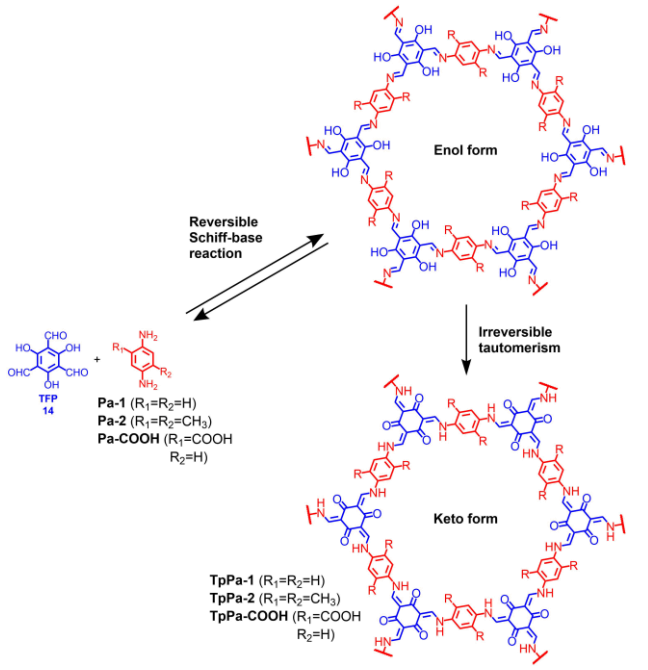

Scheme 9 Schematic representation of the synthesis of **TpPa-1**, **TpPa-2** and **Tp-Pa-COOH**.

In 2018, Liu, Cui and co-workers have reported homochiral crystallization of a series of COFs with controlled handedness by imine condensations of triformylphloroglucinol (**14**, Fig. 2) with achiral diamine or triamine linkers in the presence of chiral catalysts.[78] As stated above, the presence of the carbonyl group connected by a carbon–carbon double bond and an *N*-substituted amine in enaminones allow the system to act as bidentated ligands for metal ions. Thus, upon treatment of the enaminone-containing COF with $Cu(OAc)_2$ in the presence of *N*,*N*-diisopropylethylamine (DIEA) homochiral COF-metalated materials are formed, which can be used as Lewis acidic catalysts. X-ray absorption fine structure (XAFS) analysis was used to determine the Cu coordination environment in the copper-containing COF. The scattering path distances and degeneracies derived from these fits are consistent with tetrahedral coordination of the Cu centers with one O and one N atom of the COF and two O atoms of the acetate. ICP-OES results reveal that the Cu loading amount in the metalated COF is 1.2 wt %. In addition, the solid obtained after post-synthetic modification of the enaminone groups with Cu^{II} ions was found to be a recyclable heterogeneous catalyst for the asymmetric Henry reaction of nitroalkanes with aldehydes.

As it was stated above, there was a previous example of a metalated (with cobalt ions) Salen-based COF (Scheme 4) used to catalyze the Henry reaction with catalytic activities ranging between only traces to above 90%.[66] Nevertheless, the achiral nature of this COF prevented its use for asymmetric catalysis. In contrast, the homochiral metalated (with Cu ions) COF reported by Liu and co-workers[78] has been used to catalyze the addition of nitromethane to 4-bromobenzaldehyde in the presence of DIEA to afford the corresponding β-nitroalcohol with 10% conversion of aldehyde and 35% enantiomeric excess (ee). It is worth mentioning that when more DIEA, an additive to accelerate the Henry reaction, was used the conversion of aldehyde could increase up to 90% in 48 h, but with very low or no enantioselectivity. This is due to the fact that elevated levels of DIEA may destroy the crystallinity of the COF. Concerning with the recycling tests, the catalytic activity starts to decrease after three recycles. In spite of the very low enantioselectivity, this seminal work paves the way for the development of new chiral porous solids consisting of only achiral building blocks to be used in asymmetric catalysis.

Pyridine moieties can act as a base catalyst and a nitrogen donor to bind metal species and therefore they are attractive catalytic systems. Ma and co-workers reported in 2017 a chemically stable COF bearing pyridine as a platform for cascade catalysis.[85] The COF was obtained by reaction between triformylphloroglucinol (**14**, Fig. 2) and 2,5-diaminopyridine (**34**, Figs. 2, 3) thus providing a COF with β–ketoenamine linkages. By using the standard conditions for the solution-infiltration method, a mixture of the COF and $Pd(OAc)_2$ was stirred to immobilize Pd within the COF. XPS analysis shows that pyridinic nitrogens coordinate with the Pd species. In addition, it reveals that Pd species are also coordinated with the secondary amine of the β-ketoenamine linkage. Furthermore, carefully controlled conditions allow the synthesis of partially metalated COFs bearing therefore two types of active sites, the Pd-pyridine moieties as well as the non-metalated pyridines. As shown above, this type of catalyst systems bearing two types of active sites are suitable for application in one-pot cascade catalysis. Thus, this hybrid COF-Pd system was tested as catalyst in cascade oxidation–Knoevenagel condensation reaction from alcohols to α,β-unsaturated dinitriles and far outperforms the corresponding homogeneous catalyst (Pd/pyridine) in terms of the turnover frequency. Furthermore, the catalyst can be recycled at least six times without a significant drop in the product yield (95% after five cycles), which highlights the heterogeneous nature of the catalytic process. This excellent behavior is due to the combined contributions of the ordered porous structure, highly accessible active sites, and the site isolated manner of the two catalytic components.

Yuan, Zhu and co-workers have recently reported the preparation of a series of multivariate covalent organic

frameworks which are functionalized not only with enaminone moieties but also with carboxyl groups (**TpPa-COOH**, Scheme 9) in the search of novel porous materials for ammonia uptake.[62] By reaction of triformylphloroglucinol (**TFP**, **14**, Fig. 2) with **Pa-1** (**22**, Fig. 2) and **Pa-COOH** (**23**, Figs. 2, 3) in different ratios of linkers it is possible to obtain a series of COFs with variable amounts of carboxylic moieties (**[HOOC]$_x$-COFs**, X = 0, 17, 33, 50, and 100, Scheme 9). The simultaneous presence of –N-H, –C=O and –COOH fragments can serve as proton-donating or proton-accepting groups for hydrogen-bonding interactions, which can significantly enhance the affinity to ammonia. Larger amounts of carboxylic moieties in the pores produced decreased NH_3 uptakes which was attributed to the reduced porous surface. Thus, the COF derivative with the best ammonia uptake was **[HOOC]$_{17}$-COF**. This product was immersed in chloride salt solutions (M = Ca^{II}, Mn^{II}, and Sr^{II}) to integrate the metal ions in the carboxylated structure to achieve the first case of an open metal site in a COF architecture. Two O (from –C=O of –COOH and COF skeleton) and one N (from –N-H) atoms coordinate to one metal ion in the **[HOOC]$_{17}$-COF** framework to form a stabilized double six-membered ring structure. This coordination pattern is in agreement with the fact that elemental analysis reveals the almost equal content of metal ion and –COOH group in **[MOOC]$_{17}$-COFs** (M = Ca^{II}, Mn^{II}, and Sr^{II}). Interestingly, PXRD patterns reveal that the metalated COFs retain the same crystallinity as the precursor COF even after metal ion incorporation. It is also worth mentioning that the metal ions are uniformly dispersed in the COF structure and no metallic nanoparticles are visible by using TEM.

These metalated COF materials with synergistic multivariate and open metal sites show excellent adsorption capacities (14.3 and 19.8 mmol g^{-1} at 298 and 283 K, respectively) and isosteric heat (Qst) of 91.2 kJ mol^{-1} for ammonia molecules. This contribution enables the development of tailor-made porous materials with tunable pore-engineered surface for ammonia uptake.

3.4. COF-Metals based on COFs with hydrazone linkages

In 2011, with the aim of widening the range of possible materials that could be achieved through any kind of linkage, Yaghi and co-workers reported a pioneering work aimed at the synthesis of COFs with hydrazone groups as strong organic linkages given that hydrazones are typically much less prone to hydrolysis than imines.[53] Shortly after, in 2012, Jiang and co-workers reported the synthesis of a molybdenum-doped COF catalyst (**Mo-COF**) linked by a hydrazine linkage *via* a facile two-step bottom-up approach.[79] The COF was obtained by reaction between 1,3,5-triformylphloroglucinol (**14**, Fig. 2) and terephthalohydrazide (**49**, Fig. 2) in dimethylacetamide (DMA) under solvothermal reaction conditions. The subsequent treatment of a refluxing mixture of the COF in methanol with $MoO_2(acac)_2$ affords the corresponding **Mo-COF** (Scheme 10). FTIR analysis of the **Mo-COF** confirmed the successful incorporation of molybdenum into the framework backbone through a stable coordination bond. TGA analysis showed that the metalated COF is stable up to 260 °C and characterization by XPS confirmed the strong coordination of Mo with the salicylaldehyde benzoyl hydrazine groups of the COF. ICP-MS analysis showed that the density of the active Mo sites reached as high as 2.0 mmol g^{-1}, which is 5-10 times higher than ever reported for a Mo complex grafted on insoluble materials such as a mesoporous sieves, MWCNTs and polymers.[120]

To show that **Mo-COF** was catalytically active, the performance of **Mo-COF** as a nanochannel-reactor in the context of the epoxidation of cyclohexene was evaluated showing conversions above 99% with selectivity above 70%. Furthermore, upon the completion of the reaction the catalyst could be easily recovered in almost quantitative yield by simple filtration and could be used repeatedly without significant degradation of the catalytic performance after four cycles.

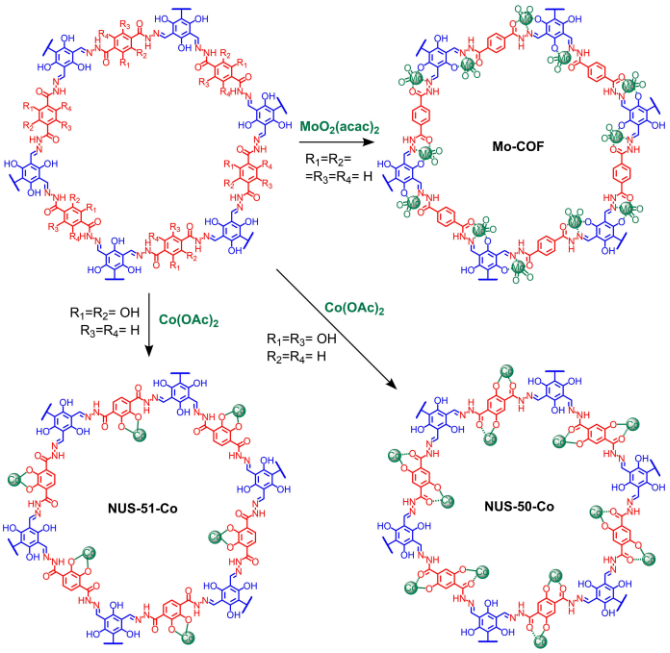

Scheme 10 Post-synthetic metalation of a hydrazone-based COF with Mo or Co to afford catalytically active metal-COFs.

In 2018, Zhao and co-workers reported the synthesis of two hydroxy-rich hydrazone-based COFs which can be synthesized in pure water by reaction between triformylphloroglucinol (**14**, Fig. 2) with either 2,5-dihydroxyterephthalohydrazide (**50**, Fig. 2) or 2,3-dihydroxyterephthalohydrazide (**51**, Fig. 2, 3). The pristine COFs were post-synthetically modified by incorporation of Co^{II} through impregnation by simply stirring in a methanolic solution of $Co(OAc)_2$.[73] A uniform distribution of Co element throughout the framework is observed in the TEM-elemental mapping. TGA measurements combined with ICP-MS analysis collectively suggest around 20 wt % loading of Co^{II} in the COFs. The XPS analysis suggests the delocalized nature of the two oxygen species after Co^{II} coordination and indicates no contribution from the nitrogen species in Co^{II} anchoring. In contrast with the previous **Mo-COF** based on COFs with hydrazine linkage (Scheme 10), which were stable only up to 260 °C, these COFs are thermally stable up to 375 °C.

The post-synthetic Co^{II} ions impart Lewis acidic sites, which prove effective in catalyzing the cyanosilylation reaction of various aldehydes with size selectivity to yield important cyanohydrin intermediates. These COFs do not show any steady decrease in activity, confirming their good stability and recyclability under the catalytic conditions.

3.5. COF-Metals based on COFs with boronic ester linkages

The limited availability of metalated 3D-COFs is probably attributed to the synthetic challenge of utilizing the appropriate geometrically shaped monomers that can not only produce crystalline polymeric networks but also form strong complexes with metal ions. McGrier and co-workers reported in 2016 one of the few examples, together with **COF-505** (Scheme 8), of metalated 3D-COFs. This 3D-COF, named **DBA-3D-COF**, can be obtained by reaction between the C_3-symmetric π-electron conjugated dehydrobenzoannulene (**DBA**, **54**, Figs. 2, 3) and the tetrahedral tetra-(4-dihydroxyborylphenyl)methane monomer (**65**, Fig. 2) under solvothermal conditions (Scheme 11).[74] The linkers formed in the polymerization reactions are boronate ester five-membered rings which are formed by the reaction of boronic acid moieties present in **65** and catechol units present in **DBA**. This kind of linkages based on boronate ester five-membered rings enable the synthesis of highly crystalline COFs owing to their high reversibility.[121-123]

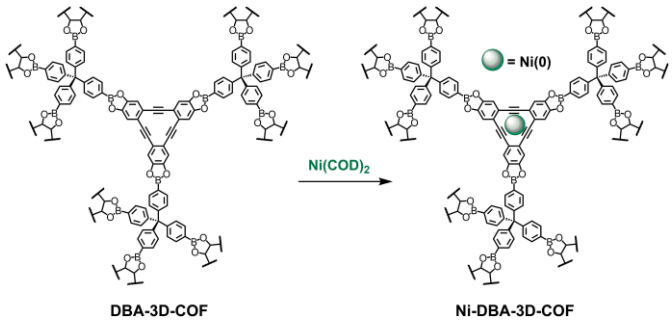

Scheme 11 Metalation of **DBA-3D-COF** with $Ni(COD)_2$ to produce **Ni-DBA-3D-COF**.

DBA derivatives exhibit planarity and metal binding properties which are comparable to that of porphyrin and phthalocyanine ligands, which typically use hard nitrogen atoms to bind metals. In contrast, **DBA** derivatives are neutral compounds that contain soft ligands capable of donating 2–4 electrons per alkyne depending on the electronic demand of the metals. Thus, **DBA-3D-COF** can be easily metalated upon treatment of ~35 mg of the COF with a solution containing 10 wt % $Ni(COD)_2$ dissolved in 1 mL of dry toluene. ICP-AES analysis indicates that ~10.1 wt % of Ni is incorporated into **Ni-DBA-3D-COF**. Retention of crystallinity and preservation of the framework following metalation with $Ni(COD)_2$ is confirmed by the PXRD profile of the formed **Ni-DBA-3D-COF**. XPS analysis of $Ni(COD)_2$ and **Ni-DBA-3D-COF** indicates that the Ni(0) atoms do not interact at the boronate ester linkage, but rather they bind with the alkynyl units of **DBA**, thus confirming the post-synthetic modification of the COF.

Both **DBA-3D-COF** and **Ni-DBA-3D-COF** display great uptake capacities for ethane and ethylene gas. Taking into account that **DBA** monomers also have the ability to bind Li, Ca, and other low oxidation state transition metals,[92] this contribution paves the way for the potential use of metalated DBA-based COFs in applications related to catalysis, gas storage and separations among others.

3.6. COF-Metal nanoparticles

Post-synthetic treatment of COFs through metal-ligand interactions can be used not only to confine metal ions into COFs but also to graft metal nanoparticles (NPs). Thus, Banerjee and co-workers reported the production of COF-supported Au NPs and Pd NPs hybrid materials with high catalytic activity in nitrophenol reduction and Sonogashira coupling, respectively.[124, 125] However, the pore size of the COF support (~1.8 nm) is too small for the relatively larger size of NPs (5 ± 3 nm for Au NPs and 7 ± 3 nm for Pd NPs) which indicates surface deposition of NPs rather than encapsulation inside the pores.

Thomas, Pratti and co-workers showed that encapsulation of NPs inside the cavities of COFs is critical to control the size through confinement of nanoparticle growth and that the lack of control of the nanoparticle size is likely due to weak interactions between COF support and metal NPs.[126] In this regard, it has been shown that the introduction of heteroatom functionalities within the pores of COFs is an efficient strategy for the immobilization of metal nanoparticles. Thus, several articles have been described in which covalent organic frameworks have been used to immobilize nanoparticles based among others on Au,[125] Co,[127] Pd[128] or Ru.[129] With this in mind, Gu, Zhang and co-workers proposed that the presence of strong anchoring groups inside the pores would facilitate the binding of metal ions/nanoparticles and formation of nucleation sites inside the cavities, thus enabling confined growth of nanoparticles and control of their particle size. Thus, they synthesized a thioether-containing COF (**Thio-COF**, Scheme 12) and showed that the presence of thioether groups inside the cavity is crucial for the size-controlled synthesis of Au NPs, serving as nucleation sites for metal deposition and NP growth upon treatment of the COF with K_2PdCl_4 or K_2PtCl_4 in methanol and water.[130] The efficient metal–ligand interaction (e.g., the charge transfer from Pt nanoparticles to S atoms) is confirmed by using XPS measurements which showed that the binding energy of the Pt $4f_{7/2}$ peak of Pt(0) species in **PtNPs@COF** had a higher value compared to that of pure Pt NPs, while the binding energy of S 2p in **PtNPs@COF** had a negative shift compared to that of S in **Thio-COF**. Interestingly, they found that the hybrid material based on Pt NPs shows excellent catalytic activity in nitrophenol reduction while that based on Pd NPS efficiently catalyzes the Suzuki-Miyaura coupling reaction. This last contribution is a good example of how efficient post-synthetic treatment of COFs through metal-ligand interactions can be used not only to confine small molecules into COFs but also metal nanoparticles.

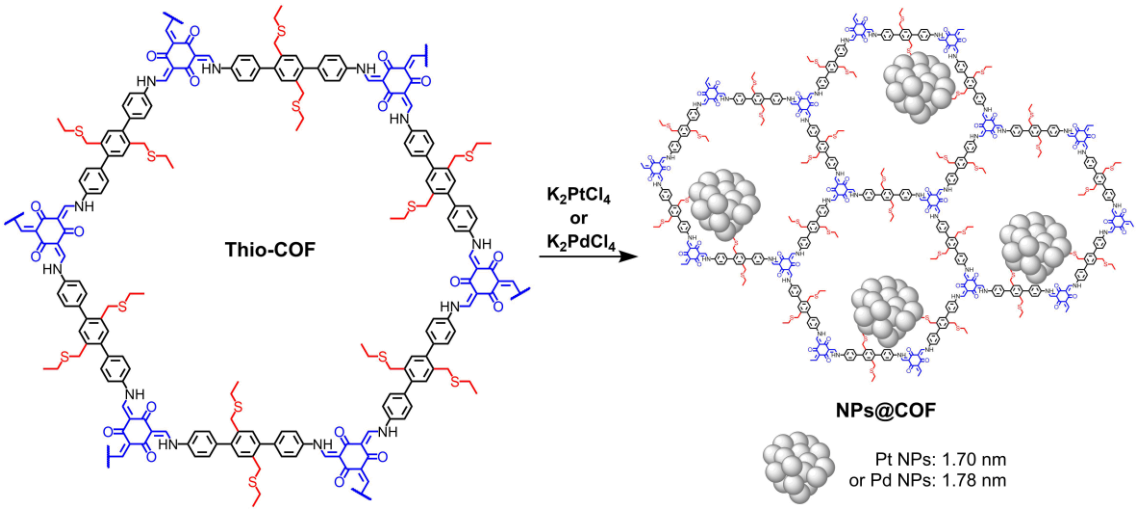

Scheme 12 Structure of **Thio-COF** and schematic representation of the synthesis of **Thio-COF** supported **PtNPs@COF** and **PdNPs@COF**.

4. Post-synthetic modification of covalent organic frameworks by backbone modification

4.1. Post-synthetic modification of covalent organic frameworks by chemical conversion of linkages

Reversibility of the COF linkage is essential to obtain ordered materials by error correction and defect healing[61, 119, 131] and therefore the linkage and its chemistry dictate the fundamental physical and chemical properties as well as the inherent limitations of COFs. Thus, the intrinsic reversibility of the linkages within COFs sometimes limits fundamental materials properties such as crystallinity or environmental stability towards chemical solvents, constraining their practical applications. For example, COFs with boroxine linkages are susceptible to water or protic solvents.[1, 132, 133] On the other hand, COFs based on the C=N imine bond, a more robust linkage, represent the most abundant and well-studied COFs that show improved hydrothermal stability.[9] However, the chemical stability of some imine-based COFs is still not completely satisfactory given that they sometimes undergo hydrolysis under strongly acidic conditions or exchange with amines due to the reversible nature of imines.[134]

Hence, in the preparation of COFs a competition between reversibility and stability is stablished, which is dominated by subtle changes in the reaction conditions. The development of linkages relies therefore on serendipity in the optimization of reaction conditions that allow for sufficient reversibility to let crystallinity emerge. In order to circumvent this dilemma, Yaghi and co-workers recently developed a strategy which was already explored to stabilize molecular cages formed by dynamic covalent chemistry[135] as well as for the synthesis of crystalline "unfeasible" zeolites.[136] The strategy involves a reversible order-inducing step under thermodynamic control and subsequently arresting this order *via* a post-synthetic treatment.[35] Thus, the chemical linkage of the COF needs to be converted from a reversible to an irreversible type of bond in a topochemical fashion in order to arrest COFs in their crystalline state.

As in other post-synthetic modifications, a COF is subjected to a reaction normally carried out in molecular organic chemistry, leading to a completely new COF for which making new linkages is no longer subject to the trial and error and inherent uncertainties of *de novo* synthesis. The seminal chemical conversion of linkages in two-dimensional COFs developed by Yaghi and co-workers involved a method of deriving amide-linked COFs from their corresponding imine-linked frameworks.[35] The synthetic procedure for the amidation reaction involved treatment of imine-based COFs with sodium chlorite (11 equiv per imine functionality), acetic acid (10 equiv), and 2-methyl-2-butene (100 equiv) in dioxane (Scheme 13). The progress of the reaction was monitored by Fourier-transform infrared (FTIR) spectroscopy and ^{13}C cross-polarization magic angle spinning (CP-MAS) NMR spectroscopy providing evidence of excellent conversion. Although the powder X-ray diffraction (PXRD) measurements indicate slight unit cell changes, no significant structural rearrangement of the material was observed during the transformation. An important outcome of this transformation is the difference between the stabilities of the imine and amide materials which is most striking in the case of acidic conditions, where the amides retain crystallinity while the corresponding imines are nearly or completely dissolved and the remaining material is rendered amorphous.

In 2018 Cui and co-workers have demonstrated that the scope of this strategy is not limited to 2D-COFs but it can also be extended to 3D-COFs.[137] Thus, TADDOL-containing **CCOF-6** was synthesized from **CCOF-5** (Scheme 13) according to the procedure mentioned above and developed by Yaghi and co-workers. Conversion of the materials from imine to amide was confirmed by FTIR and ^{13}C CP-MAS NMR spectroscopies. PXRD

analysis indicates that the symmetry of **CCOF-5** (space group P2) is conserved in **CCOF-6**, which is in agreement with the retention of the diamond configuration. Thus, only a slight change in unit cell parameters was found for the amide CCOF compared with the imine one. As stated above, the difference between the stabilities of imine and amide materials is striking in the case of acidic and alkaline conditions. Under these conditions the amide CCOF retained its crystallinity while the imine one was nearly dissolved and the remaining material was rendered amorphous. Both COFs have been tested as chiral stationary phases for high performance liquid chromatography (HPLC) to enantioseparate racemic alcohols and the amide COF obtained through the post-functionalization strategy shows superior separation performance compared to the pristine framework.

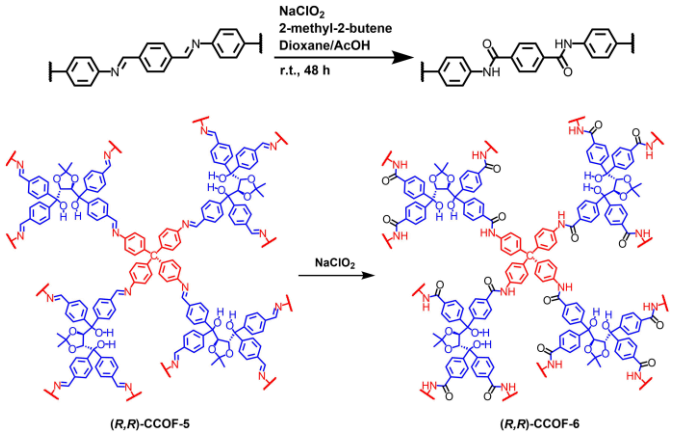

Scheme 13 Top: Conversion of imine linkages in COFs to amide-linked COFs. Bottom: Synthesis of amide-linked 3D chiral COFs from imine-linked 3D chiral COFs.

In 2018 Lotsch and co-workers have reported a post-synthetic sulfur-assisted chemical conversion of a two-dimensional imine-linked COF into a thiazole-linked COF, with full retention of crystallinity and porosity.[138] Thus, **TTT-COF** can be obtained in two successive steps: First, **TTI-COF** was infiltrated with molten sulfur at 155 °C. At this temperature sulfur has minimum viscosity, enabling mixing with the COF material. In a second step, by using a thermal treatment at higher temperature (350 °C), the conversion of the **TTI-COF** to the **TTT-COF** took place. At high temperatures elemental sulfur reacts with aromatic imines to first oxidize the imine to a thioamide, and subsequently oxidatively cyclizes the thioamide group to form a thiazole ring (Scheme 14).[139] Therefore, sulfur plays the role of oxidant (being reduced to H_2S) and of nucleophile, attaching first to the imine carbon and afterwards to the phenyl ring on the nitrogen side of the imine. ^{13}C and ^{15}N solid state NMR (ssNMR) was used to probe the imine to thiazole conversion and retention of the framework structure.

Although this approach requires the use of harsher reaction conditions than the imine-to-amide oxidation, the generated framework is stable against more drastic chemical conditions. Thus, thiazole-linked COFs retain their crystallinity under more alkaline conditions (12 M KOH versus 1 M NaOH) and also in presence of reducing agents such as hydrazine and $NaBH_4$.

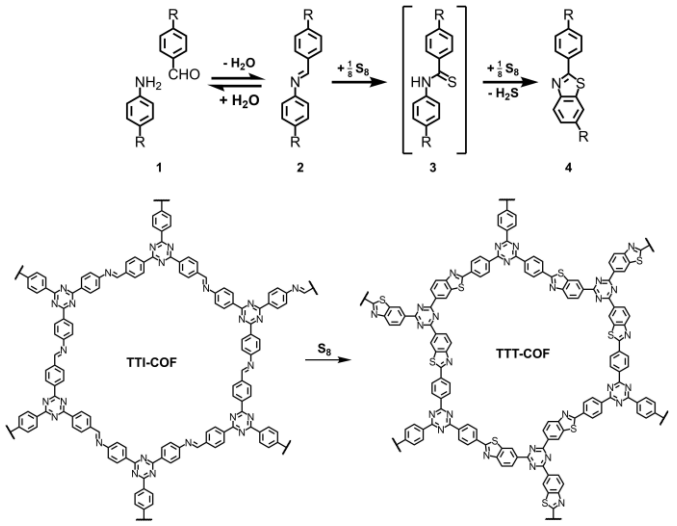

Scheme 14 Imine to thiazole transformation in **TTI-COF**. Top: Schematic drawing of the reaction of an amine and an aldehyde (**1**) to form an imine (**2**), subsequent reaction with elemental sulfur to yield a thioamide as an intermediate (**3**), and finally a thiazole (**4**). Bottom: Schematic drawing of the sulfurization reaction of the **TTI-COF** to form the thiazole-based **TTT-COF**.

One important challenge in the field of COFs is the potential of constructing a periodic conjugated 2D framework with covalently linked aromatic ring systems, from which exceptional electronic and magnetic properties are predicted.[140] In this respect, the imine linkage has revealed as a better choice than other dynamic bonds as it serves as an sp^2-hybridized unit readily inserted into a π-extended framework to open up conjugation pathways. However, because of the strongly polarized nature of the C=N bonds, the resulting imine-based frameworks only exhibit limited π-electron delocalization between the linked units.[141] With the aim to provide a general strategy to reinforce strong covalent bonding and extended π-electron delocalization in the same framework, Liu and co-workers have recently reported a facile post-synthetic transformation of imine covalent organic frameworks into ultrastable crystalline porous aromatic frameworks.[142] The strategy involves kinetically fixing of the reversible imine linkages *via* an aza-Diels-Alder cycloaddition reaction with arylacetylene derivatives in the presence of $BF_3{\cdot}Et_2O$ and chloranil in toluene (Scheme 15).

The quinoline-linked COFs obtained not only retain crystallinity and porosity, but also display dramatically enhanced chemical stability over their imine-based COF precursors. In fact, these COFs are among the most robust COFs up-to-date that can withstand strong acidic (12 M HCl), basic (14 M NaOH) and redox ($KMnO_4$, $NaBH_4$) environments, surpassing the chemical stability of the amide- and thiazole-linked COFs mentioned above. Interestingly, owing to the chemical diversity of the cycloaddition reaction and structural tunability of COFs, the pores of COFs can be readily engineered to realize pre-designed surface functionality.

These seminal examples of post-synthetic modification of covalent organic frameworks by chemical conversion of linkages pave the way to the synthesis of crystalline, porous and even aromatic frameworks that are difficult to obtain *de novo*. Access to this kind of materials will facilitate even more the practical applications of organic framework materials that require enhanced chemical stability, semiconducting properties or pore surface functionality.

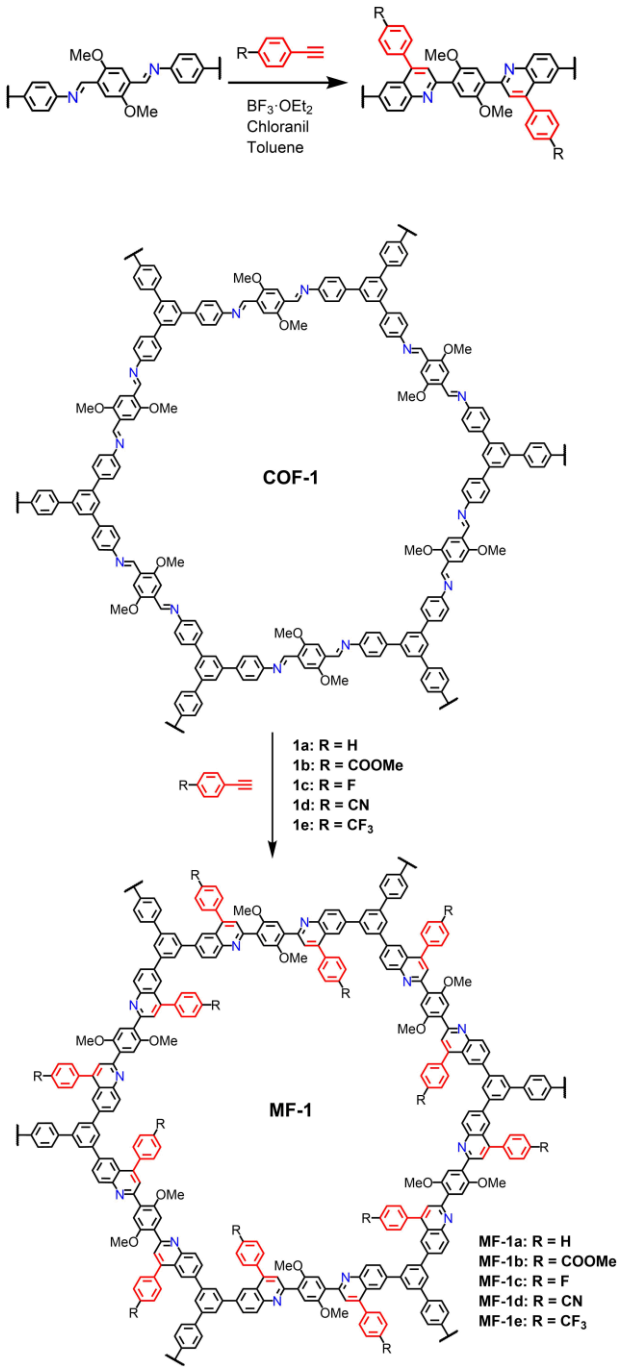

Scheme 15 Reaction scheme showing the transformation of one lattice unit of **COF-1** into **MF-1ae** *via* post-synthetic modification of **COF-1** through an aza-DA reaction.

4.2. Post-synthetic modification of covalent organic frameworks by linker exchange

The syntheses of COFs follow the principle of dynamic covalent chemistry (DCC), which is based on reversible chemical reactions that allow covalent bond formation and breaking under thermodynamic control.[40, 41, 143-145] Such a feature is key for the syntheses of COFs because it endows the process of COFs formation with the possibility of self-correction, which secures their crystalline structures. However, little attention has been paid to the use of the principle of DCC for the post-synthesis modification of COFs. This contrasts with the extensive use of post-synthetic modification *via* linker or metal cation replacement in metal organic frameworks (MOFs), which leads to the in situ MOF-to-MOF transformation. This strategy has been generally recognized to be a powerful tool to prepare functional MOFs which are difficult or inaccessible *via de novo* synthesis.[146] Taking into account that reversible bond formation is a common feature in both COFs and MOFs, it can be envisaged that the building-block-exchange-based framework-to-framework transformation strategy might also be applicable to COFs.

Thus, in 2017, Zhao and co-workers showed that the dynamic nature of the bond also allows for the linkers of a COF to be exchanged post-synthetically, yielding an isostructural material with different pore metrics while retaining crystallinity.[134] In order to perform the study, the synthesis of two different COFs (**TP-COF-BZ** and **TP-COF-DAB,** Scheme 16), was carried out and the subsequent in situ COF-to-COF transformation *via* building block exchange (BBE) was investigated. For the synthesis of both COFs, the tetratopic building block [1,1′:3′,1″-terphenyl]-3,3″,5,5″-tetracarbaldehyde (**19**, Fig. 2), in which a benzene unit is chosen as the core and two aldehyde groups are introduced to the ends of its two branches, has been designed and synthesized. On the other hand, 1,4-diaminobenzene (**DAB**, **22**, Fig. 2) and benzidine (**BZ**, **28**, Fig. 2) were selected as the ditopic linear linkers respectively for the synthesis of **TP-COF-DAB** and **TP-COF-BZ**.

TP-COF-BZ exhibits lower crystallinity and thermal stability in comparison with **TP-COF-DAB**. Furthermore, 1,4-diaminobenzene is more active than benzidine as a result of the electron-donating amine groups at the *para* position. Taking into account these two facts, Zhao and co-workers attempted the transformation of **TP-COF-BZ** into **TP-COF-DAB** through substituting benzidine units in **TP-COF-BZ** with 1,4-diaminobenzene. To drive the equilibrium toward **TP-COF-DAB**, excessive 1,4-diaminobenzene was added. The addition of 10 equiv of 1,4-diaminobenzene gives rise to the best result. A time-dependent transformation experiment showed that after 4 h the transformation has nearly completed.

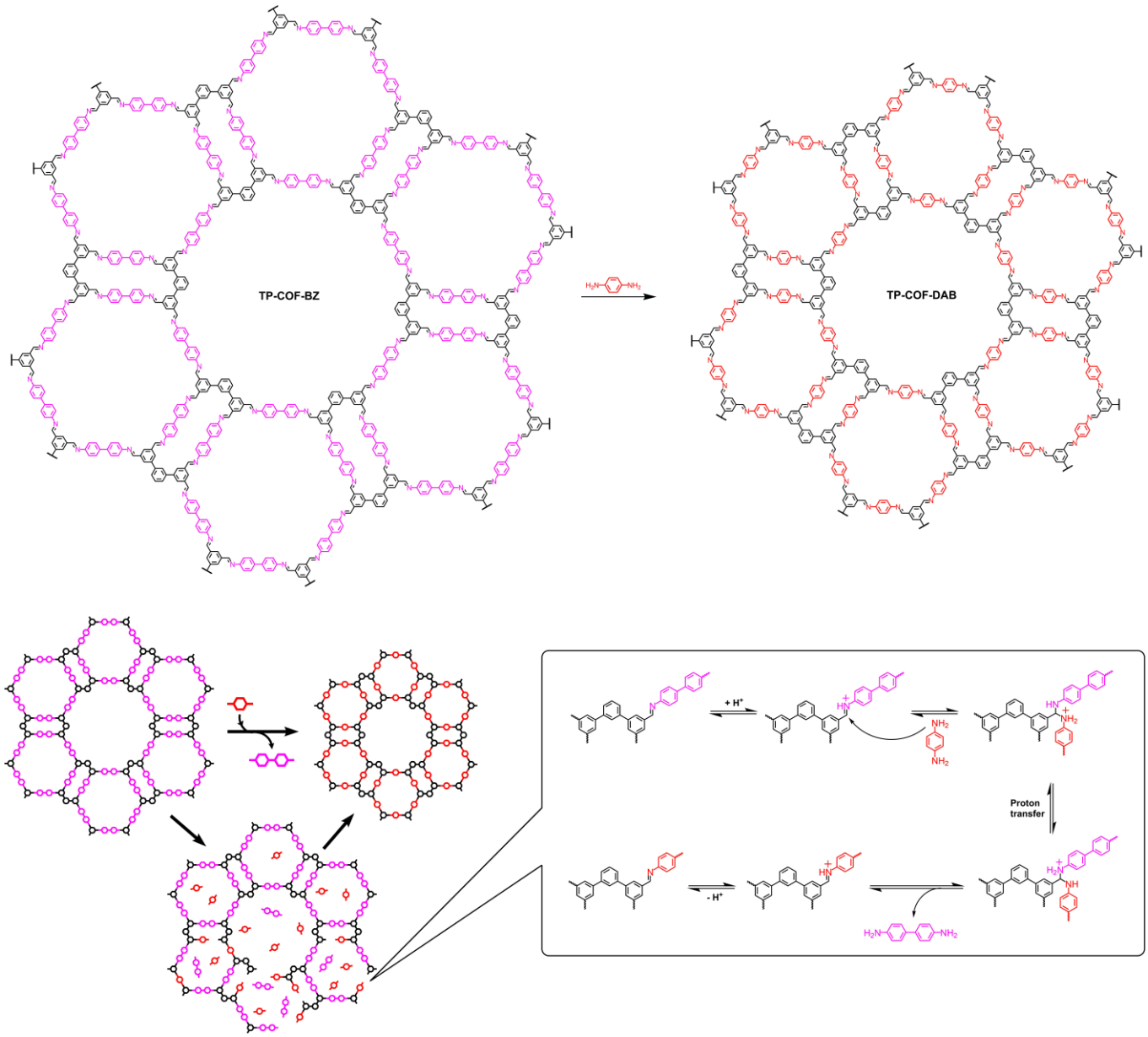

Scheme 16 Top. Transformation of **TP-COF-BZ** into **TP-COF-DAB** in the presence of 1,4-diaminobenzene. **Bottom.** Proposed process for the transformation. Note: Only one unit was illustrated for clarity.

The transformation process was also followed by photographing and the study showed that retention of insoluble materials was observed throughout the whole transformation course. This fact together with ^{1}H NMR analysis of the ratio of 1,4-diaminobenzene/benzidine in the polymers obtained at different transformation time intervals clearly indicate that exchange of linkers proceeds in a heterogeneous way. On the basis of the above experimental results, a transformation mechanism, as illustrated in Scheme 16, has been proposed. During the transformation, the intermediate polymers with partial replacements of monomers exist as insoluble solids, and the diamines stay in solution. Therefore, the replacement reactions should occur at the solid-solution interface.

By following an analogous dynamic covalent chemistry (DCC)-based post-synthetic approach at the solid–liquid interface *via* building block exchange (BBE), Horike and co-workers prepared hierarchical structures for an imine-linked COF system.[147] To start, two imine-linked COFs were prepared by the condensation of benzene-1,3,5-tricarbaldehyde (**13**, Fig. 2) with 1,4-diaminobenzene (**22**, Fig. 2) or 1,4-diaminonaphthalene (**36**, Fig. 2) under solvothermal conditions to yield respectively COFs based on benzene or naphthalene moieties. Afterwards, a solid–liquid reaction for the benzene-based COF and 1,4-diaminonaphthalene *via* post-synthetic imine exchange was conducted using different amounts of equivalents of 1,4-diaminonaphthalene. By means of this strategy, new COFs containing both naphthalene and benzene moieties in different

ratios are obtained. It is observed that the post-synthetic exchange process improves the framework crystallinity. An interesting outcome of this study is the analysis of the morphology of the new COFs. High-angle annular dark-field scanning transmission electron microscopy (HAADF-STEM) measurements suggests the gradual replacement of 1,4-diaminobenzene with 1,4-diaminonaphthalene in **COF-Ph** with the retention of the original particle morphology. Furthermore, the BET surface areas of the optimized mixed-linker COFs were two-fold greater than those of their parent phases on account of the improvement of crystallinity *via* the post-linker exchange process.

Interestingly, when the inverse BBE was carried out it was found to be much harder to displace 1,4-diaminonaphthalene with 1,4-diaminobenzene. Using the same reaction conditions led once again to COFs containing both naphthalene and benzene moieties, but the percentage of exchanged monomer was about half as in the previous case. This can be explained due to the stronger π-π interactions in the naphthalene-based COF, which make it harder to displace this monomer. This result highlights the importance of considering not only the relative reactivity of the exchanging monomers, but also the stability and the strength of the interactions in the starting COF.

This BBE strategy has been also used to introduce functionalities incompatible with COF synthesis conditions. Thus, Yan and co-workers have applied this approach for the rational fabrication of *de novo* unreachable amino-functionalized imine-linked COFs.[148] The aim of this contribution was the incorporation of amino groups in COFs given that this functional group contains lone pairs of electrons, can form hydrogen bonds and are liable for further derivatization. However, because imine-linked COFs are fabricated *via* the polymerization of aldehydes and amines, it is a great challenge to prepare amino-functionalized imine-linked COFs *via de novo* due to the participation of amino groups in the formation of imine-linked COFs. With this aim, two COFs (**PTPA** and **PTBD**) were obtained as mother COFs *via* direct condensation of 1,3,5-tris(4-formylphenyl)triazine (**16**, Fig. 2) with 1,4-phenelynediamine (**22**, Fig. 2) and benzidine (**28**, Fig. 2), respectively. Subsequently, an amino-substituted 1,4-phenylenediamine (**26**, Figs. 2, 6) and amino-substituted benzidine (**31**, Fig. 2) were used to displace the 1,4-phenelynediamine in **PTPA** and the benzidine in **PTBD** to produce their daughter imine-based COFs endowed with amino moieties, **PTBD-NH$_2$** (Scheme 17).

The BBE process was completed after 3 days of reaction and 40 °C was the most favorable condition for the BBE preparation of **PTBD-NH$_2$** and **PTPA-NH$_2$**. This fact is remarkable because, in contrast with the traditional synthesis of COFs with high temperature, the BBE process occurs under moderate temperature. This can be rationalized taking into account that high temperature leads to the high solubility for the reactant and high reaction rate, which is unsuitable for the replacement reaction. As observed by Zhao *et al.* in the work discussed above, the more active 1,4-phenelynediamine derivative was able to readily displace benzidine, although in this case only 1 equiv of amino-substituted 1,4-phenelynediamine was needed. On the other hand, 10 equiv of amino-substituted benzidine where need to displace 1,4-phenylendiamine, corroborating the hypothesis that monomer reactivity is a key factor when designing BBE reactions. This strategy not only extends for the first time the amino-function into COF materials, but also paves the way for the preparation of other *de novo* inaccessible functionalized COFs.

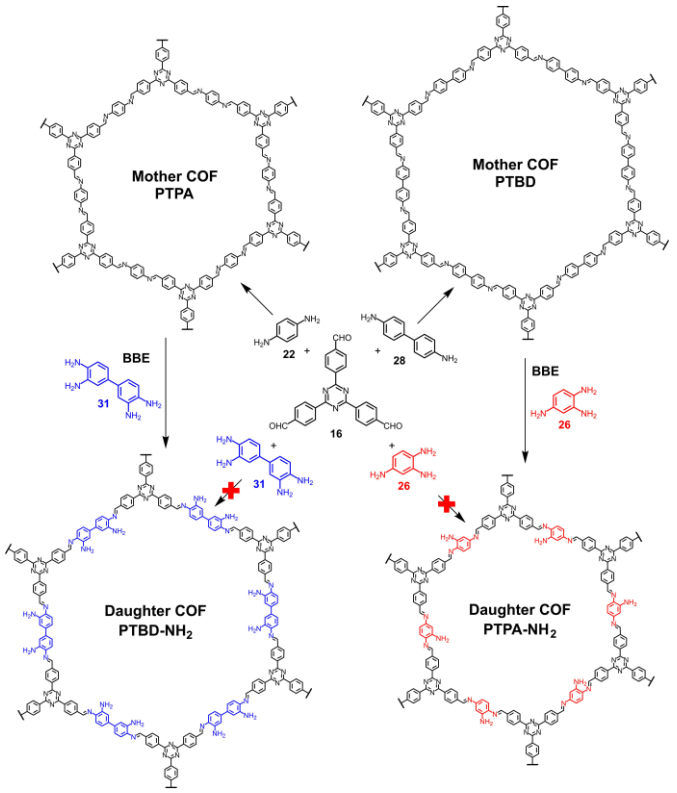

Scheme 17 Preparation of *de novo* unreachable COFs **PTBD-NH$_2$** and **PTPA-NH$_2$** through the BBE strategy.

Another challenge in the synthesis of COFs is the incorporation of linkages with limited reversibility. The characteristic reversibility of dynamic covalent chemistry not only leads to crystallinity through dynamic error correction during synthesis but also diminishes the resulting material's chemical stability. With the aim to address this stability problem, in 2018, new functionalities were incorporated into COFs by post-synthetic linker exchange in order to bring about subsequent reactivity that leads to modified linkages.[149] The study was carried out with imine-linked **ILCOF-1** based on 1,4- phenylenediamine (**22**, Fig. 2) and 1,3,6,8-tetrakis(4-formylphenyl)-pyrene (**18**, Fig. 2) which was converted through consecutive linker substitution and oxidative cyclization to two isostructural covalent organic frameworks, having thiazole and oxazole linkages (Scheme 18).

The synthesis of the new thiazole-linked COF, named **COF-921**, was accessed by substitution of the 1,4-phenylenediamine linkers in **ILCOF-1** with 2,5-diaminobenzene-1,4-dithiol dihydrochloride in a mixture of DMF and water (Scheme 18). It was found that performing the reaction under an atmosphere

of oxygen gave the desired product without structural degradation. On the other hand, the analogous oxazole-linked framework, named **LZU-192**, could be also accessed *via* linker exchange by using 2,5-diaminohydroquinone dihydrochloride as the new linker (Scheme 18). As in the previous case, by allowing the reaction to proceed under oxygen the imine is well-converted into the stable oxazole moiety. Chemical stability tests were carried out with the azole-containing COFs showing the increased irreversibility of the azole linkages and that this technique is capable of producing chemically stable materials. This contribution represents the first combination of building block exchange and chemical conversion of linkages in order to have access to COFs based on irreversible linkers which are not accessible *via de novo*.

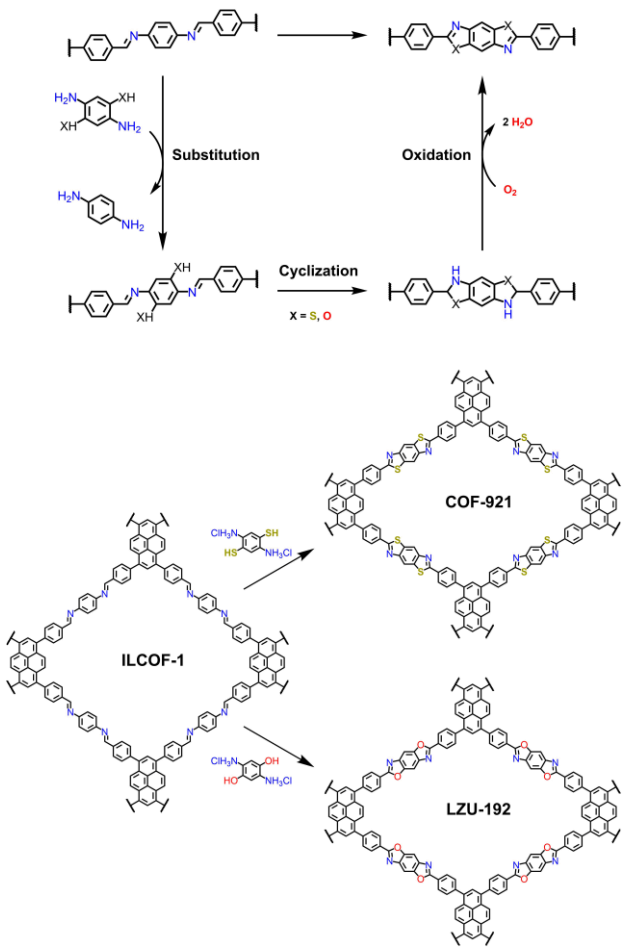

Scheme 18 Top: Proposed strategy for the synthesis of azole-linked COFs through substitution, cyclization and oxidation. Bottom: Synthesis of azole-linked **COF-921** and **LZU-192** materials from the imine precursor **ILCOF-1**.

As we have already mentioned, β-ketoenamine-linked COFs are formed by the direct condensation of multifunctional amines with triformylphloroglucinol (**14**, Fig. 2) in which imine formation is accompanied by a tautomerization that imparts increased stability.[119] While the stability is beneficial in the isolated material, it reduces the possibility of exchange processes that correct defects during the polymerization. Therefore, β-ketoenamine-linked COFs frequently exhibit smaller average crystalline domain sizes and lower surface areas and pore volumes than the parent imine-linked networks. Thus, in 2019, Dichtel and co-workers have shown that β-ketoenamine-linked COFs can be also obtained *via* BBE reactions. With this aim, a suitable imine-linked 2D-COF that is isostructural to the desired framework is formed and isolated. Subsequently, exchange is performed to give the less dynamic and more stable β-ketoenamine-linked material. It is worth noting that even the limited error-correction available to the β-ketoenamine linkage is sufficient to obtain a high-quality COF. In addition, the favorable thermodynamics of the formation of this linkage promotes complete exchange.[150] Building block exchange can be carried out by exposing these imine-linked COFs to one equivalent of triformylphloroglucinol (**14**, Fig. 2) (with respect to triformylbenzene) in a deoxygenated mixture of 1,4-dioxane, mesitylene, and 6 M acetic acid (3:3:1 volume ratio) at 120 °C for 3 days. The generality of this approach was tested with different imine-based COFs. Interestingly, the β-ketoenamine-linked COFs obtained exhibit not only higher surface areas but also higher crystallinity in comparison with previous reports as determined by PXRD. Furthermore, the stability of β-ketoenamine-linked COFs obtained by this BBE strategy compares exceptionally well to other known highly stable frameworks, including those with higher degrees of conjugation. This study certainly advances the potential of using the building block exchange strategy to improve the crystallinity and surface area of other β-ketoenamine-linked COFs, especially for those with interesting electronic, redox and optical properties that rely on improved long-range order.

Very recently this strategy has been extended to 3D-COFs. In fact, the first dimensional transformation between a 3D-COF and a 2D-COF has been reported by using this linker exchange approach to replace a tetragonal monomer with a planar one.[151]

4.3. Post-functionalization of COFs *via* cycloaddition reactions

In 2015, Jiang and co-workers reported for the first time a photo-responsive, structurally dynamic COF by condensation of 1,3,5-benzenetriboronic acid (**64**, Fig. 2) and 2,3,6,7-tetrahydroxyanthracene (**56**, Fig. 2) under solvothermal conditions.[152] One interesting feature of this COF is that the anthracene columns in **Ph-An-COF** are configured in a face-on-face π-stacking mode with a vertical interlayer separation of 3.4 Å between two anthracene units. This type of stacking mode and the suitable distance (<4.2 Å) is favorable for photoinduced [4π+4π] cycloaddition. Thus, irradiation of the COF films onto a quartz substrate under Ar with 360 nm light produces the cycloaddition of the anthracene units in the π-columns, transforming the planar 2D sheets into concavo-convex polygon skeletons. The photoinduced structural transformation is accompanied by a change in gas storage capability and monotonic decrease of the fluorescence intensity because the resulting cycloaddition dimers are not luminescent. Interestingly, these photoinduced hierarchical transformations are reversible by virtue of the thermally allowed reversibility of the cycloaddition reaction. Therefore, the anthracene units are recovered quantitatively upon heating the samples at 100 °C.

This contribution represents a good example of how COFs can behave as smart materials in which properties such as gas adsorption or luminescence can be controlled by external stimuli.

In 2016, Banerjee and co-workers used anthracene-containing COFs in order to take advantage of the susceptibility towards [4+2] cycloaddition reactions of anthracene[153] for post-synthetic functionalization. Thus, the anthracene-containing COF (**DaTP**, Scheme 19) can be subjected to a [4+2] Diels–Alder cycloaddition reaction with the dienophile *N*-hexylmaleimide upon heating at 160 °C for 24 hours.[154] A relevant feature of this post-synthetic strategy is that the cycloaddition disturbs the π-π stacking of the COF layers and produces a loss of planarity in the anthracene units, which results in exfoliation to yield covalent organic nanosheets (CON). Even free-standing CON thin films with tunable thickness at air–water interfaces can be prepared through simple layer-by-layer techniques.

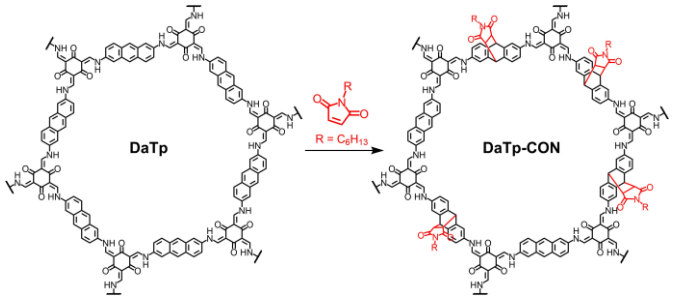

Scheme 19 Synthesis of **DaTp-CON** *via* Diels-Alder cycloaddition reaction.

This chemical exfoliation technique certainly represents an efficient tool for COF manipulation toward thin-film layer-by-layer assembly.

5. Functional group interconversion

The presence of ordered and well-defined pores in COFs opens the possibility of incorporating pendant groups which can undergo functional group interconversion. This strategy, commonly known as pore-wall engineering or channel-wall modification, is a very versatile approach to introduce new functionalities into COFs. In principle, most of the reactions developed for the covalent post-synthetic modification of traditional polymers are also applicable to COFs, even though limitations regarding minimization of side reactions, difficulty in product purification, and size and solubility limitations must be taken into account. Moreover, reactions involving heterogeneous catalysts or insoluble byproducts present a challenge when applied to COFs. Out of the wide variety of reactions available in organic chemistry, by far the most commonly used for functional group interconversion in COFs are (i) addition reactions, and (ii) substitution reactions.

Addition reactions used in post-polymerization modifications are often identical to their molecular counterparts. In this way, a functional group on the COF pore will react with, in most cases, a small molecule in an addition reaction. This class encompasses click chemistry reactions, which are the most widely used reactions for functional group interconversion. Thus, click chemistry has been used to introduce aliphatic and aromatic groups, acids, esters, amines, alcohols, thiols, fullerenes or radicals among other moieties.[155-161] Similarly, acid groups have been incorporated into COFs by ring opening reaction of phenol groups with succinic anhydride.[162, 163] Another example is the amidation[164] and amidoximation[164, 165] of nitriles with NaOH or NH_2OH respectively. Finally, a strategy named inverse vulcanization has been used to anchor polysulfides directly to COFs pores *via* strong C-S bonds.[166, 167]

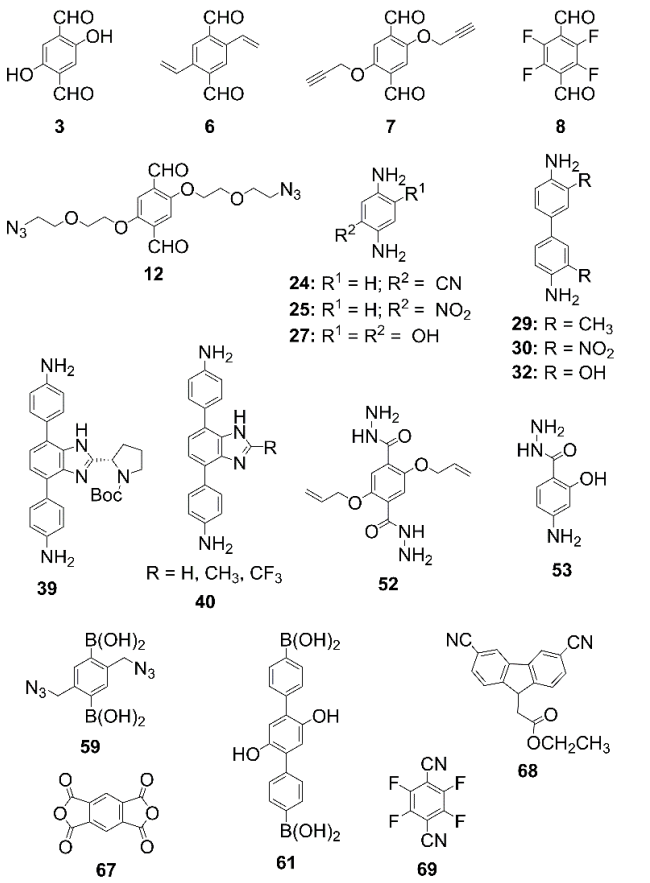

Fig. 6 Monomers used for the post-synthetic modification of COFs by functional group interconversion.

Regarding substitution reactions, a wide variety has been used for post-polymerization modifications. This comprises the acylation[168] and etherification[169, 170] of phenol groups with acyl chlorides and alkyl bromides respectively. Amidation reactions have also been carried out either with the carbonyl moiety attached to the COF, in the form of an activated ester,[171] or with the amine moiety present in the pores, by reaction with acetic anhydride.[172] Oxidations and reductions have also been applied, with examples being the phenol oxidation to quinones,[160] or the nitro[172, 173] and azide[174] reduction to amines. Other examples of substitution reactions can be found in the aromatic nucleophilic substitution of aryl fluorides,[175] the halogenation of alkyl chains[176] or the formation of salts with lithium[177] or sodium[178] atoms.

Table 2 Reactions used for the post-synthetic modification of COFs *via* functional group interconversion.

PSM reaction	COF	Monomers	Application	Ref.
CuAAC reactions	X%RTrz-COF-5	55+59+58	Selective adsorption of CO_2 over N_2	155
	100%EsTrz-NiPc-COF	57-Ni+59+58	--------	155
	$[C_{60}]_y$-ZnPc-COF	57-Zn+59+58	Photoinduced electron transfer and charge separation	159
	$[Pyr]_x$-H_2P-COF	43+7+4	Catalyst for the Michael addition reaction	156
	$[R]_x$-H_2P-COF	43+7+4	CO_2 adsorbent	157
	$[TEMPO]_{x\%}$-NiP-COF	44-Ni+7+4	Capacitive energy storage	183
	$[(S)\text{-Py}]_x$-TPB-DMTP-COF	41+7+4	Catalyst for the asymmetric Michael reaction	184
	T-COF-X	41+7+4	---------	161
	TEMPO-COF	41+7+4	Cathode for lithium-ion batteries	160
	$[Uracil]_x$-TPB-DMTP-COF	41+7+4	Nucleobase recognition in aqueous media	185
	TPB-DMTP-COF-SH	41+7+4	Hg capture from contaminated water	158
Thiol-ene reactions	COF-S-SH	41+6	Hg capture from contaminated water	189
	COF-VF	41+6	Coating to afford superhydrophobic substrates	190
	Cross-linked COF membrane	14+52	Catalyst for chlorobenzenes dechlorination in water	191
	COF-102-SPr	65+66	----------	188
Inverse vulcanization	mp-COF-graft-PS	41+7+4	Cathode for lithium organic batteries	167
	S-COF-V	41+6	Cathode for lithium-sulfur batteries	166
SNAr	COF-F-S	42+8	Cathode for lithium-sulfur batteries	175
Activated ester to amide	biomolecules@COF	42+67	Chiral stationary phase for HPLC	171
Ester hydrolysis	CTF-CSU37@post	68	Selective adsorption of CO_2 over N_2	198
Ester ammonolysis	CTF-CSU36@post	68	Selective adsorption of CO_2 over N_2	198
Nitrile amidoximation	COF-TpDb-AO	14+24	U capture from contaminated water	165
	COF-316-C(NOH)NH_2	55+69	--------	164
Nitrile amidation	COF-316-$CONH_2$	55+69	--------	164
Nitrile hydrolysis	JUC-505-COOH	55+69	Removal of antibiotics from water	201
Nitrile reduction	JUC-505-NH_2	55+69	Removal of antibiotics from water	201
Azide reduction	X%[NH_2]-COF	41+12+1	Per- and polyfluorinated alkyl substances (PFAS) capture from contaminated water	174
BOC deprotection	LZU-72	13+39	--------	202
	LZU-76	14+39	Catalyst for the asymmetric aldol reaction	202
Imidazolate formation	Li-ImCOF	13+41	Single-ion conducting solid-state electrolyte	177
Ring opening reaction	$[HO_2C]_{x\%}$-H_2P-COF	43+3+1	Selective adsorption of CO_2 over N_2	162
	3D-COOH-COF	20+32	Selective adsorption of Nd^{III} over Sr^{II} and Fe^{III}	163
Acylation reaction	$[R]_{x\%}$-H_2P-COF	43+3+1	Selective adsorption of CO_2 over N_2	168
Phenol deprotonation	COF-ONa	41+3	Enzyme adsorption	178
Williamson reaction	$[Et_4NBr]_{x\%}$-Py-COF	47+3+1	Catalyst for the *N*-formylation of amines	169
	$[BE]_{x\%}$-TD-COF	41+3+4	Catalyst in the reduction of CO_2	170
Isothiocyanate coupling	T-COF-OFITC	55+61	--------	204
	COF-5-FITC	55+58	--------	204
Phenol oxidation to quinones	DABQ-TFP-COF	14+27	Cathode for organic rechargeable batteries	160
Reduction of nitro to amine groups	TpPa-NH_2	14+25	---------	173
	TpBD(NH_2)$_2$	14+30	Lactic acid adsorption	172
Amide formation	TpBD($NHCOCH_3$)$_2$	14+30	Lactic acid adsorption	172
	ATTO633 modified COF	55+63+58	----------	213
Michael addition	PEG-modified COF	62+58	----------	213
Bromination	TpBD-MeBr	14+29	Anion exchange membrane fuel cells	176
Amine quaternization	TpBD-MeQA$^+OH^-$			
Epoxy ring opening	TpASH-Glc	14+53	Drug delivery	207
Silylation	TpASH-APTES			
Amide formation	TpASH-FA			
Epoxy ring opening	TpASH-Glc	14+53	H_2S detection and imaging in live cells and deep tissue	209
Silylation	TpASH-NPHS			

5.1. Copper catalyzed azide-alkyne cycloaddition (CuAAC) reactions

Researchers in the (nano) materials and polymer sciences have been continuously searching for well-defined ligation strategies that can be effectively used in the presence of a wide range of different functional groups typically encountered in these fields. Important requirements for successful ligation strategies are orthogonality to other functional groups, high selectivity, compatibility with water and other protic solvents and, if possible, with almost quantitative yields. In this regard, Sharples and co-workers[179] developed the approach known as click chemistry, that was defined as a set of stringent criteria that a process must meet to be useful in this context and which can be listed as modular and wide in scope, high efficiency and high yields, no or inoffensive byproducts, stereospecific, readily available starting materials and reagents, no solvent or a benign solvent, and simple purification techniques.[180] Although there are several efficient organic reactions that have been claimed to be click reactions since they fulfilled all or some of the above mentioned click chemistry criteria, the Huisgen 1,3-dipolar azide–alkyne cycloaddition is probably the most important exponent. In its classical thermal version, this chemical transformation is characterized by broad tolerance to diverse functional groups and reaction conditions as well as by high reliability. Nevertheless, it was not until the finding of the copper(I)-catalyzed variant of this reaction by the groups of Meldal[181] and Fokin and Sharpless[182] that the current potential of this coupling technology was shown. On the practical level, the copper(I) catalyst can be generated in situ using copper(II) sulfate and sodium ascorbate as reducing agent.

From all of the above, it was not surprising that the first post-synthetic modification in COFs by covalent bond formation reported in 2011 by Jiang and co-workers made use of the copper catalyzed azide-alkyne cycloaddition (CuAAC) click reaction.[155]

With this aim they used **COF-5** as scaffold, which is a typical mesoporous COF that consists of triphenylene at the corners and phenylene on the walls of a boronate ester-linked two-dimensional (2D) hexagonal skeleton. Azide groups were incorporated to the 2 and 5 positions of the phenylene unit of 1,4-benzenediboronic acid (**58**, Fig. 2) to yield the azide-appended benzenediboronic acid (**59**, Figs. 2, 6), which was utilized as wall block for the condensation reaction with hexahydroxytriphenylene (**55**, Fig. 2). The azide units in the skeletons are reactive groups that can click with various alkynes for pre-designable functionalization (Scheme 20). Interestingly, the content of azide units on the pore walls can be tuned using a three-component condensation system with **55** as the corners and a mixture of **58** and **59** as the walls. Thus, changing the ratio of **58** to **59** allows the regulation of the overall azide content on the walls. The wide scope of the strategy is demonstrated by the compatibility with (i) different moieties, including long alkyl chains, polar ester groups or large pyrene moieties; and (ii) a different COF scaffold, **N_3-NiPc-COF**, which was functionalized with ester groups. Furthermore, in 2014, Jiang and co-workers broadened the scope of this strategy with the synthesis of an electron-donor COF based on phthalocyanine moieties and with azide functionalities (Scheme 20). They demonstrated that the pores can be also post-functionalized *via* the CuAAC click reaction to afford a COF with covalently bound electron-acceptor [60]fullerene moieties in the pores (**$[C_{60}]_y$-ZnPc-COFs**).[159] This strategy represents a general protocol for constructing COFs with photoelectric donor–acceptor structures with great potential for charge separation and photoenergy conversion.

The CuAAC click reaction is not only compatible with COFs based on boronic esters in the backbone but it can also be used to post-functionalize COFs based on imine linkages. Thus, in 2014, Jiang and co-workers reported the synthesis of an imine-based COF with pendant alkyne moieties in the pores (Scheme 21, **$[HC{\equiv}C]_X$-H_2P-COFs**, X = 25, 50, 75, and 100 (X = 0: **H_2P-COF**)). The number x indicates the percentage of linkers with the alkyne moieties versus the unsubstituted linkers based upon the ratios of reactants. This alkyne-functionalized COFs were subsequently functionalized *via* the CuAAC click reaction with pyrrolidine units containing azide moieties.[156]

By means of this strategy, aqueous organocatalytic COFs (**$[Pyr]_X$-H_2P-COFs**, Scheme 21a) have been synthesized combining a number of striking catalytic features, including significantly enhanced activity, good recyclability and high capability to perform transformation under continuous flow conditions.

In a following study, the same **$[HC{\equiv}C]_X$-H_2P-COFs** were further post-functionalized *via* the CuAAC click reaction to incorporate different moieties including alkyl chains, carboxylic acid, ester, alcohol and amino groups (Scheme 21b). Thus, these COFs offer an ideal platform for pore-wall surface engineering aimed at anchoring a variety of functional groups ranging from hydrophobic to hydrophilic units and from basic to acidic moieties with tunable loading contents.[157] In addition, Jiang and co-workers demonstrated that this strategy can be used to efficiently screen for suitable pore structures for use as CO_2 adsorbents.

An analogous alkyne-containing COF but based on metalated porphyrins (**$[HC{\equiv}C]_{X\%}$-NiP-COF**; X=0, 50, and 100, Scheme 21c), was used by Jiang and co-workers to immobilize open-accessible polyradicals on the pore walls of the COF.[183] The number x indicates the percentage of linkers with the acetylene versus the OH-containing linkage based upon the ratios of reactants. The radical frameworks with openly accessible polyradicals immobilized on the pore walls experienced rapid and reversible redox reactions, giving rise to capacitive energy storage with high capacitance, robust cycle stability and high-rate kinetics. This result has paved the way for the further functionalization of the pores with redox-active species toward the development of COFs for energy storage.

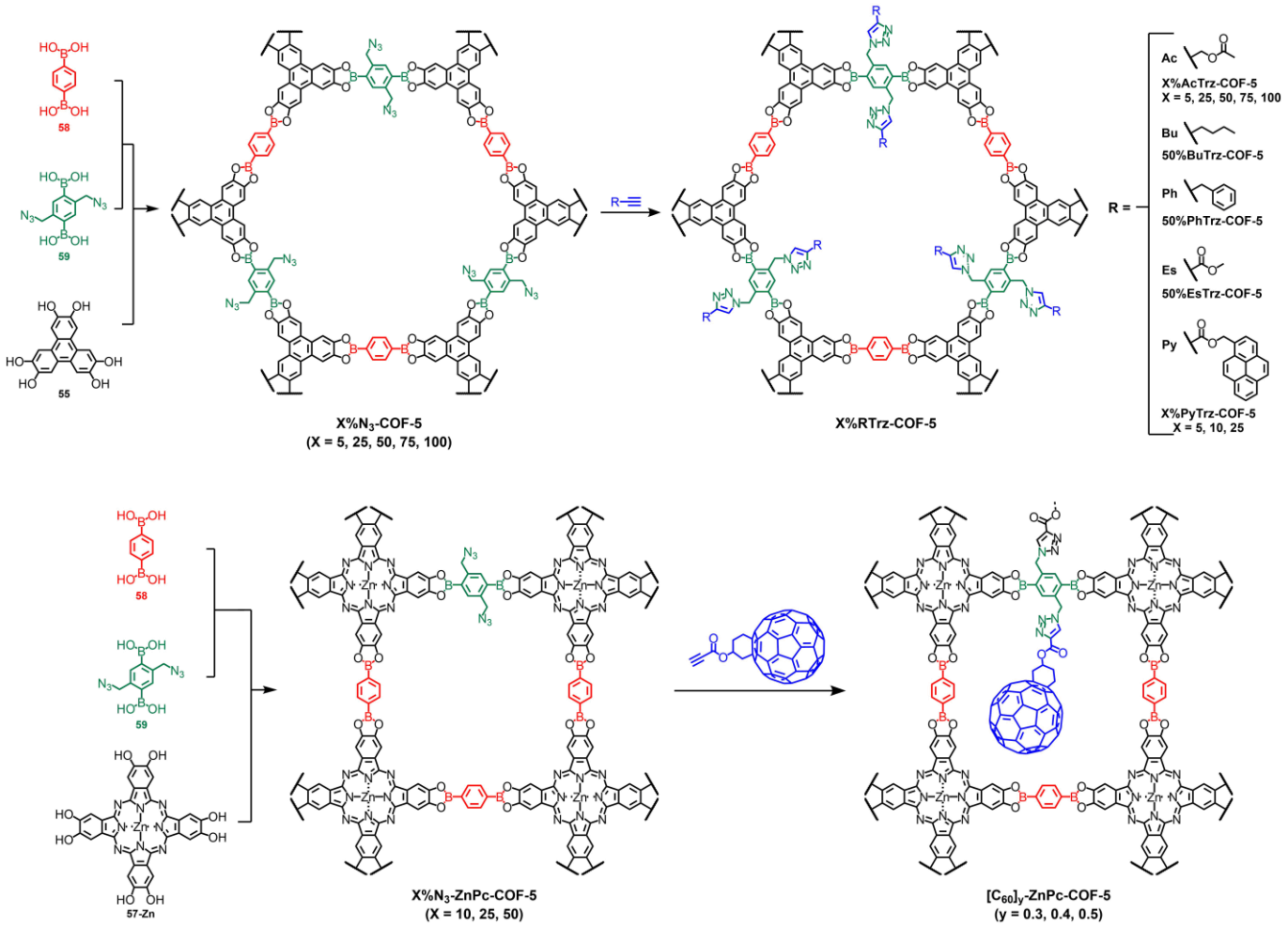

Scheme 20 Top: Synthesis of **X%N3-COF-5** with different contents (*X* = 5, 25, 50, 75 and 100) of azide moieties and covalent post-synthetic pore wall functionalization *via* click reaction with alkynes to anchor various organic groups onto COF walls (**X%RTrz-COF-5**). Bottom: Synthesis of **X%N3-ZnPc-COF** with different contents (*X* = 10, 25, 50) of azide moieties and covalent post-synthetic pore wall functionalization *via* click reaction with an alkyne-containing fullerene to prepare **[C60]y-ZnPc-COFs** as segregated donor–acceptor arrays.

Another interesting scaffold which has been used for post-functionalization *via* CuAAC of alkyne functionalized COFs is depicted in Scheme 22. It can be obtained by reaction between 2,5-dimethoxyterephthalaldehyde (**DMTA**, **4**, Fig. 2) and 1,3,5-tris-(4-aminophenyl)benzene (**41**, Fig. 2). It possesses fully conjugated rings, tight π-stacking and excellent chemical stability. Modified versions of this COF can be prepared by using a three-component system with **41**, **4**, and 2,5-bis(2-propynyloxy)terephthalaldehyde (**BPTA**, **7**, Figs. 2, 6). The stoichiometry of **DMTA** and **BPTA** can be varied to produce the COF series (COF-x, x = 0, 25, 50, 75, 100). The number x indicates the percentage of linkers with the acetylene versus the ether linkage based upon the ratios of reactants (Scheme 22).[184] In the first modification of this COF, Jiang and co-workers carried out CuAAC post-synthetic modification with an azide-containing chiral pyrrolidine, thus providing chiral COFs which can be used as chiral heterogeneous organocatalyst for the asymmetric Michael reaction with high catalytic activity, enantioselectivity and recyclability.

Further modifications of this scaffold with other azide containing moieties have been recently reported. Thus, Johnson and co-workers prepared a series of COFs that possess a tunable density of covalently bound nitroxyl radicals within the COF pores.[161] Feng, Wang and co-workers have prepared a similar COF with bound nitroxyl radicals within the COF pores and used them in combination with other redox-active COFs as cathode materials for lithium-ion batteries.[160] Somoza, Zamora, Segura and co-workers have recently modified this COF *via* CuAAC post-synthetic modification with a nucleobase. The nucleobase-modified COF has been successfully used for the selective recognition of the complementary nucleobase in water. The results obtained show how the confinement of the base-pair inside the COF's pores allows a remarkable selective recognition in aqueous media.[185]

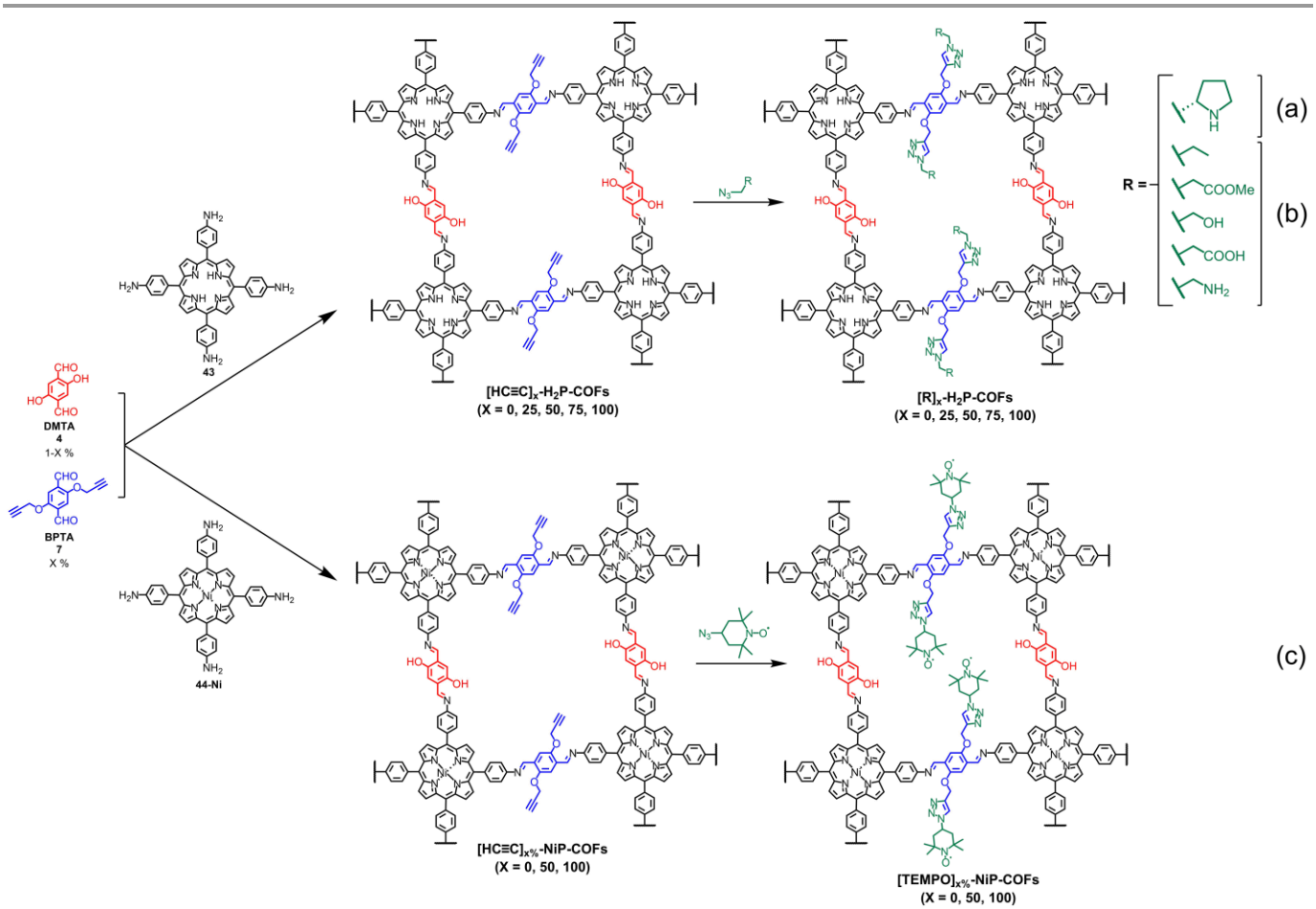

Scheme 21 General strategy for the pore surface engineering of porphyrin-containing imine-linked COFs *via* a condensation reaction and click chemistries. (a) Pyrrolidine containing COFs with catalytic activity. (b) COFs with different functional groups in the pores used as CO_2 adsorbents. (c) COFs with immobilized polyradicals for capacitive energy storage.

Segura, Mancheño and co-workers have modified this same COF *via* CuAAC post-synthetic modification and incorporated thiol functionalities.[158] The incorporation of thiol groups into the COF was accomplished by the reaction of a bisazide, namely 1,2-bis(2-azidoethyl)disulfane, with **[HC≡C]$_{0.5}$-TPB-DMTP-COF** followed by treatment with the Cleland reagent (dithiothreitol, DTT). This strategy allows the simultaneous incorporation in this highly porous organic framework of the thiol groups and the characteristic triazole moieties of the CuAAC reaction. The cooperative effect of triazole and accessible thiol (–SH) functionalities within the pores allows this material to capture Hg^{II} ranging from trace levels to highly concentrated solutions with outstanding efficiency. Thus, the material shows a record saturation mercury uptake capacity and can effectively reduce the Hg^{II} concentration from 10 mg L^{-1} to an extremely low level of 1.5 mg L^{-1} in only 10 minutes, which is below the acceptable limits in drinking water standards (2 mg L^{-1}). These remarkable results offer new prospects for the use of imine-based COFs for environmental remediation and the decontamination of aqueous media, a matter of great importance for populations at risk due to mercury pollution, especially in underdeveloped areas.

5.2. Thiol-ene reactions

While the Cu^{I} catalyzed alkyne-azide (CuAAC) reaction is still the preeminent click reaction, the thiol-ene reaction also meet the relevant criteria to be accurately described as click and accounts for the current renewed interest in this classical chemistry.[186] Thiol-ene reactions involve the addition of thiols to carbon-carbon double bonds under mild conditions and with high efficiency. There are two main categories of thiol-ene reactions: (i) the catalyzed thiol-Michael addition of a thiol to an electron-deficient carbon-carbon double bond and (ii) the free-radical thiol-ene addition of a thiol to an electron-rich/electron-poor double bond. The thiol-ene free radical addition has been gaining prominence in the field of coatings and surfaces due to the spatial and temporal control enabled by UV-initiation, rapid kinetics and insensitivity to oxygen.[187]

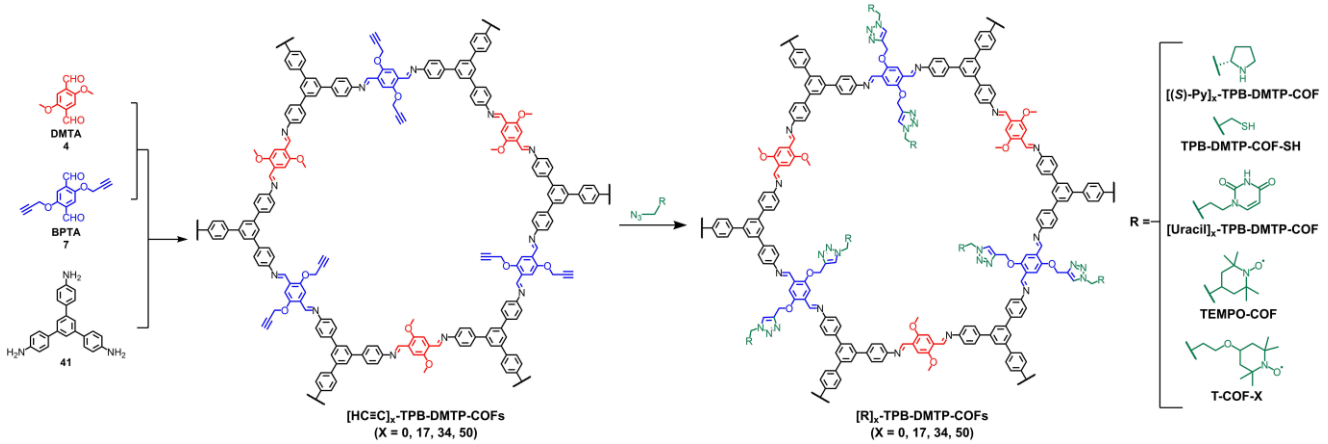

Scheme 22 Synthesis and functionalization of **[HC≡C]x-TPB-DMTP-COF** *via* click chemistry.

The first reported thiol-ene free radical addition reaction with a COF system was described by Dichtel and co-workers in 2013[188] and we will specifically comment it in the section dedicated to the monomer truncation strategy for the internal functionalization of three-dimensional COFs. A second example of this strategy was reported by Ma and co-workers, who used a post-synthetically modified COF *via* thiol-ene reaction for mercury removal.[189] With this aim, they designed a vinyl-functionalized COF (**COF-V**) which can be obtained by condensation reaction between 2,5-divinylterephthalaldehyde (**6**, Figs. 2, 6) and 1,3,5-tris(4-aminophenyl)benzene (**41**, Fig. 2). Further thiol-ene reaction with 1,2-ethanedithiole in the presence of AIBN as radical initiator provided the corresponding COF functionalized with thiol moieties (**COF-S-SH**, Scheme 23). This new material removes mercury from aqueous solutions and air, affording Hg^{II} and Hg^{0} capacities of 1350 and 863 mg g^{-1}. This contribution is a new example of the exceptional potential of COFs for high performance environmental remediation.

In 2018, Ma and co-workers have used the thiol-ene click reaction to graft fluorinated compounds onto the same vinyl-functionalized COF (**COF-V**, Scheme 23) in order to integrate superwettability within COFs for functional coating.[190] Taking advantage from the bulk superhydrophobicity of the COF crystals and the feasibility of COF synthesis, they can be used as a coat or in situ integrated within various substrates such as melamine foam and magnetic liquids. Interestingly, once applied, this renders them superhydrophobic. These novel materials share the attributes of general superhydrophobic surfaces, such as self-cleaning and waterproofing with the unique functions resulting of the intrinsic properties of COFs highlighting the opportunity to design smart materials.

Dong and co-workers have incorporated thiol-functionalized polysiloxane to an allyl-decorated COF in which Pd nanoparticles had been previously supported.[191] Thiol-ene reaction between the thiol-functionalized polysiloxane and the allyl-decorated COF with Pd nanoparticles provides an efficient way to produce a stand-alone and elastic membrane. This membrane is permanently porous, robust, processable, uniform and water permeable. Furthermore, it can be used to construct highly efficient membrane-based microreactor for continuous-flow operation to catalyze chlorobenzenes (CBs) dechlorination in water at room temperature. This approach provides an innovative synthetic methodology for the fabrication of self-standing and covalently cross-linked COF-based and metal nanoparticles-loaded membranes.

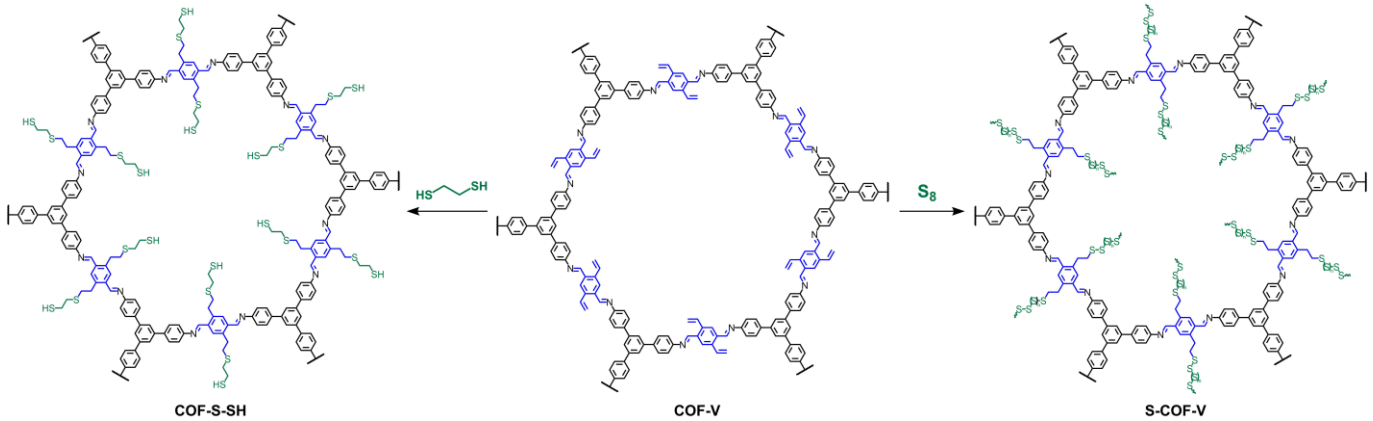

Scheme 23 Post-synthetic modification of **COF-V** by thiol-ene reaction with 1,2-ethanediole to afford **COF-S-SH** and by inverse vulcanization with sulfur to yield **S-COF-V**.

5.3. Inverse vulcanization

Related with the above thiol-ene reaction is a post-synthetic graft-polymerization strategy named inverse vulcanization which has been developed by Pyun and co-workers in order to prepare polymers with a high sulfur content directly from elemental sulfur for their use as active cathode materials in Li-S batteries.[192, 193] This strategy allows for sulfur loading and robust C-S binding through thermally activated radical polymerization between sulfur and vinyl groups. Thus, Xu, Chen and co-workers have recently immobilized sulfur within the pores of the vinyl functionalized **COF-V** *via* the inverse vulcanization strategy (Scheme 23).[166] The procedure involves uniform mixing of **COF-V** and elemental sulfur by grinding. Subsequent thermal treatment at 155 °C under vacuum in a sealed tube enable the fluid of molten liquid sulfur to be infiltrated into the pores. To ensure the ring-opening polymerization (ROP) of S_8 and fully copolymerization between the polysulfur diradicals and vinyl groups, further heat treatment at elevated temperature of 200 °C is required.

When this material is used as cathode for Li-S batteries the characteristic shuttle effect of polysulfides can be efficiently suppressed owing to the synergetic chemical covalent binding with the vinyl groups and physical confinement by the mesoporous channels. Analysis of the Li-S batteries indicate high initial capacity of 1400 mA h g^{-1}, which retained 959 mA h g^{-1} after 100 cycles at 0.2 C representing one of the best performances of reported COF-based sulfur cathodes.

A similar strategy based on the inverse vulcanization process has been also used by Zhang, Awaga and co-workers but using an alkyne modified COF instead of the vinyl analogue. They have also used the materials as cathodes for rechargeable lithium organic batteries with a capacity of 425 mA h g^{-1} at a rate of 250 mA g^{-1} in the initial cycle and with good cycling performance.[167]

These contributions show how this graft polymerization strategy represents a facile method for developing high performance rechargeable lithium organic batteries by using catalyst- and solvent-free reaction conditions with the low cost and environmentally benign sulfur.

5.4. Aromatic Nucleophilic substitution of aryl fluorides

Aromatic nucleophilic substitution (SNAr) strategies for the incorporation of sulfur into aryl moieties are appealing due to their low environmental impact, mild conditions and no requirement for transition metal catalysis. A number of S-arylations proceeding through a SNAr pathway have been developed.[194] An efficient S-arylation reaction based in SNAr takes place with aromatic rings endowed with fluorine substituents. Thus, in 2018, Kuang, Zhang and co-workers have reported the synthesis of a porous 2D-COF (**COF-F**, Scheme 24) with high content of aromatic fluoride substituents on the backbone which can undergo SNAr reaction with sulfur.[175] **COF-F** contains tetrafluoro benzene moieties with enhanced reactivity in SNAr reactions between sulfur and aromatic fluoride which can be used for the covalent attachment of sulfur to the COF skeleton under suitable conditions. Thus, the reaction is carried out in two steps. First a mixture of elemental sulfur and polymer in 3:1 weight ratio is heated at 160 °C for 15 h to ensure sufficient impregnation of molten linear sulfur chains in the polymer pores. Afterwards the mixture is heated at 350 °C for another 15 h to assist the SNAr reaction between aromatic fluoride and sulfur to covalently link sulfur to the polymer backbone yielding **COF-F-S** (Scheme 24). After the physical and chemical confinement of sulfur through this post-functionalization approach, the COF material still shows some structural order. Interestingly, because of its higher porosity, this crystalline **COF-F** provides higher sulfur loading (60 wt %) and more structural order after sulfur confinement compared to analogous amorphous macromolecular materials.

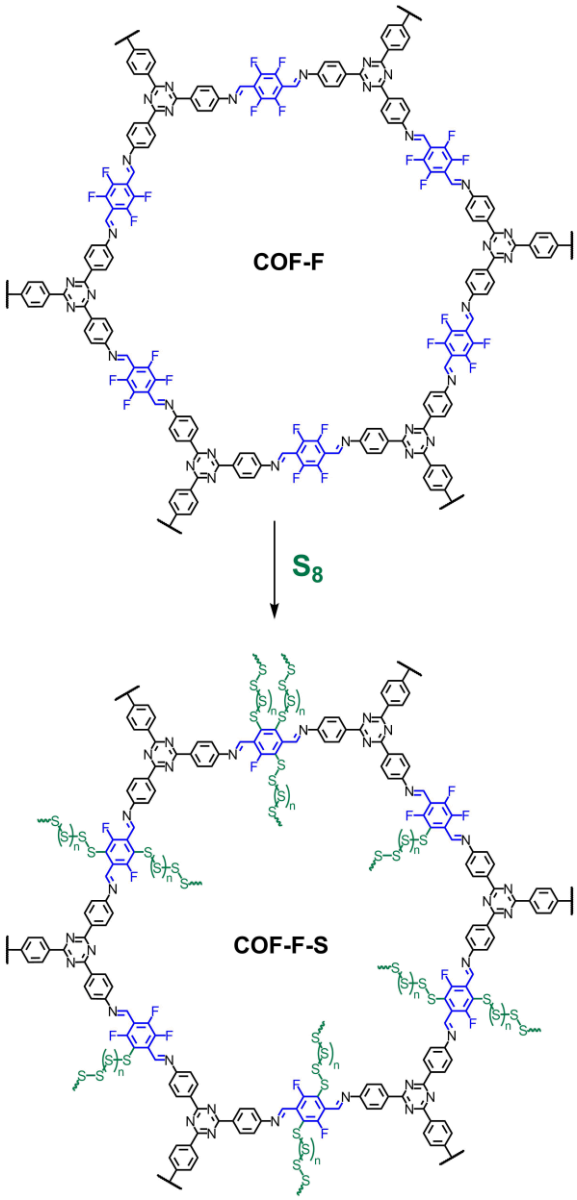

Scheme 24 Post-synthetic modification of **COF-F** by SNAr with sulfur.

The study of the performance of **COF-F-S** as cathode material in lithium-sulfur batteries in comparison with parent analogous amorphous macromolecular materials indicates that the high porosity derived from the AA stacked 2D-COF structure is advantageous because it allows high sulfur loading, efficient ion transport, fast reaction kinetics and increased electrical conductivity.

5.5. Post-polymerization Modifications of ester groups including active esters

Following the seminal work of the groups of Ringsdorf and Ferruti,[195, 196] many studies have shown the benefits of using polymeric active esters from simple polymer chemistry to materials and life science and beyond. Thus, although active esters are very classical reactive groups, they still represent one of the most useful groups for post-polymerization modifications. The main reasons for the extensive use of this post-polymerization strategies are: (i) that the reaction between amines and active esters proceeds under very mild conditions (including room temperature) with almost quantitative yields of the corresponding amides and (ii) the reaction proceeds without the auxiliary usage of a metal catalyst.

This strategy has been recently used to immobilize biomolecules such as enzymes into covalent organic frameworks. With this aim, Zhang, Chen, Ma and co-workers carried out the synthesis of a COF bearing carboxylate groups.[171] The corresponding COF (**TS-COF-1**) was obtained under solvothermal conditions by reaction between pyromellitic dianhydride (**67**, Figs. 2, 6) and 1,3,5-tris-(4-aminophenyl)triazine (**42**, Fig. 2) (Scheme 25). It is worth pointing out that the condensation reaction of an anhydride and a primary amine possesses a two-step mechanism.[197] First, the anhydride reacts with the primary amine to form amic acid intermediates *via* a spontaneous ring opening process. Second, by increasing the reaction temperature above 150 °C, the amic acid dehydrates to form an imide group. Thus, carboxylate groups (-COOH) can exist as residuals during this condensation reaction. In fact, by using toluidine blue O (**TBO**) assay and acid-base titration, good amount of COOH residues (*ca.* 6%) were determined to be in the COF. In order to create activated ester functionalities, the COF was reacted with 1-ethyl-3-(3-dimethylaminopropyl) carbodiimide (**EDC**) and *N*-hydroxysuccinimide (**NHS**). The subsequent reaction of this COF with biomolecules containing amino groups such as amino acids or peptides afforded the corresponding COFs with the biomolecules covalently anchored on the channel walls of the COF (Scheme 25).

In this contribution it is shown that the **biomolecules⊂COFs** obtained can serve as chiral stationary phases towards various racemates in both normal and reverse phase high-performance liquid chromatography (HPLC). This study therefore paves the way for the application of COFs in chiral separation and related fields.

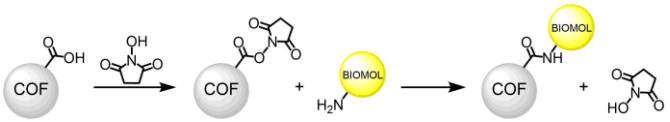

Scheme 25 Scheme of the covalent strategy to bond various biomolecules with carboxylate-containing COFs.

Other ester groups have been also used for post-synthetic modifications. Thus, Yu and co-workers have shown that COFs endowed with ester groups within the pores can be post-functionalized by hydrolysis chemistry of the ester groups upon treatment with hydrochloric acid to yield the free carboxylic acid or by ammonolysis of the ester groups upon treatment with hydrazine hydrate to yield the corresponding acetohydrazide groups.[198] This type of surface modification through hydrolysis or hydrazide chemistry has shown to be cost-effective and highly throughput. In addition, the reaction conditions avoid the contamination of pores by metal nanoparticles.

5.6. Post-functionalization of nitrile groups

Amidoxime is the chelating group of choice to impart COFs with a specific functionality as uranium capturers given that it has been proven to be the state-of-the-art moiety for uranium mitigation.[199, 200] However, although the incorporation of amidoxime moieties into 2D-COFs is attractive, the direct incorporation into imine-based COFs is difficult given the incompatibility of the amidoxime group with the imine-based COF synthesis as it is prone to react with the building units and therefore inhibit the COF formation. Nevertheless, given that amidoxime groups are readily formed through the reaction of hydroxylamine with cyano groups, nitrile-functionalized COFs are suitable precursors for the target 2D-COFs endowed with amidoxime moieties. Thus, Ma and co-workers reported the synthesis of a nitrile-functionalized COF (**COF-TpDb**) by reaction between 2,5-diaminobenzonitrile (**24**, Figs. 2, 6) and triformylphloroglucinol (**14**, Fig. 2) under solvothermal conditions. The resultant COF was then amidoximated by treatment with hydroxylamine in methanol to afford the amidoxime-functionalized COF material (**COF-TpDb-AO**, Scheme 26).[165]

The amidoxime-functionalized COF is able to reduce various uranium contaminated water samples from 1 ppm to less than 0.1 ppb within several minutes. Thus, it far outperforms other macromolecular amorphous analogs in terms of adsorption affinities, capacities and kinetics. This is a good example of the benefits of post-synthetic functionalization of COFs for their implementation in environmental remediation.

Very recently, Yaghi and co-workers have also incorporated amide and amidoxime functionalities into COFs. The amidoxime functionality was obtained by nucleophilic attack of hydroxylamine to the nitrile functional groups as shown above. On the other hand, amide functionalities can be obtained by nitrile hydrolysis in concentrated aqueous NaOH.[164] Interestingly, in a separate work Yan, Valtchev and co-workers refluxed the same COF with concentrated NaOH in EtOH/H_2O

and the nitrile groups were further hydrolyzed to carboxylic acids.[201] Moreover, treatment with $LiAlH_4$ reduced the nitrile to the corresponding amine, highlighting the versatility of nitrile groups for post-synthetic modification.

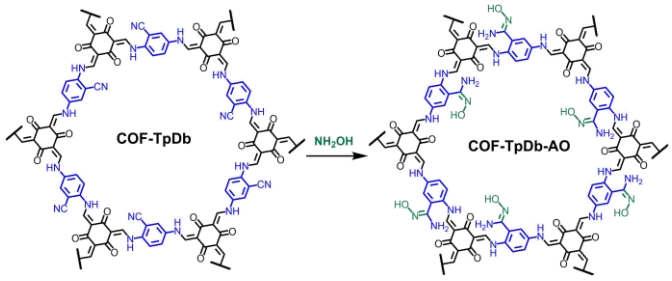

Scheme 26 Scheme for the chemical transformation of the cyano groups of **COF-TpDb** to amidoxime groups to yield **COF-TpDb-AO**.

5.7. Post-functionalization by reduction of azides

Surface waters throughout the world are contaminated by per- and polyfluorinated alkyl substances (PFAS) such as 2-propoxypropionate (GenX). With the aim of developing novel COF derivatives with rapid uptake and high affinity for adsorbing GenX and other PFAS, Dichtel and co-workers addressed the synthesis of porous COFs bearing amine groups in the pores that interact with the anionic headgroup of PFAS, along with ample hydrophobic surface area that further support adsorption.[174]

The amine functional groups were loaded into the final COF in a controlled manner by condensing 1,3,5-tris(4-aminophenyl)-benzene (**41**, Fig. 2) with a mixture of terephthalaldehyde (**1**, Fig. 2) and a dialdehyde bearing azide-functionalized ethylene glycol side chains (**12**, Figs. 2, 6). The polymerization was carried out with various molar ratios of **1** and **12** to synthesize COFs (**X%[N_3]–COFs**) that average 6, 4.5, 3, 1.5, 1, 0.5, and 0.06 azides, respectively, per layer within each hexagonal pore. The **X%[N_3]–COFs** were subsequently reduced to the corresponding **X%[NH_2]–COFs** by PPh_3 in CH_3OH. The complete reduction of azides to amines was spectroscopically confirmed. This strategy allows for the incorporation of a varying density of amine functionalities into the pores of imine-linked COFs while maintaining high surface areas (≥1000 $m^2\ g^{-1}$). It was found that the highest uptake of GenX at high concentrations ($[GenX]_0$ = 0.2 and 50 mg L^{-1}) corresponds to **20%[NH_2]–COF** while **28%[NH_2]–COF** exhibited the most rapid and the highest uptake of GenX and 12 other PFAS at environmentally relevant concentrations. This is an excellent example of how the well-defined structure of COFs with high surface area together with the tunable pore size and controlled amount of amine groups allow finding optimum characteristics for materials in order to improve their performance as adsorbents.

5.8. Deprotection of BOC-protected amines

As it was mentioned above, Jiang and co-workers carried out CuAAC post-synthetic modification of an achiral COF with an azide-containing chiral pyrrolidine providing chiral COFs.[184] In 2016 Wang and co-workers reported an alternative method for the direct construction of chiral crystalline COFs from chiral building blocks. Thus, chiral COFs can be obtained from the direct condensation of an *N*-Boc-protected pyrrolidine-based chiral building block (**39**, Figs. 2, 6) with 1,3,5-triformylbenzene (**13**, Fig. 2) and triformylphloroglucinol (**14**, Fig. 2), respectively. The BOC group can be post-synthetically cleaved by applying heat or acidic conditions (Scheme 27). The chiral COFs obtained are structurally robust and highly active as organocatalysts in asymmetric aldol reaction.[202]

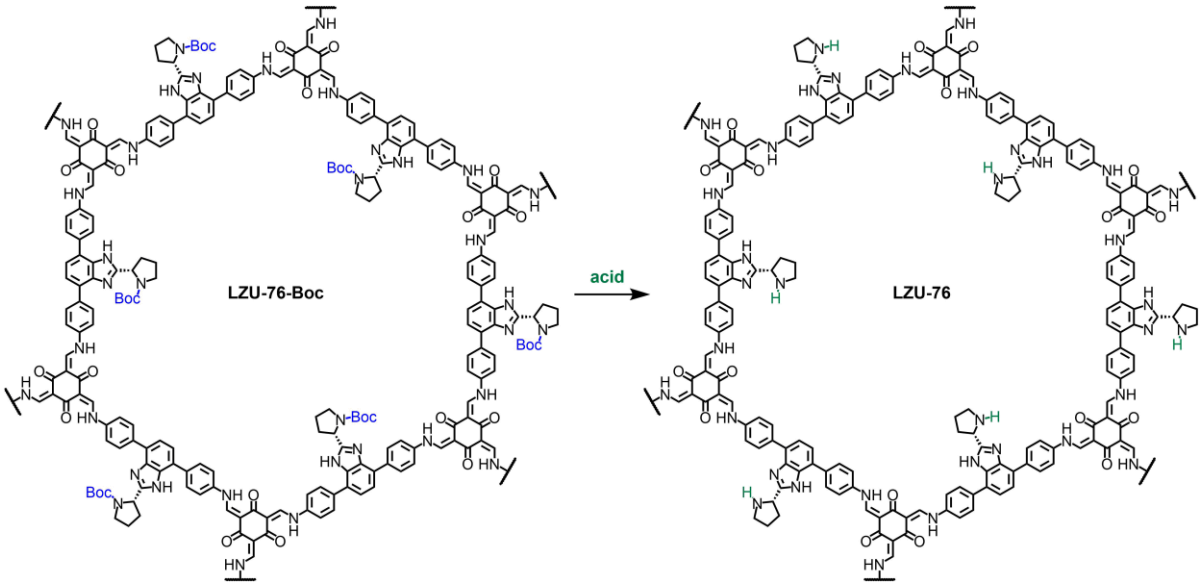

Scheme 27 Schematic representation of the post-synthetic deprotection of COFs bearing BOC-protected pyrrolidine moieties.

5.9. Post-Functionalization of imidazole groups

Imidazole and metal imidazolates have been extensively used in porous materials, especially for the construction of zeolitic imidazolate frameworks (ZIFs),[203] but until very recently they had not been incorporated into COFs. Thus, in 2019 Lee, Zhang and co-workers achieved the post-synthetic functionalization of imidazole groups in order to create ionic COFs.[177] Through the condensation of imidazole-bearing linear diamines (**40**, Figs. 2, 6) with 1,3,5-triformylbenzene (**13**, Fig. 2) they synthetized a series of COFs (**R-ImCOFs**) with different electron-withdrawing or electron-donating side-chains (R = H, CH_3, CF_3). Subsequent treatment with *n*-BuLi in hexane solution led to the formation of lithium-imidazolate COFs (**R-Li-ImCOFs**). The crystalline structure of the materials is mostly preserved after the PSM, except for **CH_3-Li-ImCOF** where some degree of amorphization was observed.

The presence of negatively charged groups immobilized in the well-ordered channels only allow the movement of the loosely bound lithium cations. Therefore, these materials behave as excellent single-ion conductors, with conductivities up to $7.2 \cdot 10^{-3}$ S cm^{-1} and activation energies as low as 0.10 eV. Moreover, conductivity could be tuned with the different side-chains: electron-withdrawing groups provide a looser lithium-imidazolate ion pairing, leading to a higher ion conductivity and explaining the observed **CF_3-Li-ImCOF** > **H-Li-ImCOF** > **CH_3-Li-ImCOF** order of conductivity.

5.10. Post-Functionalization of phenolic groups

Because of the small size of the hydroxyl group and the ready accessibility of monomers bearing this group, several examples of post-functionalization of COFs containing hydroxyl groups have been reported. Thus, in 2015 Jiang and co-workers showed that COFs endowed with phenol groups within the pores undergo a quantitative ring opening reaction with succinic anhydride that decorates the channel walls with open carboxylic acid groups (Scheme 28).[162] By adjusting the content of phenol groups on the channel it is possible to tune the content of carboxylic acid units on the channel walls. It is worth mentioning that this reaction not only proceeds smoothly and cleanly but also, in contrast to metal-catalyzed azide–alkyne or other click reactions, this ring opening reaction is free of metal catalysts which excludes the formation of metal nanoparticles that would contaminate the channels. Furthermore, this channel-wall functionalization strategy has shown to be efficient to convert a conventional COF into a material with outstanding CO_2 adsorption with high capacity, selectivity, reusability and separation productivity for flue gas. Therefore, channel-wall functional engineering is a powerful strategy to develop COFs for high-performance gas storage and separation.

A similar strategy have been recently used by Fang, Valtchev and co-workers for the synthesis of a 3D carboxy-functionalized COF through post-synthetic modification of a hydroxy-functionalized COF (Scheme 28).[163] Interestingly, this COF functionalized with carboxylate groups displays high metal loading capacities and excellent adsorption selectivity for Nd^{III} over Sr^{II} and Fe^{III}. This study therefore represents another good example of the potential of functionalized COFs in environmentally related applications.

COFs containing phenol groups have been also post-synthetically functionalized *via* acylation reactions. Thus, Gao and co-workers have reported the synthesis of COFs endowed with azobenzene and stilbene groups *via* acylation reactions of the COFs with different phenol content on their channel walls (**[HO]$_{x\%}$-H_2P-COFs**, Scheme 28) with azobenzene and stilbene derivatives endowed with carbonyl chloride functionalities. The CO_2 uptake and CO_2/N_2 selectivity of these COFs have been evaluated and it has been determined that the selectivity is greatly increased by the introduction of the 4-phenylazobenzoyl group with CO_2-philic and N_2-phobic features.[168]

The acidic feature of the phenolic groups has been used by Ma and co-workers to prepare the corresponding sodium phenoxides in basic media.[178] Thus, by treatment of a COF bearing phenol groups on their channel walls with a NaOH aqueous solution it is possible to obtain the corresponding COF with sodium phenoxide functionalities within the channel walls. In order to get insight into the effect of pore hydrophobicity for enzyme uptake, the COF with the -ONa functionality was compared with an isoreticular COF with -OMe groups. The enzyme lipase uptake capacity of the COF with -ONa groups is significantly lower than that of the isoreticular COF with -OMe functionalities thus showing that the hydrophobic pore environment is favorable for the infiltration of lipase in the pores of the COFs. Therefore, post-synthetic functionalization is also an efficient strategy for the tuning of the hydrophilic/hydrophobic characteristics of these materials.

The Williamson reaction for the synthesis of ethers has been also used for the modification of phenol-containing COFs by reaction with suitable alkyl bromides in basic media. Thus, Gao and co-workers have recently immobilized ionic liquids onto COFs *via* the Williamson ether reaction between the phenol group in **[HO]$_{x\%}$-Py-COFs** and (2-bromoethyl)triethyl-ammonium bromide ionic liquid in the presence of K_2CO_3 in dry DMF (Scheme 29).[169] By controlling the content of phenol groups it is possible to modulate the ionization degree on the channel walls of the COFs termed as **[Et_4NBr]$_{x\%}$-Py-COFs** (X = 25, 50). These ionic COFs have shown to be efficient metal-free heterogeneous catalysts for *N*-formylation reactions of different amines with CO_2 and $PhSiH_3$. The possibility of modifying these COFs through other charged guest molecules by means of ion exchange make them a promising platform for other interesting materials for catalysis or gas separation.

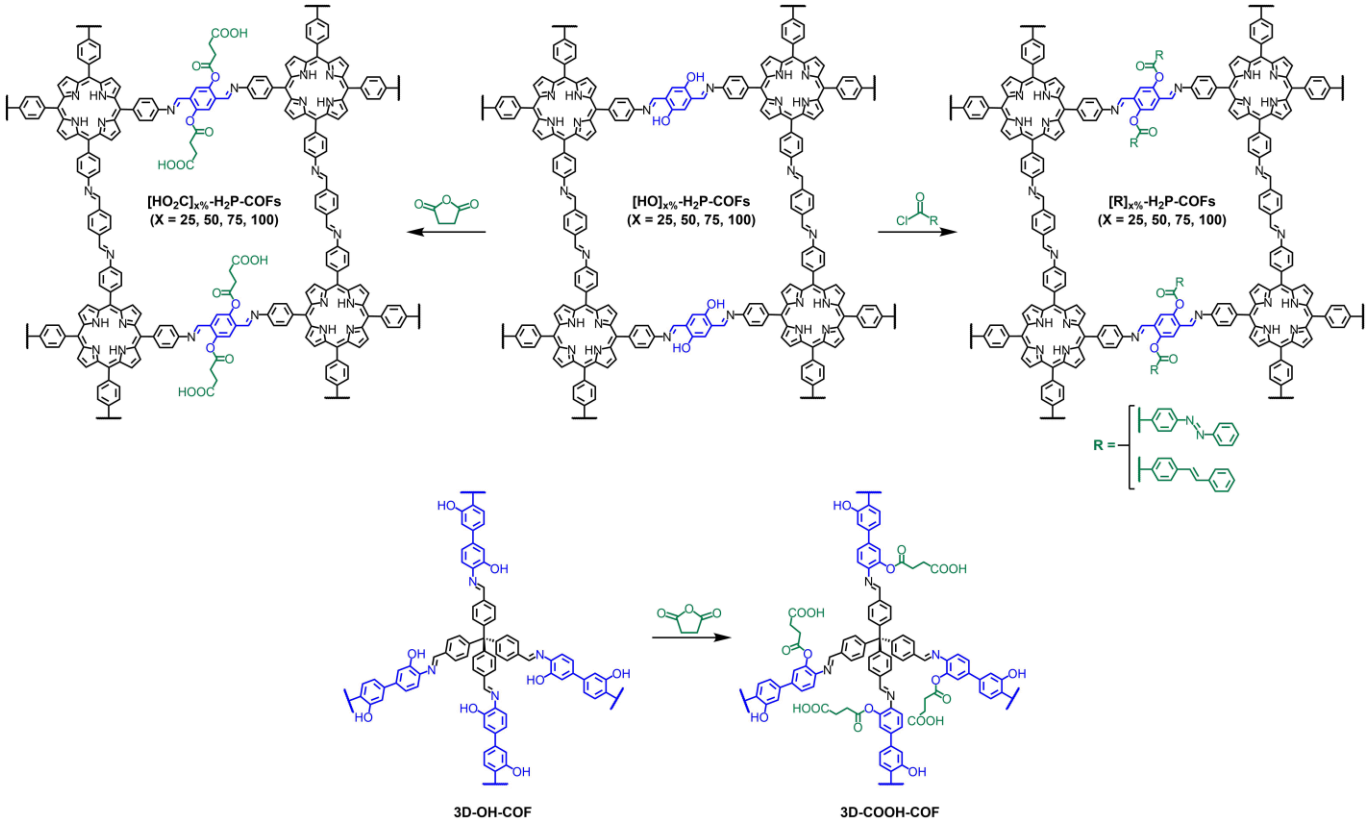

Scheme 28 Schematic representation of the post-functionalization of COFs containing phenolic groups. Top: Scheme of the ring opening reaction of **[HO]$_{x\%}$-H$_2$P-COFs** with succinic anhydride to yield **[HO$_2$C]$_{x\%}$-H$_2$P-COFs** with channel walls functionalized with carboxylic acid and with azobenzene and stilbene derivatives *via* acylation reaction. Bottom: Scheme of the preparation of a 3D-COF with carboxylate groups through post-synthetic decoration.

Ding, Chen, Han and co-workers have also used the Williamson ether reaction to anchor a zwitterionic betaine group endowed with a reactive bromoalkyl functionality into COFs bearing phenol groups in the pores.[170] The zwitterionic group-functionalized COFs present high activity as heterogeneous catalyst in the reduction of CO_2 with amine and phenylsilane to produce formamides, aminals, and methylamines, respectively, with high yield and selectivity.

Medina, Bein and co-workers have also shown the reactivity of COFs bearing phenolic groups with fluorescent dyes endowed with reactive isothiocyanate functionalities to yield COFs functionalized with fluorescent dyes through *o*-thiocarbamate linkages (Scheme 30).[204] The mild reaction conditions of this post-synthetic modification method also allow for the COF to retain its porosity and crystallinity as key features.

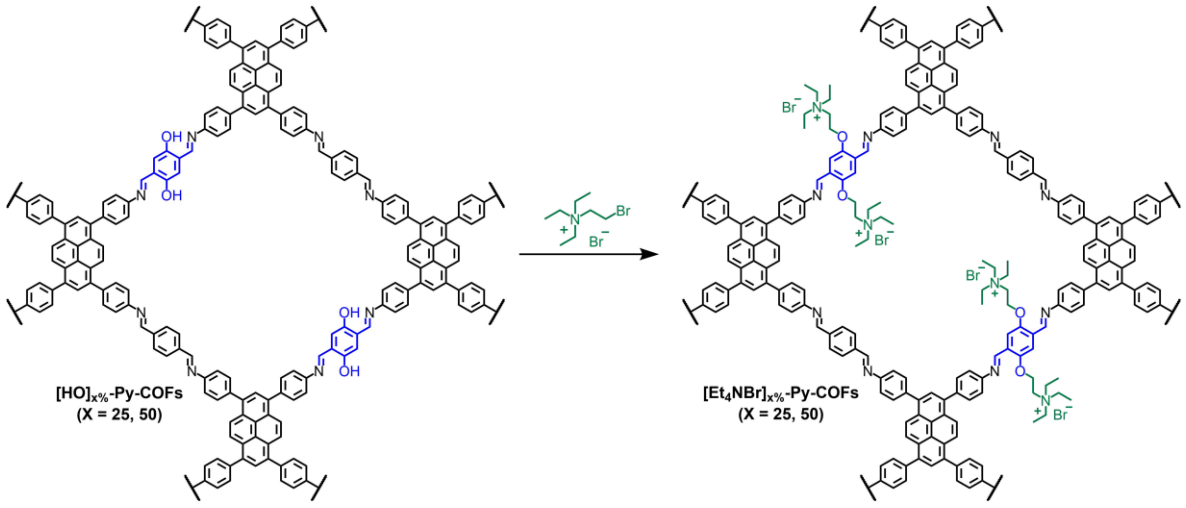

Scheme 29 Synthesis of **[Et$_4$NBr]$_{x\%}$-Py-COFs** with the ionization of channel walls through the Williamson ether reaction of **[HO]$_{x\%}$-Py-COFs** with (2-bromoethyl)triethylammonium bromide.

Another interesting characteristic of dihydroxybenzene derivatives is their ability to be oxidized to the corresponding quinones. In fact, the oxidation of hydroquinone to *p*-benzoquinone has received considerable attention in the literature.[205] Thus, Feng, Wang and co-workers have incorporated *p*-benzoquinone moieties in the skeleton of COFs by a post-synthetic procedure *via* oxidation of suitable dihydroxybenzene precursors.[160] Direct reaction between 2,5-diamino-1,4-benzoquinone (**DABQ**, Scheme 31) and 1,3,5-triformylphloroglucinol (**TFP**, **14**, Fig. 2) only afford amorphous solids. An alternative strategy involves first condensation between 2,5-diamino-1,4-dihydroxybenzene (**DABH**, **27**, Figs. 2, 6) dihydrochloride and 1,3,5-triformylphloroglucinol to obtain **DABH-TFP-COF**. The -OH groups were then subjected to sequential oxidization with O_2 and NEt_3 to yield the corresponding **DABQ-TFP-COF** (Scheme 31). The full oxidization of hydroxyl to carbonyl groups was confirmed by FTIR analysis. The redox-active 2D-COF obtained was subsequently delaminated into 2D few layer nanosheets and used for the development of organic rechargeable battery cathodes. The exfoliated COF with shorter Li^+ diffusion pathways, in comparison with the pristine COFs, allows a higher use efficiency of redox sites and faster kinetics for lithium storage.

5.11. Post-Functionalization of nitro groups

Kim and co-workers have developed a post-synthetic strategy for the modification of covalent organic frameworks using a technique based in the continuous flow of microdroplets and used this strategy to transform COFs endowed with nitro groups into COFs with amino functionalities.[173] The aim of this strategy is to develop an effective, fast and serial process for the synthesis of COFs and their post-synthetic modification avoiding long separation and purification steps. With this purpose, organic building units for the synthesis of COFs are confined in continuously moving droplets in a transparent capillary for 15 min at 100 °C in order to obtain crystalline COFs. Furthermore, in-line post-synthetic modification of these COFs is also demonstrated by the conversion of **TpPa-NO_2** to **TpPa-NH_2** *via* a serial microfluidic approach (Fig. 7). Thus, droplets containing the grown **TpPa-NO_2** particles are directly fed into a T-micromixer, where they spontaneously merge with a $SnCl_2$ solution after careful optimization of the flow rates. The merged droplets moved through a coiled capillary in a heating bath maintained at 50 °C for only 10 min. FTIR and PXRD analysis of the product obtained show that the reduction of the nitro groups was selectively and precisely carried throughout the framework, which was made possible by the fairly accessible pores of the **TpPa-NO_2** backbone. This strategy is a relevant step forward to decrease the long separation and purification steps in order to facilitate mass production of suitably functionalized COFs for desired activities.

5.12. Sequential pore wall post-synthetic modification of COFs

After all the examples shown above, it can be concluded that post-synthetic modification as a strategy for the incorporation of functional groups in the pores of covalent organic frameworks is well established. In fact, there are even a few examples of sequential post-synthetic modification.

In 2016, Medina, Bein and co-workers developed a novel approach for the synthesis of a COF bearing an amine functional group in the pores through a post-synthetic reduction reaction. They first synthesized a COF featuring nitro functionalities in the pores which act as protective groups for the final desired amino groups. The nitro groups can be reduced upon treatment of the COF with $SnCl_2 \cdot 2H_2O$ to yield the amine functionalized COF. In order to demonstrate the accessibility of the amino groups in the pores, a subsequent post-synthetic modification step, the aminolysis of acetic anhydride, was performed to obtain an amide functionalized COF. Thus, a two-step post-synthetic modification in a COF was efficiently carried out.[172]

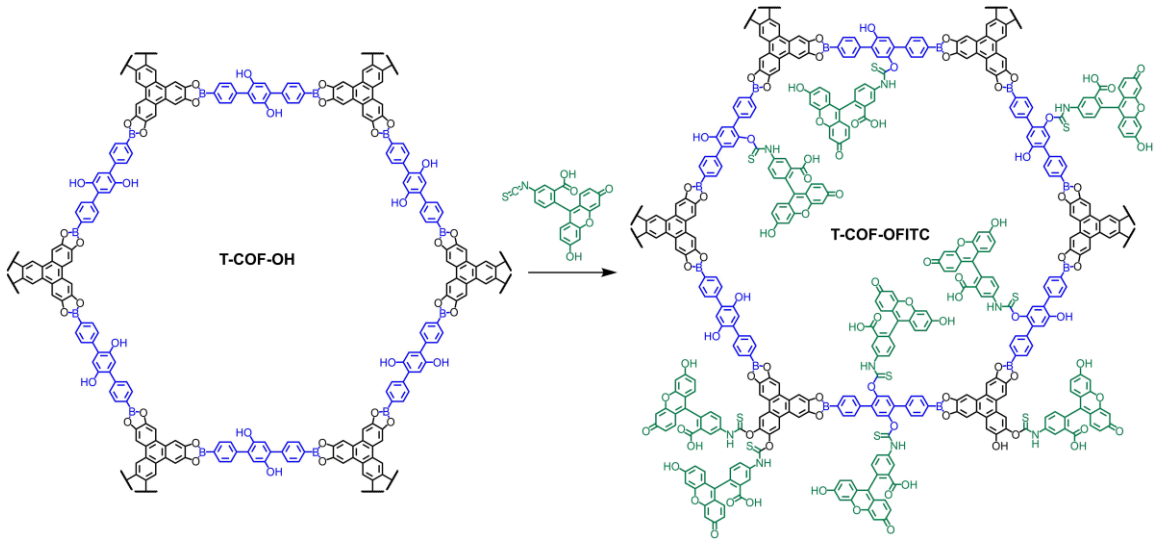

Scheme 30 Schematic representation of the post-synthetic modification reaction of a COF containing phenolic groups with a fluorescent dye endowed with an isothiocyanate functionality to yield a COF functionalized with fluorescent dyes through *o*-thiocarbamate linkages.

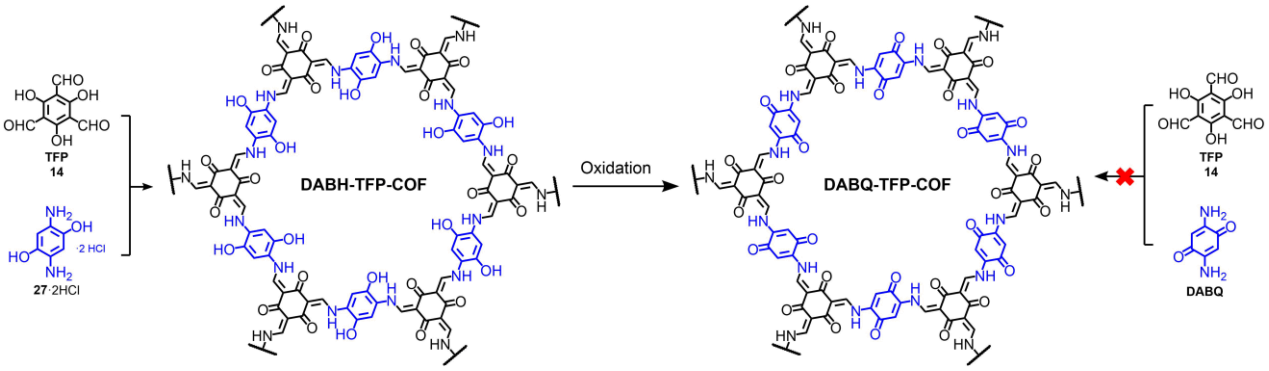

Scheme 31 Synthesis route for **DABQ-TFP COF** containing a post-synthetic step based in the oxidation of the hydroquinone moieties to benzoquinone units.

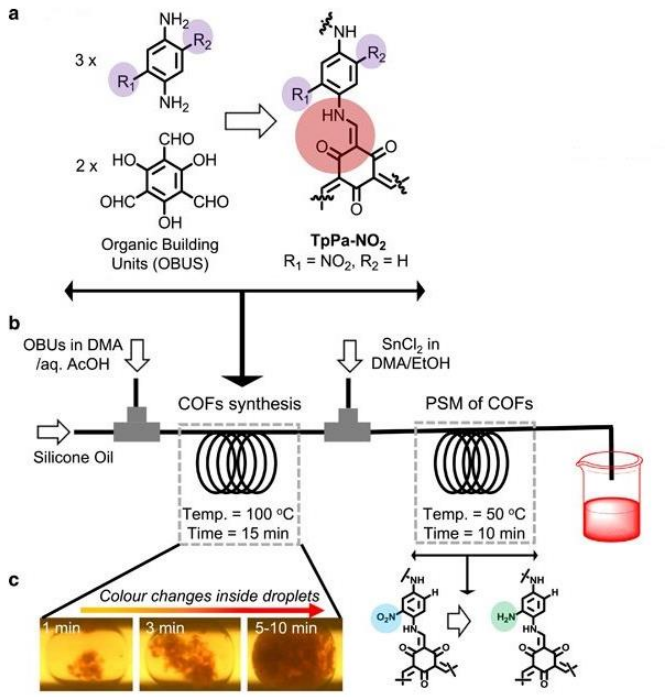

Fig. 7 (a) Schematic representation of the **TpPa-NO$_2$** COF formation; (b) representation of the synthesis of the COFs and serial post-synthetic modification of **TpPa-NO2** to **TpPa-NH2**; (c) monitoring the 'in-droplet' reaction progress (15 min, 100 °C) using dynamic color changes and filling of the droplet with a deep-red precipitate. Adapted from *NPG Asia Materials*, 2018, **10**, e456, licensed under CC BY 4.0 International License.

Yan and co-workers reported in 2017 the synthesis of a quaternary-ammonium-functionalized COF for anion conduction *via* heterogeneous sequential post-synthetic modification.[176] **TpBD-Me**, a COF with biphenyl moieties substituted with methyl groups, was first synthesized by a Schiff base aldehyde-amine condensation reaction *via* a solvothermal method. A Wohl-Ziegler reaction[206] was carried out to perform the heterogeneous bromination of **TpBD-Me** by treatment with *N*-bromosuccinimide (NBS) to give **TpBD-MeBr**. Subsequent quaternization was accomplished by treatment of a dispersion of **TpBD-MeBr** with aqueous trimethylamine. **TpBD-MeQA$^+$Br$^-$** powder (in Br^- form) was then treated with a KOH solution to be converted into **TpBD-MeQA$^+$OH$^-$** (Scheme 32). The as-prepared COF was compressed into membranes and then fully converted into the HCO_3^- form. Anion conductivity of the COF membrane in HCO_3^- form was measured by a four-electrode method under water-immersed conditions showing a conductivity of 5.3 mS cm^{-1} at 20 °C. Thus, this quaternary-ammonium-functionalized COF provides a new option for the development of anion exchange membrane fuel cells.

Banerjee and co-workers carried out post-synthetic modifications of a COF to yield functionalized targeted covalent organic nanosheets (CONs) for targeted delivery of 5-fluorouracil to breast cancer cells.[207] Fabrication of the targeted drug delivery system often requires surface amine ($-NH_2$) groups in order to be used for anchoring targeting ligands for the site-specific drug delivery.[208] Therefore a synthetic route is needed to produce COFs with surface amine groups for further sequential post-synthetic modifications. Considering the above mentioned advantages of hydroxyl functionalities for post-synthetic modifications, 4-aminosalicylhydrazide (**53**, Figs. 2, 6) was selected as one of the linker units for the construction of the targeted phenol functionalized COF (**TpASH**, Fig. 8). A first post-synthetic step consisted on the transformation of the phenolic hydroxyl groups to alkyl hydroxyl groups in the presence of glycidol (Glc) through an epoxy ring opening to yield **TpASH-Glc** CONs. The subsequent conversion of these surface alkyl hydroxyl groups to amines in the presence of APTES to afford amine functionalized CONs (**TpASH-APTES**) was the second step involved. Finally, the conjugation of the cellular targeting ligand folic acid (FA) was the third step that finally yielded the corresponding folate conjugated targeted CONs (**TpASH-FA**) (Fig. 8).

It is worth pointing out that this post-synthetic modification resulted in simultaneous chemical delamination and functionalization to targeted CONs. Furthermore, the targeted CONs showed sustained release of the drug to the cancer cells through receptor mediated endocytosis, which led to the death of cancer cells by apoptosis. Although the use of CONs-based drug delivery systems is still in a nascent stage in comparison with other biocompatible polymer-based systems, this work represents a first step toward the development of CONs-based targeted drug delivery systems.

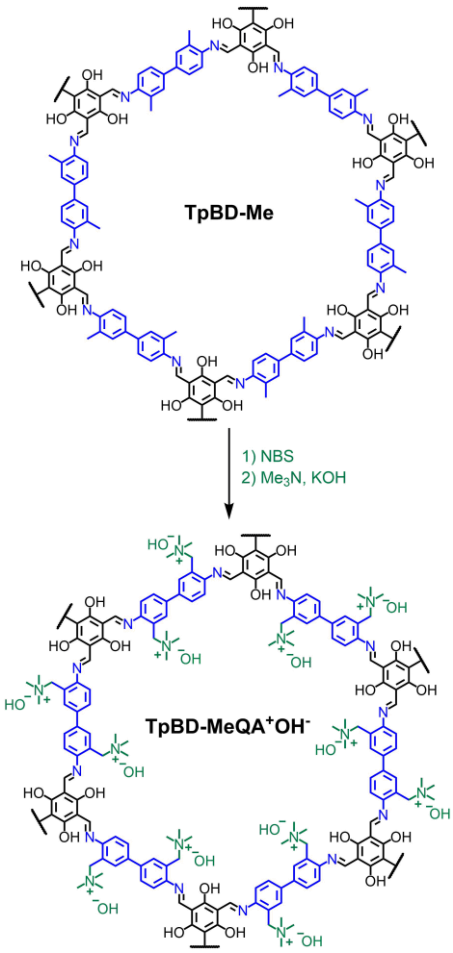

Scheme 32 Sequential post-synthetic modification of **TpBD-Me**.

The same basic scaffold as in the previous example, **TpASH** (Fig. 8), has been used by Zhang and co-workers to produce a two-photon fluorescent COF nanoprobe with enhanced chemical stability and photostability.[209] The idea of this work is to combine the respective advantages of small-molecule probes and COFs by creating a hybrid probe. Thus, the phenolic hydroxyl present in **TpASH** is appropriate for the post-synthesis conjugation with a fluorescent probe *via* a sequential post-synthetic modification. The first step is common with the strategy discussed above and involves the alkylation of **TpASH** by using glycidol *via* epoxide ring opening. The thus established presence of multiple glycols in close vicinity then served to create a strong trivalent link between the two-photon fluorescent probe, a 4-amino-1,8-naphthalimide (NPHS) derivative endowed with a 3-aminopropyltriethoxysilane (APTES) unit, and the COF. The prepared two-photon fluorescent COF nanoprobe, namely **TpASH-NPHS**, exhibits excellent photostability, limited cytotoxicity and long-term bioimaging capability and it has been already used to detect and image H_2S in live cells and deep tissues under NIR excitation. This seminal result will probably stimulate the development of other fluorescent COF nanoprobes for nanomedicine and biosensing.

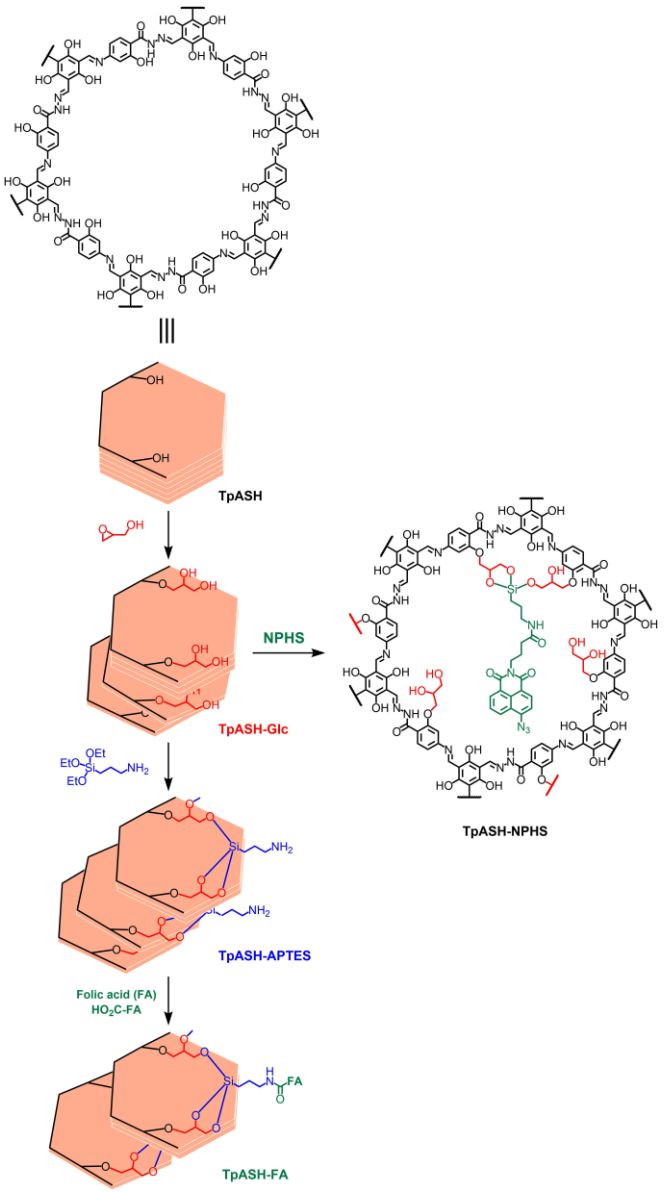

Fig. 8 Sequential post-synthetic modification scheme of **TpASH** to functionalized targeted CONs (**TpASH-FA**) and a two-photon fluorescent COF nanoprobe (**TpASH-NPHS**).

In a recent article, Lin and co-workers performed a sequential pore-wall post-synthetic modification combining functional group interconversion and metalation.[210] Thus, a core-shell magnetic nanoparticle-COF bearing hydroxyl groups in the pores was first subjected to ring opening reaction with succinic anhydride affording a carboxylic acid-grafted COF. Subsequent treatment with pamidronic acid introduced phosphate groups in the pores, which were used in a final step to immobilize Zr^{IV} ions. The as-prepared material was applied to the enrichment of phosphopeptides, showing high adsorption capacity and selectivity.

6. Monomer truncation strategy for the functionalization of COFs

The incorporation of truncated monomers has different effects on the crystallinity of COFs and it has been used as an efficient strategy both for the internal post-functionalization of three-dimensional COFs and for the outer surface functionalization of 2D-COFs.[4]

6.1. Monomer truncation strategy for the internal functionalization of three-dimensional COFs

Dichtel and co-workers have developed an interesting strategy that provides functionalized COFs suitable for post-synthetic modification.[211] The strategy involves the condensation of a polyfunctional monomer with a monomer bearing fewer reactive groups. The role of the truncated monomer in the crystallization depends on the relative rates of bond formation and exchange. Thus, the truncated monomer is incorporated throughout the network when growth is faster than exchange. In this case, the network grows around these defect sites. On the other hand, the truncated monomer will preferentially reside at the faces of the growing crystal when exchange is rapid relative to framework growth. Under these conditions, the truncated monomer will preferentially reside at the faces of the growing crystal, thus providing a way to control its shape, size and even surface functionality.

By operating in the slow exchange regime, Dichtel and co-workers utilized this strategy to functionalize the interior of a boroxine-linked 3D-COF (**COF-102**) derived from the dehydration of tetrakis(boronic acid) (**65**, Fig. 2).[212] For this purpose, a second monomer (**66**, Fig. 2) incorporating an allyl group in place of one phenylboronic acid moiety was included in the crystallization. It was possible to evaluate the percent incorporation of the truncated monomer into the COF lattice by ^{1}H NMR spectroscopy after the material was digested in CD_3CN/D_2O (3:1 v/v). Interestingly, the percent incorporations were very close to the feed ratios of the monomers used in the synthesis, up to feed ratios of 33%.

Furthermore, Dichtel and co-workers have also demonstrated the feasibility of post-synthetic functionalization of this 3D-COF. Samples of the allyl-derivative of **COF-102** with 22% allyl loading have been subjected to typical thiol-ene reaction conditions by adding propanethiol to a THF solution containing a photoinitiator (Scheme 33). Powder X-ray diffraction (PXRD) confirmed the long-range order and identical network topologies of the COF before and after the thiol-ene reaction.[188]

This strategy obviates the need to derivatize 3D-COF monomers with additional reactive moieties, which is synthetically inconvenient due to their high symmetry and compact structure.

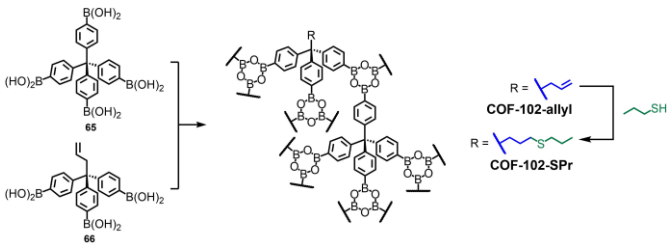

Scheme 33 Co-crystallization of tetra(boronic acid) with truncated monomer bearing an allyl moiety to produce an internally functionalized 3D-COF and post-synthetic *via* thiol-ene reaction.

6.2. Monomer truncation strategy for the outer surface functionalization of 2D-COFs

Bein and co-workers have used the monomer truncation strategy for the synthesis of a 2D-COF. They have shown that by applying monoboronic acids as modulators together with 2,3,6,7,10,11-hexahydroxytriphenylene (**55**, Fig. 2) and benzene-1,4-diboronic acid (**58**, Fig. 2) in the solvothermal synthesis of a COF it is possible to influence and optimize the crystallinity, domain size and porosity of the resulting framework.[213] An important outcome of this strategy is that the modulator is expressed at the outer surface of individual COF crystallites and therefore the functional group of a substituted truncated modulator is pointing away from the COF, rendering it easily accessible for subsequent reactions. This is especially interesting in cases where a modification on the outer surface of a COF domain is sufficient. This strategy is also relevant for the incorporation of sterically demanding functional groups which might prove very difficult to incorporate into close-packed 2D-COFs and to convert in post-modification reactions. As a proof of concept, Bein and co-workers carried out the attachment of a fluorescent dye and even coated the COF crystallites with a shell of methoxypolyethylene glycol maleimide (PEG-maleimide) *via* a Michael-type addition. Therefore, the use of functionalized truncated modulating agents represents an efficient strategy for functionalizing the outer surface of COF crystallites thus allowing the modification of their physical, chemical or electronic properties.

Conclusions

The work carried out during more than a decade in the field of covalent organic frameworks has paved the way for the development of new families of robust, stable, ordered and highly accessible porous materials with associated functionalities in their framework. These characteristics have allowed research on COFs to address some of the important challenges identified in materials science when searching for advanced solids for separation, catalysis, energy storage, adsorption, sensors, electronic or photoluminescence devices. Some of these applications very often depend on the presence of chemical functionality at the organic building blocks. However, some functionalities cannot be introduced into COFs directly *via de novo* syntheses but can be accessed through post-synthesis modification (PSM) strategies.

Metal complexation through coordination chemistry has allowed the incorporation of a variety of active metal species into covalent organic frameworks with regular channels, controlled diameter and with uniformly distributed organic ligands. The interaction of the uniformly distributed organic ligands with metal active sites allows for the effective isolation of the active sites of the catalyst at the molecular level. These highly dispersed and uniformly distributed catalytic points are responsible for the excellent catalytic properties obtained for these materials. Thus, metalated covalent organic frameworks have been used as efficient heterogeneous **catalysts** in a variety of reactions including Suzuki-Miyaura, Henry, nitroaromatic hydrogenation, silica-based cross-coupling reactions of silanes and aryl halides, selective oxidation of alkenes, C-H borylation, cyanosilylation of aldehydes, cycloaddition of epoxides with CO_2 to form cyclic carbonates or CO_2 reduction to CO among others. They have also acted as catalyst in tandem reactions such as the Heck-epoxidation tandem reaction, in cascade oxidation-Knoevenagel condensation from alcohols to α,β-unsaturated dinitriles and they have been also used as electrocatalyst for the oxygen evolution reaction.

A completely different approach developed by Yaghi and co-workers based on metalated COFs is the post-synthetic strategy that involves the reversible removal of Cu^{I} from COFs constructed from helical organic threads based on copper(I)-bisphenanthroline moieties. By removing the Cu^{I} ions, the individual 1D square ribbons in the demetalated form are held together only by mechanical interlocking of rings. This strategy provides a remarkable example of how the **mechanical properties** of a COF can be modified through post-synthetic modification.

Another important strategy toward post-synthetic modification of COFs involves the **backbone modification**. Different approaches have been addressed with this aim. The first one faces the question of the competition between reversibility and stability in the preparation of COFs which is dominated by subtle changes in the reaction conditions. This strategy involves a reversible order-inducing step under thermodynamic control for the synthesis of the protoCOF in which the order is subsequently arrested *via* a post-synthetic treatment to provide the target COF. Thus, the **chemical linkage of the COF is converted from a reversible to an irreversible type of bond in a topochemical fashion** in order to arrest COFs in their crystalline state. By means of this strategy, the COFs obtained not only retain crystallinity and porosity, but also are among the most robust COFs up-to-date that can withstand strong acidic, basic and redox environments. A second approach related with backbone modification involves the building-block-exchange-based **framework-to-framework transformation**. The dynamic nature of the bonds allows for the linkers of a COF to be exchanged post-synthetically, yielding an isostructural material with different pore metrics while retaining crystallinity. Thus, this strategy allows the use of protoCOF structures (i.e., the utilization of a parent COF as a template) for the evolution of new COF structures with completely new components and therefore paves the way for the future incorporation of new linkers with interesting electronic, redox and optical properties that rely on improved long-range order. The third strategy for backbone modification deals with the post-functionalization of COFs *via* **cycloaddition reactions**. With this aim, anthracene-containing COFs are used in order to take advantage of the susceptibility towards [4+2] cycloaddition. Cycloaddition disturbs the π–π stacking of the COF layers and produces a loss of planarity in the anthracene units, which results in exfoliation to **yield covalent organic nanosheets (CON)**. Even free-standing CON thin films with tunable thickness at air–water interfaces can be prepared through simple layer-by-layer techniques. This chemical exfoliation technique certainly represents an efficient tool for COF manipulation toward thin-film layer-by-layer assembly.

Functional group interconversion offers the endless repertoire of organic synthesis for the post-synthetic modification of COFs. The first post-synthetic modification in COFs by covalent bond formation reported in 2011 by Jiang and co-workers made use of the copper catalyzed azide-alkyne cycloaddition (CuAAC) click reaction. Following this seminal work, a great variety of reactions have been used successfully for the post-synthetic modification of COFs including the thiol-ene reaction, the aromatic nucleophilic substitution of aryl fluorides, the reaction of activated esters with amines, the amidoximation of nitrile-containing COFs by treatment with hydroxylamine and the reduction of azide- and nitro-containing COFs to the corresponding amine-containing COFs. Specially versatile are those COFs endowed with phenolic groups which have been reacted with acid chlorides in acylation reactions, with anhydrides in ring opening reactions, with suitable alkyl bromides in basic media through the Williamson ether reaction, with isothiocyanates to yield *o*-thiocarbamate linkages and with NaOH aqueous solution to obtain the corresponding COFs with sodium phenoxide functionalities within the channel walls as an efficient strategy for the tuning of the hydrophilic/hydrophobic characteristics of these materials. Thus, the post-synthetic modification of COFs by means of functional group interconversion is now well established and there are even a few examples of **sequential post-synthetic modification of COFs**.

It is also worth highlighting the **monomer truncation strategy for the functionalization of COFs**. This strategy has been successfully used both for the outer surface functionalization of 2D-COFs and for the internal functionalization of 3D-COFs.

In spite of the important contributions to the development of COFs obtained by the above reviewed post-synthetic strategies, there are still some important challenges that have to be addressed in the field. Concerning with the post-synthetic modifications that have been reported to date *via* the functional group interconversion, the versatility of this approach has been already demonstrated and the potential of this strategy for the expansion of the functional and structural diversity of COFs has been shown. However, efforts toward the

sequential pore wall post-synthetic modification of COFs will be necessary in order to expand the number of functional porous COFs available and to enhance the performance of COFs in a growing number of relevant applications.

On the other hand, the library of organic linkers that have been utilized in the syntheses of metalated, catalytically active COFs is still limited. Thus, the nature of the organic linkers has to be broadened in order to improve structural stability in aqueous acidic/alkaline media and to increase the accessible surface area, which is of particular importance for substrate and product diffusion. Furthermore, efforts should be dedicated to the design of COFs that can be used as an auspicious platform for integrating multiple metal components, considering that the functionality, spatial arrangement and density of metallic active sites can be precisely managed. By means of this strategy, a great potential can be envisaged for the use of multifunctional COFs as heterogeneous cascade catalysts.

In addition, more work is needed in order to take advantage of the principles of dynamic covalent chemistry for post-synthesis modification of COFs. Thus, it will be of main importance to explore in depth the in situ COF-to-COF transformation between COFs *via* heterogeneous linker exchange in order to face the important challenges in the developments of novel covalent organic frameworks which are related with the structural complexity and transformation of COFs. In this respect, the development of approaches to fabricate hierarchical COF architectures with controlled domain structures still remains a scientific challenge.[30]

It is also of great importance to develop novel methods that use the intrinsic reversibility of the linkers in COFs to introduce linkers with functionalities incompatible with COF synthesis conditions or which cannot be added through more established covalent post-synthetic modifications for COFs such as the functional group interconversion.

In conclusion, post-polymerization modification methods offer efficient ways to produce functional covalent organic frameworks with a variety of applications. We clearly show that the post-polymerization modification approach is rapidly developing and will certainly expand in the future. Active research on the production of novel covalent organic frameworks together with novel post-polymerization modifications strategies will contribute to the development of new applications for these unique materials.

Conflicts of interest

There are no conflicts to declare.

Acknowledgements

Financial support from Spanish Government (Project MAT2016-77608-C3-2-P) and the UCM (INV.GR.00.1819.10759) is acknowledged. The authors wish to give credit to the scientists who have participated in the development of this research field whose names are cited in the references.

Notes and references

1. A. P. Côté, A. I. Benin, N. W. Ockwig, M. Keeffe, A. J. Matzger and O. M. Yaghi, *Science*, 2005, **310**, 1166.
2. U. Díaz, D. Brunel and A. Corma, *Chem. Soc. Rev.*, 2013, **42**, 4083-4097.
3. C. Sanchez, B. Julián, P. Belleville and M. Popall, *J. Mater. Chem.*, 2005, **15**, 3559-3592.
4. M. S. Lohse and T. Bein, *Adv. Funct. Mater.*, 2018, **28**, 1705553.
5. X. Feng, X. Ding and D. Jiang, *Chem. Soc. Rev.*, 2012, **41**, 6010-6022.
6. S.-Y. Ding and W. Wang, *Chem. Soc. Rev.*, 2013, **42**, 548-568.
7. J. W. Colson and W. R. Dichtel, *Nat. Chem.*, 2013, **5**, 453.
8. P. J. Waller, F. Gándara and O. M. Yaghi, *Acc. Chem. Res.*, 2015, **48**, 3053-3063.
9. J. L. Segura, M. J. Mancheño and F. Zamora, *Chem. Soc. Rev.*, 2016, **45**, 5635-5671.
10. U. Díaz and A. Corma, *Coord. Chem. Rev.*, 2016, **311**, 85-124.
11. S. Kandambeth, K. Dey and R. Banerjee, *J. Am. Chem. Soc.*, 2019, **141**, 1807-1822.
12. C. S. Diercks and O. M. Yaghi, *Science*, 2017, **355**, eaal1585.
13. M. Dogru and T. Bein, *Chem. Commun.*, 2014, **50**, 5531-5546.
14. J. Zhou and B. Wang, *Chem. Soc. Rev.*, 2017, **46**, 6927-6945.
15. C.-Y. Lin, D. Zhang, Z. Zhao and Z. Xia, *Adv. Mater.*, 2018, **30**, 1703646.
16. X. Zhan, Z. Chen and Q. Zhang, *J. Mater. Chem. A*, 2017, **5**, 14463-14479.
17. M.-X. Wu and Y.-W. Yang, *Chin. Chem. Lett.*, 2017, **28**, 1135-1143.
18. A. K. Mandal, J. Mahmood and J.-B. Baek, *ChemNanoMat*, 2017, **3**, 373-391.
19. F. Zhao, H. Liu, D. S. Mathe, A. Dong and J. Zhang, *Nanomaterials*, 2018, **8**, 15.
20. T. Banerjee, K. Gottschling, G. Savasci, C. Ochsenfeld and B. V. Lotsch, *ACS Energy Lett.*, 2018, **3**, 400-409.
21. Y. Yan, T. He, B. Zhao, K. Qi, H. Liu and B. Y. Xia, *J. Mater. Chem. A*, 2018, **6**, 15905-15926.
22. Y. Song, Q. Sun, B. Aguila and S. Ma, *Adv. Sci.*, 2018, **6**, 1801410.
23. S. Dalapati, C. Gu and D. Jiang, *Small*, 2016, **12**, 6513-6527.
24. S. B. Alahakoon, C. M. Thompson, G. Occhialini and R. A. Smaldone, *ChemSusChem*, 2017, **10**, 2116-2129.
25. L. Ma, X. Feng, S. Wang and B. Wang, *Mater. Chem. Front.*, 2017, **1**, 2474-2486.
26. W. Zheng, C.-S. Tsang, L. Y. S. Lee and K.-Y. Wong, *Mater. Today Chem.*, 2019, **12**, 34-60.
27. S. Yuan, X. Li, J. Zhu, G. Zhang, P. Van Puyvelde and B. Van der Bruggen, *Chem. Soc. Rev.*, 2019, DOI: 10.1039/C8CS00919H.
28. Y. Yusran, Q. Fang and S. Qiu, *Isr. J. Chem.*, 2018, **58**, 971-984.
29. N. Huang, P. Wang and D. Jiang, *Nat. Rev. Mater.*, 2016, **1**, 16068.
30. Y. Jin, Y. Hu and W. Zhang, *Nat. Rev. Chem.*, 2017, **1**, 0056.
31. D. Rodríguez-San-Miguel, P. Amo-Ochoa and F. Zamora, *Chem. Commun.*, 2016, **52**, 4113-4127.
32. X.-H. Liu, C.-Z. Guan, D. Wang and L.-J. Wan, *Adv. Mater.*, 2014, **26**, 6912-6920.
33. R. P. Bisbey and W. R. Dichtel, *ACS Cent. Sci.*, 2017, **3**, 533-543.
34. W. Zhao, L. Xia and X. Liu, *CrystEngComm*, 2018, **20**, 1613-1634.

35. P. J. Waller, S. J. Lyle, T. M. Osborn Popp, C. S. Diercks, J. A. Reimer and O. M. Yaghi, *J. Am. Chem. Soc.*, 2016, **138**, 15519-15522.
36. C. J. Hawker and K. L. Wooley, *Science*, 2005, **309**, 1200.
37. J.-F. Lutz, J.-M. Lehn, E. W. Meijer and K. Matyjaszewski, *Nat. Rev. Mater.*, 2016, **1**, 16024.
38. H.-C. J. Zhou and S. Kitagawa, *Chem. Soc. Rev.*, 2014, **43**, 5415-5418.
39. L. Chen, Q. Chen, M. Wu, F. Jiang and M. Hong, *Acc. Chem. Res.*, 2015, **48**, 201-210.
40. S. J. Rowan, S. J. Cantrill, G. R. L. Cousins, J. K. M. Sanders and J. F. Stoddart, *Angew. Chem. Int. Ed.*, 2002, **41**, 898-952.
41. Y. Jin, C. Yu, R. J. Denman and W. Zhang, *Chem. Soc. Rev.*, 2013, **42**, 6634-6654.
42. W. Zhang and Y. Jin, *Dynamic Covalent Chemistry: Principles, Reactions, and Applications*, Wiley-VCH, Weinheim, 2017.
43. K. Biradha and R. Santra, *Chem. Soc. Rev.*, 2013, **42**, 950-967.
44. S. I. Stupp and L. C. Palmer, *Chem. Mater.*, 2014, **26**, 507-518.
45. J. D. Badjić, A. Nelson, S. J. Cantrill, W. B. Turnbull and J. F. Stoddart, *Acc. Chem. Res.*, 2005, **38**, 723-732.
46. E. K. Richman and J. E. Hutchison, *ACS Nano*, 2009, **3**, 2441-2446.
47. J. D. Wuest, *Chem. Commun.*, 2005, **0**, 5830-5837.
48. R. Chakrabarty, P. S. Mukherjee and P. J. Stang, *Chem. Rev.*, 2011, **111**, 6810-6918.
49. M. Yoshizawa, J. K. Klosterman and M. Fujita, *Angew. Chem. Int. Ed.*, 2009, **48**, 3418-3438.
50. R. Robson, *J. Chem. Soc., Dalton Trans.*, 2000, **0**, 3735-3744.
51. R. W. Tilford, W. R. Gemmill, H.-C. zur Loye and J. J. Lavigne, *Chem. Mater.*, 2006, **18**, 5296-5301.
52. F. J. Uribe-Romo, J. R. Hunt, H. Furukawa, C. Klöck, M. O'Keeffe and O. M. Yaghi, *J. Am. Chem. Soc.*, 2009, **131**, 4570-4571.
53. F. J. Uribe-Romo, C. J. Doonan, H. Furukawa, K. Oisaki and O. M. Yaghi, *J. Am. Chem. Soc.*, 2011, **133**, 11478-11481.
54. S. Dalapati, S. Jin, J. Gao, Y. Xu, A. Nagai and D. Jiang, *J. Am. Chem. Soc.*, 2013, **135**, 17310-17313.
55. C. R. DeBlase, K. E. Silberstein, T.-T. Truong, H. D. Abruña and W. R. Dichtel, *J. Am. Chem. Soc.*, 2013, **135**, 16821-16824.
56. Q. Fang, Z. Zhuang, S. Gu, R. B. Kaspar, J. Zheng, J. Wang, S. Qiu and Y. Yan, *Nat. Commun.*, 2014, **5**, 4503.
57. E. Jin, M. Asada, Q. Xu, S. Dalapati, M. A. Addicoat, M. A. Brady, H. Xu, T. Nakamura, T. Heine, Q. Chen and D. Jiang, *Science*, 2017, **357**, 673.
58. C. R. DeBlase and W. R. Dichtel, *Macromolecules*, 2016, **49**, 5297-5305.
59. F. García and M. M. J. Smulders, *J. Polym. Sci. A*, 2016, **54**, 3551-3577.
60. L. Chen, S. Rangan, J. Li, H. Jiang and Y. Li, *Green Chem.*, 2014, **16**, 3978-3985.
61. S.-Y. Ding, J. Gao, Q. Wang, Y. Zhang, W.-G. Song, C.-Y. Su and W. Wang, *J. Am. Chem. Soc.*, 2011, **133**, 19816-19822.
62. Y. Yang, M. Faheem, L. Wang, Q. Meng, H. Sha, N. Yang, Y. Yuan and G. Zhu, *ACS Cent. Sci.*, 2018, **4**, 748-754.
63. H. Wang, F. Jiao, F. Gao, Y. Lv, Q. Wu, Y. Zhao, Y. Shen, Y. Zhang and X. Qian, *Talanta*, 2017, **166**, 133-140.
64. X. Chen, N. Huang, J. Gao, H. Xu, F. Xu and D. Jiang, *Chem. Commun.*, 2014, **50**, 6161-6163.
65. H. Vardhan, G. Verma, S. Ramani, A. Nafady, A. M. Al-Enizi, Y. Pan, Z. Yang, H. Yang and S. Ma, *ACS Appl. Mater. Interfaces*, 2019, **11**, 3070-3079.
66. L.-H. Li, X.-L. Feng, X.-H. Cui, Y.-X. Ma, S.-Y. Ding and W. Wang, *J. Am. Chem. Soc.*, 2017, **139**, 6042-6045.
67. W. Seo, D. L. White and A. Star, *Chem. Eur. J.*, 2017, **23**, 5652-5657.
68. J. Wang, X. Yang, T. Wei, J. Bao, Q. Zhu and Z. Dai, *ACS Appl. Bio Mater.*, 2018, **1**, 382-388.
69. J. Romero, D. Rodriguez-San-Miguel, A. Ribera, R. Mas-Ballesté, T. F. Otero, I. Manet, F. Licio, G. Abellán, F. Zamora and E. Coronado, *J. Mater. Chem. A*, 2017, **5**, 4343-4351.
70. E. M. Johnson, R. Haiges and S. C. Marinescu, *ACS Appl. Mater. Interfaces*, 2018, **10**, 37919-37927.
71. H. B. Aiyappa, J. Thote, D. B. Shinde, R. Banerjee and S. Kurungot, *Chem. Mater.*, 2016, **28**, 4375-4379.
72. W. Leng, R. Ge, B. Dong, C. Wang and Y. Gao, *RSC Adv.*, 2016, **6**, 37403-37406.
73. T. Kundu, J. Wang, Y. Cheng, Y. Du, Y. Qian, G. Liu and D. Zhao, *Dalton Trans.*, 2018, **47**, 13824-13829.
74. L. A. Baldwin, J. W. Crowe, D. A. Pyles and P. L. McGrier, *J. Am. Chem. Soc.*, 2016, **138**, 15134-15137.
75. Q. Sun, B. Aguila, J. Perman, N. Nguyen and S. Ma, *J. Am. Chem. Soc.*, 2016, **138**, 15790-15796.
76. Y. Liu, Y. Ma, Y. Zhao, X. Sun, F. Gándara, H. Furukawa, Z. Liu, H. Zhu, C. Zhu, K. Suenaga, P. Oleynikov, A. S. Alshammari, X. Zhang, O. Terasaki and O. M. Yaghi, *Science*, 2016, **351**, 365.
77. M. Mu, Y. Wang, Y. Qin, X. Yan, Y. Li and L. Chen, *ACS Appl. Mater. Interfaces*, 2017, **9**, 22856-22863.
78. X. Han, J. Zhang, J. Huang, X. Wu, D. Yuan, Y. Liu and Y. Cui, *Nat. Commun.*, 2018, **9**, 1294.
79. W. Zhang, P. Jiang, Y. Wang, J. Zhang, Y. Gao and P. Zhang, *RSC Adv.*, 2014, **4**, 51544-51547.
80. W. Leng, Y. Peng, J. Zhang, H. Lu, X. Feng, R. Ge, B. Dong, B. Wang, X. Hu and Y. Gao, *Chem. Eur. J.*, 2016, **22**, 9087-9091.
81. Y. Hou, X. Zhang, J. Sun, S. Lin, D. Qi, R. Hong, D. Li, X. Xiao and J. Jiang, *Micropor. Mesopor. Mat.*, 2015, **214**, 108-114.
82. S. Lin, Y. Hou, X. Deng, H. Wang, S. Sun and X. Zhang, *RSC Adv.*, 2015, **5**, 41017-41024.
83. L. Chen, L. Zhang, Z. Chen, H. Liu, R. Luque and Y. Li, *Chem. Sci.*, 2016, **7**, 6015-6020.
84. D. Sun, S. Jang, S.-J. Yim, L. Ye and D.-P. Kim, *Adv. Funct. Mater.*, 2018, **28**, 1707110.
85. Q. Sun, B. Aguila and S. Ma, *Mater. Chem. Front.*, 2017, **1**, 1310-1316.
86. S. Yang, W. Hu, X. Zhang, P. He, B. Pattengale, C. Liu, M. Cendejas, I. Hermans, X. Zhang, J. Zhang and J. Huang, *J. Am. Chem. Soc.*, 2018, **140**, 14614-14618.
87. X. Wu, X. Han, Y. Liu, Y. Liu and Y. Cui, *J. Am. Chem. Soc.*, 2018, **140**, 16124-16133.
88. J. Hynek, J. Zelenka, J. Rathouský, P. Kubát, T. Ruml, J. Demel and K. Lang, *ACS Appl. Mater. Interfaces*, 2018, **10**, 8527-8535.
89. Y. Liu, C. S. Diercks, Y. Ma, H. Lyu, C. Zhu, S. A. Alshmimri, S. Alshihri and O. M. Yaghi, *J. Am. Chem. Soc.*, 2019, **141**, 677-683.
90. P. G. Cozzi, *Chem. Soc. Rev.*, 2004, **33**, 410-421.
91. C. J. Barona-Castaño, C. C. Carmona-Vargas, J. T. Brocksom and T. K. De Oliveira, *Molecules*, 2016, **21**, 310.
92. W. J. Youngs, C. A. Tessier and J. D. Bradshaw, *Chem. Rev.*, 1999, **99**, 3153-3180.
93. J. Sedó, J. Saiz-Poseu, F. Busqué and D. Ruiz-Molina, *Adv. Mater.*, 2013, **25**, 653-701.
94. S. Pal, in *Pyridine*, ed. P. P. Pandey, IntechOpen, 2018, DOI: 10.5772/intechopen.76986.
95. C. Kaes, A. Katz and M. W. Hosseini, *Chem. Rev.*, 2000, **100**, 3553-3590.
96. J. W. Buchler, in *Porphyrins*, ed. D. Dolphin, Academic Press, New York, 1978, vol. 1, ch. 10, p. 389.

97. K. M. Kadish, K. M. Smith and R. Guilard, in *The Porphyrin Handbook*, Academic Press, San Diego, CA, 2000, vol. 3.
98. H. Zhang, M. Zhao, X. He, Z. Wang, X. Zhang and X. Liu, *The Journal of Physical Chemistry C*, 2011, **115**, 8845-8850.
99. C. Li, J. Li, F. Wu, S.-S. Li, J.-B. Xia and L.-W. Wang, *The Journal of Physical Chemistry C*, 2011, **115**, 23221-23225.
100. K. Srinivasu and S. K. Ghosh, *The Journal of Physical Chemistry C*, 2013, **117**, 26021-26028.
101. E. C. Constable, in *Advances in Inorganic Chemistry*, ed. A. G. Sykes, Academic Press, 1989, vol. 34, pp. 1-63.
102. G. Singh, P. A. Singh, A. K. Sen, K. Singha, S. N. Dubeya, R. N. Handa and J. Choi, *Synth. React. Inorg. Met. Org. Chem.*, 2002, **32**, 171-187.
103. A. de la Peña Ruigómez, D. Rodríguez-San-Miguel, K. C. Stylianou, M. Cavallini, D. Gentili, F. Liscio, S. Milita, O. M. Roscioni , M. L. Ruiz-González, C. Carbonell, D. Maspoch, R. Mas-Ballesté, J. L. Segura and F. Zamora, *Chem. Eur. J.*, 2015, **21**, 10666-10670.
104. T. P. Yoon and E. N. Jacobsen, *Science*, 2003, **299**, 1691.
105. C. Baleizão and H. Garcia, *Chem. Rev.*, 2006, **106**, 3987-4043.
106. K. Nomura and S. Zhang, *Chem. Rev.*, 2011, **111**, 2342-2362.
107. Y. Yamada, C.-K. Tsung, W. Huang, Z. Huo, S. E. Habas, T. Soejima, C. E. Aliaga, G. A. Somorjai and P. Yang, *Nat. Chem.*, 2011, **3**, 372.
108. D. Wu, Q. Xu, J. Qian, X. Li and Y. Sun, *Chem. Eur. J.*, 2019, **25**, 3105-3111.
109. C. Zhang, S. Zhang, Y. Yan, F. Xia, A. Huang and Y. Xian, *ACS Appl. Mater. Interfaces*, 2017, **9**, 13415-13421.
110. B. Nath, W.-H. Li, J.-H. Huang, G.-E. Wang, Z.-h. Fu, M.-S. Yao and G. Xu, *CrystEngComm*, 2016, **18**, 4259-4263.
111. H. Liao, H. Wang, H. Ding, X. Meng, H. Xu, B. Wang, X. Ai and C. Wang, *J. Mater. Chem. A*, 2016, **4**, 7416-7421.
112. X. Chen, M. Addicoat, E. Jin, L. Zhai, H. Xu, N. Huang, Z. Guo, L. Liu, S. Irle and D. Jiang, *J. Am. Chem. Soc.*, 2015, **137**, 3241-3247.
113. G. Lin, H. Ding, R. Chen, Z. Peng, B. Wang and C. Wang, *J. Am. Chem. Soc.*, 2017, **139**, 8705-8709.
114. D. B. Shinde, S. Kandambeth, P. Pachfule, R. R. Kumar and R. Banerjee, *Chem. Commun.*, 2015, **51**, 310-313.
115. S. Lin, C. S. Diercks, Y.-B. Zhang, N. Kornienko, E. M. Nichols, Y. Zhao, A. R. Paris, D. Kim, P. Yang, O. M. Yaghi and C. J. Chang, *Science*, 2015, **349**, 1208.
116. M. K. Singh and D. Bandyopadhyay, *J. Chem. Sci.*, 2016, **128**, 1-8.
117. S.-B. Ren, J. Wang and X.-H. Xia, *ACS Appl. Mater. Interfaces*, 2016, **8**, 25875-25880.
118. I. Hod, M. D. Sampson, P. Deria, C. P. Kubiak, O. K. Farha and J. T. Hupp, *ACS Catalysis*, 2015, **5**, 6302-6309.
119. S. Kandambeth, A. Mallick, B. Lukose, M. V. Mane, T. Heine and R. Banerjee, *J. Am. Chem. Soc.*, 2012, **134**, 19524-19527.
120. M. Bagherzadeh, M. Zare, T. Salemnoush, S. Özkar and S. Akbayrak, *Applied Catalysis A: General*, 2014, **475**, 55-62.
121. H. M. El-Kaderi, J. R. Hunt, J. L. Mendoza-Cortés, A. P. Côté, R. E. Taylor, M. Keeffe and O. M. Yaghi, *Science*, 2007, **316**, 268.
122. E. L. Spitler and W. R. Dichtel, *Nat. Chem.*, 2010, **2**, 672.
123. E. L. Spitler, M. R. Giovino, S. L. White and W. R. Dichtel, *Chem. Sci.*, 2011, **2**, 1588-1593.
124. P. Pachfule, M. K. Panda, S. Kandambeth, S. M. Shivaprasad, D. D. Díaz and R. Banerjee, *J. Mater. Chem. A*, 2014, **2**, 7944-7952.
125. P. Pachfule, S. Kandambeth, D. Díaz Díaz and R. Banerjee, *Chem. Commun.*, 2014, **50**, 3169-3172.
126. C. E. Chan-Thaw, A. Villa, P. Katekomol, D. Su, A. Thomas and L. Prati, *Nano Lett.*, 2010, **10**, 537-541.
127. D. Mullangi, D. Chakraborty, A. Pradeep, V. Koshti, C. P. Vinod, S. Panja, S. Nair and R. Vaidhyanathan, *Small*, 2018, **14**, 1801233.
128. T. He, L. Liu, G. Wu and P. Chen, *J. Mater. Chem. A*, 2015, **3**, 16235-16241.
129. G.-J. Chen, X.-B. Li, C.-C. Zhao, H.-C. Ma, J.-L. Kan, Y.-B. Xin, C.-X. Chen and Y.-B. Dong, *Inorg. Chem.*, 2018, **57**, 2678-2685.
130. S. Lu, Y. Hu, S. Wan, R. McCaffrey, Y. Jin, H. Gu and W. Zhang, *J. Am. Chem. Soc.*, 2017, **139**, 17082-17088.
131. F. Haase, K. Gottschling, L. Stegbauer, L. S. Germann, R. Gutzler, V. Duppel, V. S. Vyas, K. Kern, R. E. Dinnebier and B. V. Lotsch, *Mater. Chem. Front.*, 2017, **1**, 1354-1361.
132. A. P. Côté, H. M. El-Kaderi, H. Furukawa, J. R. Hunt and O. M. Yaghi, *J. Am. Chem. Soc.*, 2007, **129**, 12914-12915.
133. S. Wan, J. Guo, J. Kim, H. Ihee and D. Jiang, *Angew. Chem. Int. Ed.*, 2009, **48**, 5439-5442.
134. C. Qian, Q.-Y. Qi, G.-F. Jiang, F.-Z. Cui, Y. Tian and X. Zhao, *J. Am. Chem. Soc.*, 2017, **139**, 6736-6743.
135. X.-Y. Hu, W.-S. Zhang, F. Rominger, I. Wacker, R. R. Schröder and M. Mastalerz, *Chem. Commun.*, 2017, **53**, 8616-8619.
136. M. Mazur, P. S. Wheatley, M. Navarro, W. J. Roth, M. Položij, A. Mayoral, P. Eliášová, P. Nachtigall, J. Čejka and R. E. Morris, *Nat. Chem.*, 2016, **8**, 58-62.
137. X. Han, J. Huang, C. Yuan, Y. Liu and Y. Cui, *J. Am. Chem. Soc.*, 2018, **140**, 892-895.
138. F. Haase, E. Troschke, G. Savasci, T. Banerjee, V. Duppel, S. Dörfler, M. M. J. Grundei, A. M. Burow, C. Ochsenfeld, S. Kaskel and B. V. Lotsch, *Nat. Commun.*, 2018, **9**, 2600.
139. B. Böttcher and F. Bauer, *Liebigs Ann.*, 1950, **568**, 218-227.
140. Y. Xu, S. Jin, H. Xu, A. Nagai and D. Jiang, *Chem. Soc. Rev.*, 2013, **42**, 8012-8031.
141. M. R. Rao, Y. Fang, S. De Feyter and D. F. Perepichka, *J. Am. Chem. Soc.*, 2017, **139**, 2421-2427.
142. X. Li, C. Zhang, S. Cai, X. Lei, V. Altoe, F. Hong, J. J. Urban, J. Ciston, E. M. Chan and Y. Liu, *Nat. Commun.*, 2018, **9**, 2998.
143. P. T. Corbett, J. Leclaire, L. Vial, K. R. West, J.-L. Wietor, J. K. M. Sanders and S. Otto, *Chem. Rev.*, 2006, **106**, 3652-3711.
144. A. Wilson, G. Gasparini and S. Matile, *Chem. Soc. Rev.*, 2014, **43**, 1948-1962.
145. N. Roy, B. Bruchmann and J.-M. Lehn, *Chem. Soc. Rev.*, 2015, **44**, 3786-3807.
146. P. Deria, J. E. Mondloch, O. Karagiaridi, W. Bury, J. T. Hupp and O. K. Farha, *Chem. Soc. Rev.*, 2014, **43**, 5896-5912.
147. G. Zhang, M. Tsujimoto, D. Packwood, N. T. Duong, Y. Nishiyama, K. Kadota, S. Kitagawa and S. Horike, *J. Am. Chem. Soc.*, 2018, **140**, 2602-2609.
148. H.-L. Qian, Y. Li and X.-P. Yan, *J. Mater. Chem. A*, 2018, **6**, 17307-17311.
149. P. J. Waller, Y. S. AlFaraj, C. S. Diercks, N. N. Jarenwattananon and O. M. Yaghi, *J. Am. Chem. Soc.*, 2018, **140**, 9099-9103.
150. M. C. Daugherty, E. Vitaku, R. L. Li, A. M. Evans, A. D. Chavez and W. R. Dichtel, *Chem. Commun.*, 2019, **55**, 2680-2683.
151. Z. Li, X. Ding, Y. Feng, W. Feng and B.-H. Han, *Macromolecules*, 2019, **52**, 1257-1265.
152. N. Huang, X. Ding, J. Kim, H. Ihee and D. Jiang, *Angew. Chem. Int. Ed.*, 2015, **54**, 8704-8707.
153. E. R. Thapaliya, B. Captain and F. M. Raymo, *J. Org. Chem.*, 2014, **79**, 3973-3981.

154. M. A. Khayum, S. Kandambeth, S. Mitra, S. B. Nair, A. Das, S. S. Nagane, R. Mukherjee and R. Banerjee, *Angew. Chem. Int. Ed.*, 2016, **55**, 15604-15608.
155. A. Nagai, Z. Guo, X. Feng, S. Jin, X. Chen, X. Ding and D. Jiang, *Nat. Commun.*, 2011, **2**, 536.
156. H. Xu, X. Chen, J. Gao, J. Lin, M. Addicoat, S. Irle and D. Jiang, *Chem. Commun.*, 2014, **50**, 1292-1294.
157. N. Huang, R. Krishna and D. Jiang, *J. Am. Chem. Soc.*, 2015, **137**, 7079-7082.
158. L. Merí-Bofí, S. Royuela, F. Zamora, M. L. Ruiz-González, J. L. Segura, R. Muñoz-Olivas and M. J. Mancheño, *J. Mater. Chem. A*, 2017, **5**, 17973-17981.
159. L. Chen, K. Furukawa, J. Gao, A. Nagai, T. Nakamura, Y. Dong and D. Jiang, *J. Am. Chem. Soc.*, 2014, **136**, 9806-9809.
160. S. Wang, Q. Wang, P. Shao, Y. Han, X. Gao, L. Ma, S. Yuan, X. Ma, J. Zhou, X. Feng and B. Wang, *J. Am. Chem. Soc.*, 2017, **139**, 4258-4261.
161. B. K. Hughes, W. A. Braunecker, D. C. Bobela, S. U. Nanayakkara, O. G. Reid and J. C. Johnson, *J. Phys. Chem. Lett.*, 2016, **7**, 3660-3665.
162. N. Huang, X. Chen, R. Krishna and D. Jiang, *Angew. Chem. Int. Ed.*, 2015, **54**, 2986-2990.
163. Q. Lu, Y. Ma, H. Li, X. Guan, Y. Yusran, M. Xue, Q. Fang, Y. Yan, S. Qiu and V. Valtchev, *Angew. Chem. Int. Ed.*, 2018, **57**, 6042-6048.
164. B. Zhang, M. Wei, H. Mao, X. Pei, S. A. Alshmimri, J. A. Reimer and O. M. Yaghi, *J. Am. Chem. Soc.*, 2018, **140**, 12715-12719.
165. Q. Sun, B. Aguila, L. D. Earl, C. W. Abney, L. Wojtas, P. K. Thallapally and S. Ma, *Adv. Mater.*, 2018, **30**, 1705479.
166. Q. Jiang, Y. Li, X. Zhao, P. Xiong, X. Yu, Y. Xu and L. Chen, *J. Mater. Chem. A*, 2018, **6**, 17977-17981.
167. Y. Wu, Z. Zhang, S. Bandow and K. Awaga, *Bull. Chem. Soc. Jpn.*, 2017, **90**, 1382-1387.
168. S. Zhao, B. Dong, R. Ge, C. Wang, X. Song, W. Ma, Y. Wang, C. Hao, X. Guo and Y. Gao, *RSC Adv.*, 2016, **6**, 38774-38781.
169. B. Dong, L. Wang, S. Zhao, R. Ge, X. Song, Y. Wang and Y. Gao, *Chem. Commun.*, 2016, **52**, 7082-7085.
170. Z.-J. Mu, X. Ding, Z.-Y. Chen and B.-H. Han, *ACS Appl. Mater. Interfaces*, 2018, **10**, 41350-41358.
171. S. Zhang, Y. Zheng, H. An, B. Aguila, C.-X. Yang, Y. Dong, W. Xie, P. Cheng, Z. Zhang, Y. Chen and S. Ma, *Angew. Chem. Int. Ed.*, 2018, **57**, 16754-16759.
172. M. S. Lohse, T. Stassin, G. Naudin, S. Wuttke, R. Ameloot, D. De Vos, D. D. Medina and T. Bein, *Chem. Mater.*, 2016, **28**, 626-631.
173. V. Singh, S. Jang, N. K. Vishwakarma and D.-P. Kim, *NPG Asia Mater.*, 2018, **10**, e456.
174. W. Ji, L. Xiao, Y. Ling, C. Ching, M. Matsumoto, R. P. Bisbey, D. E. Helbling and W. R. Dichtel, *J. Am. Chem. Soc.*, 2018, **140**, 12677-12681.
175. D.-G. Wang, N. Li, Y. Hu, S. Wan, M. Song, G. Yu, Y. Jin, W. Wei, K. Han, G.-C. Kuang and W. Zhang, *ACS Appl. Mater. Interfaces*, 2018, **10**, 42233-42240.
176. H. Guo, J. Wang, Q. Fang, Y. Zhao, S. Gu, J. Zheng and Y. Yan, *CrystEngComm*, 2017, **19**, 4905-4910.
177. Y. Hu, N. Dunlap, S. Wan, S. Lu, S. Huang, I. Sellinger, M. Ortiz, Y. Jin, S.-h. Lee and W. Zhang, *J. Am. Chem. Soc.*, 2019, **141**, 7518-7525.
178. Q. Sun, C.-W. Fu, B. Aguila, J. Perman, S. Wang, H.-Y. Huang, F.-S. Xiao and S. Ma, *J. Am. Chem. Soc.*, 2018, **140**, 984-992.
179. H. C. Kolb, M. G. Finn and K. B. Sharpless, *Angew. Chem. Int. Ed.*, 2001, **40**, 2004-2021.
180. C. R. Becer, R. Hoogenboom and U. S. Schubert, *Angew. Chem. Int. Ed.*, 2009, **48**, 4900-4908.
181. C. W. Tornøe, C. Christensen and M. Meldal, *J. Org. Chem.*, 2002, **67**, 3057-3064.
182. V. V. Rostovtsev, L. G. Green, V. V. Fokin and K. B. Sharpless, *Angew. Chem. Int. Ed.*, 2002, **41**, 2596-2599.
183. F. Xu, H. Xu, X. Chen, D. Wu, Y. Wu, H. Liu, C. Gu, R. Fu and D. Jiang, *Angew. Chem. Int. Ed.*, 2015, **54**, 6814-6818.
184. H. Xu, J. Gao and D. Jiang, *Nat. Chem.*, 2015, **7**, 905.
185. S. Royuela, E. García-Garrido, M. Martín Arroyo, M. J. Mancheño, M. M. Ramos, D. González-Rodríguez, Á. Somoza, F. Zamora and J. L. Segura, *Chem. Commun.*, 2018, **54**, 8729-8732.
186. A. B. Lowe, *Polym. Chem.*, 2014, **5**, 4820-4870.
187. C. Resetco, B. Hendriks, N. Badi and F. Du Prez, *Mater. Horizons*, 2017, **4**, 1041-1053.
188. D. N. Bunck and W. R. Dichtel, *Chem. Commun.*, 2013, **49**, 2457-2459.
189. Q. Sun, B. Aguila, J. Perman, L. D. Earl, C. W. Abney, Y. Cheng, H. Wei, N. Nguyen, L. Wojtas and S. Ma, *J. Am. Chem. Soc.*, 2017, **139**, 2786-2793.
190. Q. Sun, B. Aguila, J. A. Perman, T. Butts, F.-S. Xiao and S. Ma, *Chem*, 2018, **4**, 1726-1739.
191. B.-J. Yao, J.-T. Li, N. Huang, J.-L. Kan, L. Qiao, L.-G. Ding, F. Li and Y.-B. Dong, *ACS Appl. Mater. Interfaces*, 2018, **10**, 20448-20457.
192. A. G. Simmonds, J. J. Griebel, J. Park, K. R. Kim, W. J. Chung, V. P. Oleshko, J. Kim, E. T. Kim, R. S. Glass, C. L. Soles, Y.-E. Sung, K. Char and J. Pyun, *ACS Macro Lett.*, 2014, **3**, 229-232.
193. W. J. Chung, J. J. Griebel, E. T. Kim, H. Yoon, A. G. Simmonds, H. J. Ji, P. T. Dirlam, R. S. Glass, J. J. Wie, N. A. Nguyen, B. W. Guralnick, J. Park, Á. Somogyi, P. Theato, M. E. Mackay, Y.-E. Sung, K. Char and J. Pyun, *Nat. Chem.*, 2013, **5**, 518.
194. P. S. Fier and J. F. Hartwig, *J. Am. Chem. Soc.*, 2014, **136**, 10139-10147.
195. H.-G. Batz, G. Franzmann and H. Ringsdorf, *Angew. Chem. Int. Ed.*, 1972, **11**, 1103-1104.
196. P. Ferruti, A. Bettelli and A. Feré, *Polymer*, 1972, **13**, 462-464.
197. B. Lu and T. C. Chung, *Macromolecules*, 1999, **32**, 8678-8680.
198. Y. Fu, Z. Wang, X. Fu, J. Yan, C. Liu, C. Pan and G. Yu, *J. Mater. Chem. A*, 2017, **5**, 21266-21274.
199. C. W. Abney, S. Liu and W. Lin, *J. Phys. Chem. A*, 2013, **117**, 11558-11565.
200. C. W. Abney, R. T. Mayes, M. Piechowicz, Z. Lin, V. S. Bryantsev, G. M. Veith, S. Dai and W. Lin, *Energy Environ. Sci.*, 2016, **9**, 448-453.
201. X. Guan, H. Li, Y. Ma, M. Xue, Q. Fang, Y. Yan, V. Valtchev and S. Qiu, *Nat. Chem.*, 2019, DOI: 10.1038/s41557-019-0238-5.
202. H.-S. Xu, S.-Y. Ding, W.-K. An, H. Wu and W. Wang, *J. Am. Chem. Soc.*, 2016, **138**, 11489-11492.
203. A. Phan, C. J. Doonan, F. J. Uribe-Romo, C. B. Knobler, M. O'Keeffe and O. M. Yaghi, *Acc. Chem. Res.*, 2010, **43**, 58-67.
204. S. Rager, M. Dogru, V. Werner, A. Gavryushin, M. Götz, H. Engelke, D. D. Medina, P. Knochel and T. Bein, *CrystEngComm*, 2017, **19**, 4886-4891.
205. R. J. Radel, J. M. Sullivan and J. D. Hatfield, *Ind. Eng. Chem. Prod. Res. Dev.*, 1982, **21**, 566-570.
206. T. Nishiwaki and T. Goto, *Bull. Chem. Soc. Jpn.*, 1960, **33**, 26-28.
207. S. Mitra, H. S. Sasmal, T. Kundu, S. Kandambeth, K. Illath, D. Díaz Díaz and R. Banerjee, *J. Am. Chem. Soc.*, 2017, **139**, 4513-4520.

208. T. R. Cook, Y.-R. Zheng and P. J. Stang, *Chem. Rev.*, 2013, **113**, 734-777.
209. P. Wang, F. Zhou, C. Zhang, S.-Y. Yin, L. Teng, L. Chen, X.-X. Hu, H.-W. Liu, X. Yin and X.-B. Zhang, *Chem. Sci.*, 2018, **9**, 8402-8408.
210. C. Gao, J. Bai, Y. He, Q. Zheng, W. Ma, Z. Lei, M. Zhang, J. Wu, F. Fu and Z. Lin, *ACS Appl. Mater. Interfaces*, 2019, **11**, 13735-13741.
211. D. N. Bunck and W. R. Dichtel, *Chem. Eur. J.*, 2013, **19**, 818-827.
212. D. N. Bunck and W. R. Dichtel, *Angew. Chem. Int. Ed.*, 2012, **51**, 1885-1889.
213. M. Calik, T. Sick, M. Dogru, M. Döblinger, S. Datz, H. Budde, A. Hartschuh, F. Auras and T. Bein, *J. Am. Chem. Soc.*, 2016, **138**, 1234-1239.